Climate data and their characterisation for hydrological and agricultural scenario modelling across the Flinders and Gilbert catchments

A technical report to the Australian Government from the CSIRO Flinders and Gilbert Agricultural Resource Assessment, part of the North Queensland Irrigated Agriculture Strategy

Cuan Petheram[1], Ang Yang[1]

[1]CSIRO Land and Water, Canberra

December 2013

Australian Government
Department of Infrastructure and Regional Development

OFFICE OF NORTHERN AUSTRALIA
Your link to Northern Australia

Water for a Healthy Country Flagship Report series ISSN: 1835-095X

Australia is founding its future on science and innovation. Its national science agency, CSIRO, is a powerhouse of ideas, technologies and skills.

CSIRO initiated the National Research Flagships to address Australia's major research challenges and opportunities. They apply large scale, long term, multidisciplinary science and aim for widespread adoption of solutions. The Flagship Collaboration Fund supports the best and brightest researchers to address these complex challenges through partnerships between CSIRO, universities, research agencies and industry.

Consistent with Australia's national interest, the Water for a Healthy Country Flagship aims to develop science and technologies that improve the social, economic and environmental outcomes from water, and deliver $3 billion per year in net benefits for Australia by 2030. The Sustainable Agriculture Flagship aims to secure Australian agriculture and forest industries by increasing productivity by 50 percent and reducing carbon emissions intensity by at least 50 percent by 2030.

For more information about Water for a Healthy Country Flagship, Sustainable Agriculture Flagship or the National Research Flagship Initiative visit <http://www.csiro.au/flagships>.

Citation

Petheram C and Yang A (2013) Climate data and their characterisation for hydrological and agricultural scenario modelling across the Flinders and Gilbert catchments. A technical report to the Australian Government from the CSIRO Flinders and Gilbert Agricultural Resource Assessment, part of the North Queensland Irrigated Agriculture Strategy. CSIRO Water for a Healthy Country and Sustainable Agriculture flagships, Australia.

Flinders and Gilbert Agricultural Resource Assessment acknowledgments

This report was prepared for the Office of Northern Australia in the Australian Government Department of Infrastructure and Regional Development under the North Queensland Irrigated Agriculture Strategy <http://www.regional.gov.au/regional/ona/nqis.aspx>. The Strategy is a collaborative initiative between the Office of Northern Australia, the Queensland Government and CSIRO. One part of the Strategy is the Flinders and Gilbert Agricultural Resource Assessment, which was led by CSIRO. Important aspects of the Assessment were undertaken by the Queensland Government and TropWATER (James Cook University).

The Strategy was guided by two committees:

(i) the **Program Governance Committee**, which included the individuals David Crombie (GRM International), Scott Spencer (SunWater, during the first part of the Strategy) and Paul Woodhouse (Regional Development Australia) as well as representatives from the following organisations: Australian Government Department of Infrastructure and Regional Development; CSIRO; and the Queensland Government.

(ii) the **Program Steering Committee**, which included the individual Jack Lake (Independent Expert) as well as representatives from the following organisations: Australian Government Department of Infrastructure and Regional Development; CSIRO; the Etheridge, Flinders and McKinlay shire councils; Gulf Savannah Development; Mount Isa to Townsville Economic Development Zone; and the Queensland Government.

This report was reviewed by Dr Steve Charles (CSIRO), Dr Lu Zhang (CSIRO), Dr Peter Stone (CSIRO) and Dr Ian Watson (CSIRO).

The authors acknowledge the work of Professor Tom McMahon (University of Melbourne) and Dr Murray Peel (University of Melbourne) in undertaking an Ensemble Empirical Mode Decomposition (EEMD) analysis for this report. The authors would like to thank Ms Jin Teng for providing advice on the application of the empirical scaling method.

Director's foreword

Northern Australia comprises approximately 20% of Australia's land mass but remains relatively undeveloped. It contributes about 2% to the nation's gross domestic product (GDP) and accommodates around 1% of the total Australian population.

Recent focus on the shortage of water and on climate-based threats to food and fibre production in the nation's south have re-directed attention towards the possible use of northern water resources and the development of the agricultural potential in northern Australia. Broad analyses of northern Australia as a whole have indicated that it is capable of supporting significant additional agricultural and pastoral production, based on more intensive use of its land and water resources.

The same analyses also identified that land and water resources across northern Australia were already being used to support a wide range of highly valued cultural, environmental and economic activities. As a consequence, pursuit of new agricultural development opportunities would inevitably affect existing uses and users of land and water resources.

The Flinders and Gilbert catchments in north Queensland have been identified as potential areas for further agricultural development. The Flinders and Gilbert Agricultural Resource Assessment (the Assessment), of which this report is a part, provides a comprehensive and integrated evaluation of the feasibility, economic viability and sustainability of agricultural development in these two catchments as part of the North Queensland Irrigated Agricultural Strategy. The Assessment seeks to:

- identify and evaluate water capture and storage options
- identify and test the commercial viability of irrigated agricultural opportunities
- assess potential environmental, social and economic impacts and risks.

By this means it seeks to support deliberation and decisions concerning sustainable regional development.

The Assessment differs from previous assessments of agricultural development or resources in two main ways:

- It has sought to 'join the dots'. Where previous assessments have focused on single development activities or assets – without analysing the interactions between them – this Assessment considers the opportunities presented by the simultaneous pursuit of multiple development activities and assets. By this means, the Assessment uses a whole-of-region (rather than an asset-by-asset) approach to consider development.
- The novel methods developed for the Assessment provide a blueprint for rapidly assessing future land and water developments in northern Australia.

Importantly, the Assessment has been designed to lower the barriers to investment in regional development by:

- explicitly addressing local needs and aspirations
- meeting the needs of governments as they regulate the sustainable and equitable management of public resources with due consideration of environmental and cultural issues
- meeting the due diligence requirements of private investors, by addressing questions of profitability and income reliability at a broad scale.

Most importantly, the Assessment does not recommend one development over another. It provides the reader with a range of possibilities and the information to interpret them, consistent with the reader's values and their aspirations for themselves and the region.

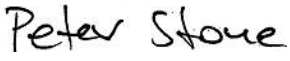

Dr Peter Stone, Deputy Director, CSIRO Sustainable Agriculture Flagship

The Flinders and Gilbert Agricultural Resource Assessment team

Project Director	Peter Stone
Project Leaders	Cuan Petheram, Ian Watson
Reporting Team	Heinz Buettikofer, Becky Schmidt, Maryam Ahmad, Simon Gallant, Frances Marston, Greg Rinder, Audrey Wallbrink
Project Support	Ruth Palmer, Daniel Aramini, Michael Kehoe, Scott Podger
Communications	Leane Regan, Claire Bobinskas, Dianne Flett[2], Rebecca Jennings
Data Management	Mick Hartcher

Activities

Agricultural productivity	Tony Webster, Brett Cocks, Jo Gentle[6], Dean Jones, Di Mayberry, Perry Poulton, Stephen Yeates, Ainsleigh Wixon
Aquatic and riparian ecology	Damien Burrows[1], Jon Brodie[1], Barry Butler[1], Cassandra James[1], Colette Thomas[1], Nathan Waltham[1]
Climate	Cuan Petheram, Ang Yang
Instream waterholes	David McJannet, Anne Henderson, Jim Wallace[1]
Flood mapping	Dushmanta Dutta, Fazlul Karim, Steve Marvanek, Cate Ticehurst
Geophysics	Tim Munday, Tania Abdat, Kevin Cahill, Aaron Davis
Groundwater	Ian Jolly, Andrew Taylor, Phil Davies, Glenn Harrington, John Knight, David Rassam
Indigenous water values	Marcus Barber, Fenella Atkinson[5], Michele Bird[2], Susan McIntyre-Tamwoy[5]
Water storage	Cuan Petheram, Geoff Eades[2], John Gallant, Paul Harding[3], Ahrim Lee[3], Sylvia Ng[3], Arthur Read, Lee Rogers, Brad Sherman, Kerrie Tomkins, Sanne Voogt[3]
Irrigation infrastructure	John Hornbuckle
Land suitability	Rebecca Bartley, Daniel Brough[3], Charlie Chen, David Clifford, Angela Esterberg[3], Neil Enderlin[3], Lauren Eyres[3], Mark Glover, Linda Gregory, Mike Grundy, Ben Harms[3], Warren Hicks, Joseph Kemei, Jeremy Manders[3], Keith Moody[3], Dave Morrison[3], Seonaid Philip, Bernie Powell[3], Liz Stower, Mark Sugars[3], Mark Thomas, Seija Tuomi, Reanna Willis[3], Peter R Wilson[2]
River modelling	Linda Holz, Julien Lerat, Chas Egan[3], Matthew Gooda[3], Justin Hughes, Shaun Kim, Alex Loy[3], Jean-Michel Perraud, Geoff Podger

Socio-economics	Lisa Brennan McKellar, Neville Crossman, Onil Banerjee, Rosalind Bark, Andrew Higgins, Luis Laredo, Neil MacLeod, Marta Monjardino, Carmel Pollino, Di Prestwidge, Stuart Whitten, Glyn Wittwer[4]

Note: all contributors are affiliated with CSIRO unless indicated otherwise. Activity Leaders are underlined. [1] TropWATER, James Cook University, [2] Independent consultant, [3] Queensland Government, [4] Monash University, [5] Archaeological Heritage Management Solutions, [6]University of Western Sydney

Shortened forms

APE	areal potential evaporation
APSIM	Agricultural Production Systems Simulator
CMIP	Coupled Model Intercomparison Project
CSIRO	Commonwealth Scientific and Industrial Research Organisation
Cv	coefficient of variation
DEM	digital elevation model
EEMD	Ensemble empirical mode decomposition
ENSO	El Niño Southern Oscillation
GCMs	global climate models
GCM-ES	global climate model output empirically scaled to provide catchment-scale variables
IMF	Intrinsic Mode Functions
IPCC AR4	the Fourth Assessment Report of the Intergovernmental Panel on Climate Change
IPO	Inter-decadal Pacific Oscillation
ITCZ	Inter-tropical Convergence Zone
MJO	Madden-Julian Oscillation
NASA	National Aeronautics and Space Administration
NQIAS	North Queensland Irrigated Agriculture Strategy
ONA	the Australian Government Office of Northern Australia
PE	potential evaporation
SOI	Southern Oscillation Index
SRES	Special Report on Emissions Scenarios

Units

MEASUREMENT UNITS	DESCRIPTION
°C	degrees Celsius
GL	gigalitres, 1,000,000,000 litres
keV	kilo-electronvolts
kL	kilolitres, 1000 litres
km	kilometres, 1000 metres
L	Litres
m	Metres
mAHD	metres above Australian Height Datum
MeV	mega-electronvolts
mg	milligrams
MJ/m^2	megajoules per metre square
ML	megalitres, 1,000,000 litres

Preface

The Flinders and Gilbert Agricultural Resource Assessment (the Assessment) aims to provide information so that people can answer questions such as the following in the context of their particular circumstances in the Flinders and Gilbert catchments:

- What soil and water resources are available for irrigated agriculture?
- What are the existing ecological systems, industries, infrastructure and values?
- What are the opportunities for irrigation?
- Is irrigated agriculture economically viable?
- How can the sustainability of irrigated agriculture be maximised?

The questions – and the responses to the questions – are highly interdependent and, consequently, so is the research undertaken through this Assessment. While each report may be read as a stand-alone document, the suite of reports must be read as a whole if they are to reliably inform discussion and decision making on regional development.

The Assessment is producing a series of reports:

- Technical reports present scientific work at a level of detail sufficient for technical and scientific experts to reproduce the work. Each of the 12 research activities (outlined below) has a corresponding technical report.
- Each of the two catchment reports (one for each catchment) synthesises key material from the technical reports, providing well-informed but non-scientific readers with the information required to make decisions about the opportunities, costs and benefits associated with irrigated agriculture.
- Two overview reports – one for each catchment – are provided for a general public audience.
- A factsheet provides key findings for both the Flinders and Gilbert catchments for a general public audience.

All of these reports are available online at <http://www.csiro.au/FGARA>. The website provides readers with a communications suite including factsheets, multimedia content, FAQs, reports and links to other related sites, particularly about other research in northern Australia.

The Assessment is divided into 12 scientific activities, each contributing to a cohesive picture of regional development opportunities, costs and benefits. Preface Figure 1 illustrates the high-level linkages between the 12 activities and the general flow of information in the Assessment. Clicking on an 'activity box' links to the relevant technical report.

The Assessment is designed to inform consideration of development, not to enable particular development activities. As such, the Assessment informs – but does not seek to replace – existing planning processes. Importantly, the Assessment does not assume a given regulatory environment. As regulations can change, this will enable the results to be applied to the widest range of uses for the longest possible time frame. Similarly, the Assessment does not assume a static future, but evaluates three distinct scenarios:

- Scenario A – historical climate and current development
- Scenario B – historical climate and future irrigation development
- Scenario C – future climate and current development.

As the primary interest was in evaluating the scale of the opportunity for irrigated agriculture development under the current climate, the future climate scenario (Scenario C) was secondary in importance to scenarios A and B. This balance is reflected in the allocation of resources throughout the Assessment.

The approaches and techniques used in the Assessment have been designed to enable application elsewhere in northern Australia.

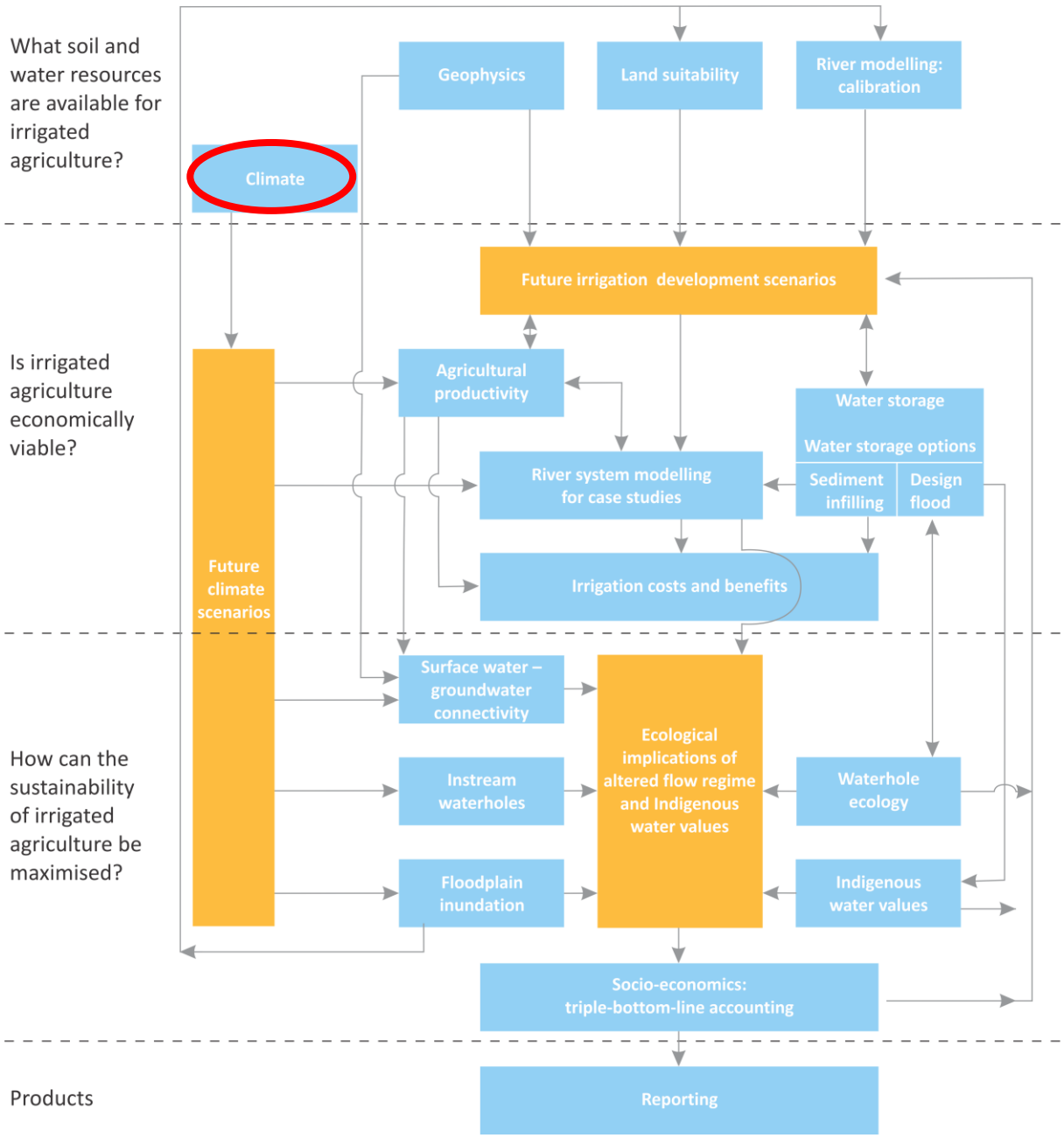

Preface Figure 1 Schematic diagram illustrating high-level linkages between the 12 activities (blue boxes)

This report is a technical report. The red oval in Preface Figure 1 indicates the activity (or activities) that contributed to this report.

The orange boxes indicate information used or produced by several activities. The red oval indicates the activity (or activities) that contributed to this technical report. Click on a box associated with an activity for a link to its technical report (or click on 'Technical reports' on <http://www.csiro.au/FGARA> for a list of links to all technical reports). Note that the Water storage activity has multiple technical reports – in this case the separate reports are listed under the activity title. Note also that these reports will be published throughout 2013, and hyperlinks to currently unpublished reports will produce an 'invalid publication' error in the CSIRO Publication Repository.

Executive summary

Climatic variables are generally considered, together with soil data, to be the most important environmental factors in determining the suitability of particular locations for agriculture. And because climate is so very closely linked to hydrology and water availability, understanding of climate and its variability is especially important in assessments of semi-arid and subtropical sites in northern Australia for irrigated land use.

Climate data for this study were assembled for the Flinders and Gilbert catchments using daily gridded SILO data (Jefferies et al. 2001) from between 1 July 1890 and 30 June 2011, referred to herein as the historical period. These data were acquired primarily for preparing a consistent set of input climate data files for the hydrological and agricultural numerical models being used by other activities in the Flinders and Gilbert Agricultural Resource Assessment, namely for river modelling, flood mapping, agricultural productivity, water storage, groundwater, and dry season pools (Preface Figure 1).

The Flinders and Gilbert Agricultural Resource Assessment is primarily focused on assessing the opportunity for irrigation with currently available environmental resources. However, given the changes in temperature and rainfall projected in the coming decades, and the sensitivity of Australian agriculture (and the natural resource base on which it depends) to that change, the effects of climate change form part of the Assessment. To this end, information from global climate model projections were used to inform the development of climate data reflecting a world where the global average surface air temperatures are 2 °C higher relative to ~1990 global temperatures. The method employed is described in this report. These synthetic future climate data will be used as input to the hydrological and agricultural numerical models used in the Assessment.

In collating and manipulating these climate data for use by the numerical models, climate statistics and maps were prepared for the Flinders and Gilbert catchments. These are presented in this report and the results are summarised below.

The mean annual rainfall, averaged over the 121-year historical period (1890 to 2011) over the Flinders and Gilbert catchments was 492 mm and 775 mm respectively. Close to 90% of rainfall across the two catchments fell during the wet season (1 November- 30 April). The highest median rainfall in both the Flinders and Gilbert catchments occurred during the months of January and February, with a median monthly value of about 100 and 200 mm, respectively. The months with the lowest median rainfall were July and August: about 0.5 mm in each of the Flinders and Gilbert catchments.

A statistical analysis called Ensemble Empirical Mode Decomposition was undertaken on four rainfall stations in the Assessment area to examine the proportion of variance in the historical monthly time series of rainfall that was due to different frequency fluctuations. It was found that approximately 90% of the variance in the historical monthly time series of rainfall was due to the annual cycle and within year variability. The remaining 10% was attributed to inter-annual variability in rainfall. An increasing trend in rainfall of between +4 and +14.5% was computed over the length of the historical period.

Although the majority of the variation in the historical monthly rainfall record was attributed to the annual cycle and within year variability, rainfall in the catchments nevertheless exhibits considerable variation from one year to the next. The highest catchment average annual rainfall in the Flinders (1310 mm) and Gilbert (2187 mm) catchments occurred in 1974, and was nearly three times the median annual rainfall. The variation of annual rainfall in the Flinders and Gilbert catchments is large compared to rainfall stations of similar mean annual rainfall elsewhere in Australia. It is also large compared to rainfall stations of similar mean annual rainfall and situated in similar climate types elsewhere in the world.

The duration of dry spells (i.e. consecutive years of annual rainfall below the median annual rainfall) in the Flinders and Gilbert catchments is comparable to other areas of eastern Australia and does not appear unusual. However, the magnitude (i.e. intensity) of dry spells in the Flinders and Gilbert catchments

appears to be larger than the majority of the rainfall stations examined in south-eastern and south-western Australia. This suggests that agriculturalists in the Flinders and Gilbert catchments would need to have especially well developed drought contingency plans.

Areal potential evaporation in the two catchments exceeds 1800 mm in most years. It exhibits a strong seasonal pattern, ranging from 200 mm per month during the build up and the wet season (October to January), to about 100 mm per month during the middle of the dry season (June to July). The high potential evaporation rates and relatively low rainfall result in a large annual rainfall deficit across most of the Assessment area. Consequently, both catchments have a high proportion of landscape with a semi-arid climate. High rainfall deficits adversely affect surface water storages. This is discussed in more detail in the companion technical report about water storage (see Preface Figure 1).

Together with the availability of water, temperature is one of the most influential climatic factors on crop productivity. Both the Flinders and Gilbert catchments experience high maximum daily temperatures, particularly during the months of October to February. Temperature considerations on crop productivity in the Flinders and Gilbert catchments are discussed in more detail in the companion technical report about agricultural productivity (see Preface Figure 1).

Based on the methods used in this report, approximately half the global climate models were found to result in a spatially averaged increase in mean annual rainfall (by up to 17% in the Flinders and 22% in the Gilbert) and half resulted in a decrease (by up to 33% in both the Flinders and Gilbert), relative to the historical climate. Importantly, approximately 60% of the models differed by less than ±10% from the historical rainfall (1890 to 2011), and it is possible for small trends to be generated by internal variability modelled by the global climate models. Hence the consensus result from the 15 global climate models is that the impacts on mean annual rainfall of a 2 °C increase in global temperatures relative to ~1990 is not likely to be major in either the Flinders or Gilbert catchments.

Contents

Figures

Tables

1 Introduction

Climatic variables are generally considered, together with soil data, to be the most important environmental factors in determining the suitability of particular locations for agriculture. And because climate is so very closely linked to hydrology and water availability, understanding of climate and its variability is especially important in assessments of semi-arid and subtropical sites in northern Australia for irrigated land use.

The Flinders and Gilbert Agricultural Resource Assessment is primarily focused on assessing the opportunity for irrigation with currently available environmental resources. However, given the changes in temperature and rainfall projected in the coming decades, and the sensitivity to that change of Australian agriculture and the natural resource base on which it depends (Hennessy et al. 2007), the effects of climate change on specific development options form part of this Assessment.

The primary purpose of this report is to: i) provide a general overview of the current climate of the Flinders and Gilbert catchments, ii) describe the methods by which the historical climate series were scaled for an increase in global temperature of 2 degree C relative to ~1990 temperatures, and iii) present the results of empirical scaling for an ensemble of 15 Global Climate Models (GCM).

This study will produce a consistent set of data on current and future climate data – for use in the companion technical reports about river modelling, flood mapping, agricultural productivity, water storage, groundwater and dry season pools (Preface Figure 1).

The remainder of this introductory section describes the Assessment area, the availability of climate data in the Flinders and Gilbert catchments, and an outline of how the original climate data were acquired. The water year, seasons and climate scenarios are then described. Section 2 provides an overview of current climate of the lower Gulf region, briefly describing the relevant atmospheric circulatory systems. Maps of key climatic parameters are then presented together with an analysis of runs of wet and dry years. Section 3 describes the methods by which the historical climate data were scaled to reflect projected climate change. The methods section contains a brief discussion on how the Assessment results, as informed by the Coupled Model Intercomparison Project (CMIP) 3 GCMs from the IPCC 2007 assessment report four (AR4), compare to the preliminary CMIP5 GCM runs that are currently being archived as part of IPCC 2014 assessment report five (AR5). This is followed by a presentation of the projected climate series. Conclusions are then provided.

1.1 Assessment area

The Assessment area encompasses the Flinders and Gilbert catchments, which are located in the Gulf region of North Queensland (Figure 1.1). The Flinders catchment has an area of 109,000 km^2 and a population of about 6000 people. The Flinders River is the longest of the Gulf Rivers and second longest Australian river course outside of the Murray-Darling Basin, and sixth longest Australian river overall. The river rises in the Great Dividing Range north-east of Hughenden, nearly 1000 km from its entry to the Gulf of Carpentaria. The Gilbert catchment has an area of 46,354 km^2 and a population of about 1200 people. The Gilbert catchment is comprised of two major rivers, the Gilbert and the Einasleigh. The Gilbert River flows in a north-westerly direction from the Great Dividing Range, 150 km south-east of Georgetown and is joined by its major tributary, the Einasleigh River, downstream of Strathmore Station, before entering the Gulf of Carpentaria.

Both catchments have a maximum elevation of about 1050 m and do not have any mountains that provide notable obstruction to large-scale atmospheric circulatory systems. While the Gilbert catchment is undulating in its mid-to-upper reaches the Flinders catchment is predominately flat (Figure 1.1). The main

land use by area in the two catchments is extensive cattle grazing. Major population centres are shown in Figure 1.1.

In this report northern Australia is defined as the area encompassed by the Timor Sea drainage division, Gulf of Carpentaria drainage division and the North-east Coast drainage division north of Cairns.

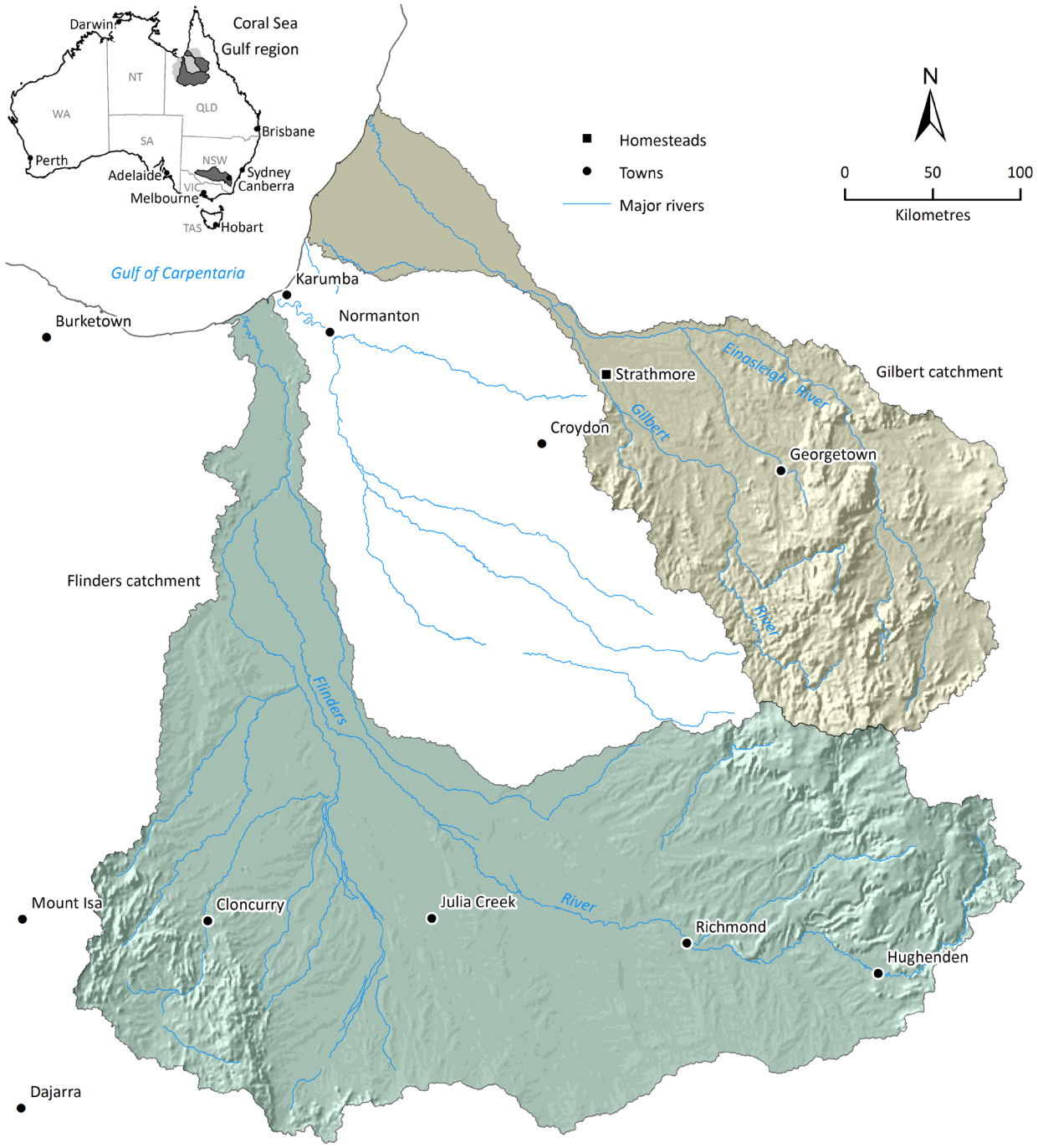

Figure 1.1 A shaded relief map of the Flinders and Gilbert catchments. The Flinders and Gilbert catchments, the Gulf region and the Murrumbidgee catchment in south-eastern Australia are shown in the small thumbnail map in top left corner

1.2 Availability of climate data

An exploratory evaluation of the spatial and temporal extent of the available climate data across the Timor Sea and Gulf of Carpentaria drainage divisions reveals that the Gulf region has the best coverage of rainfall and temperature stations across northern Australia (Appendix A). The distributions of rainfall and

maximum temperature data in the Flinders and Gilbert catchments are shown in Figure 1.2 and Figure 1.3 respectively.

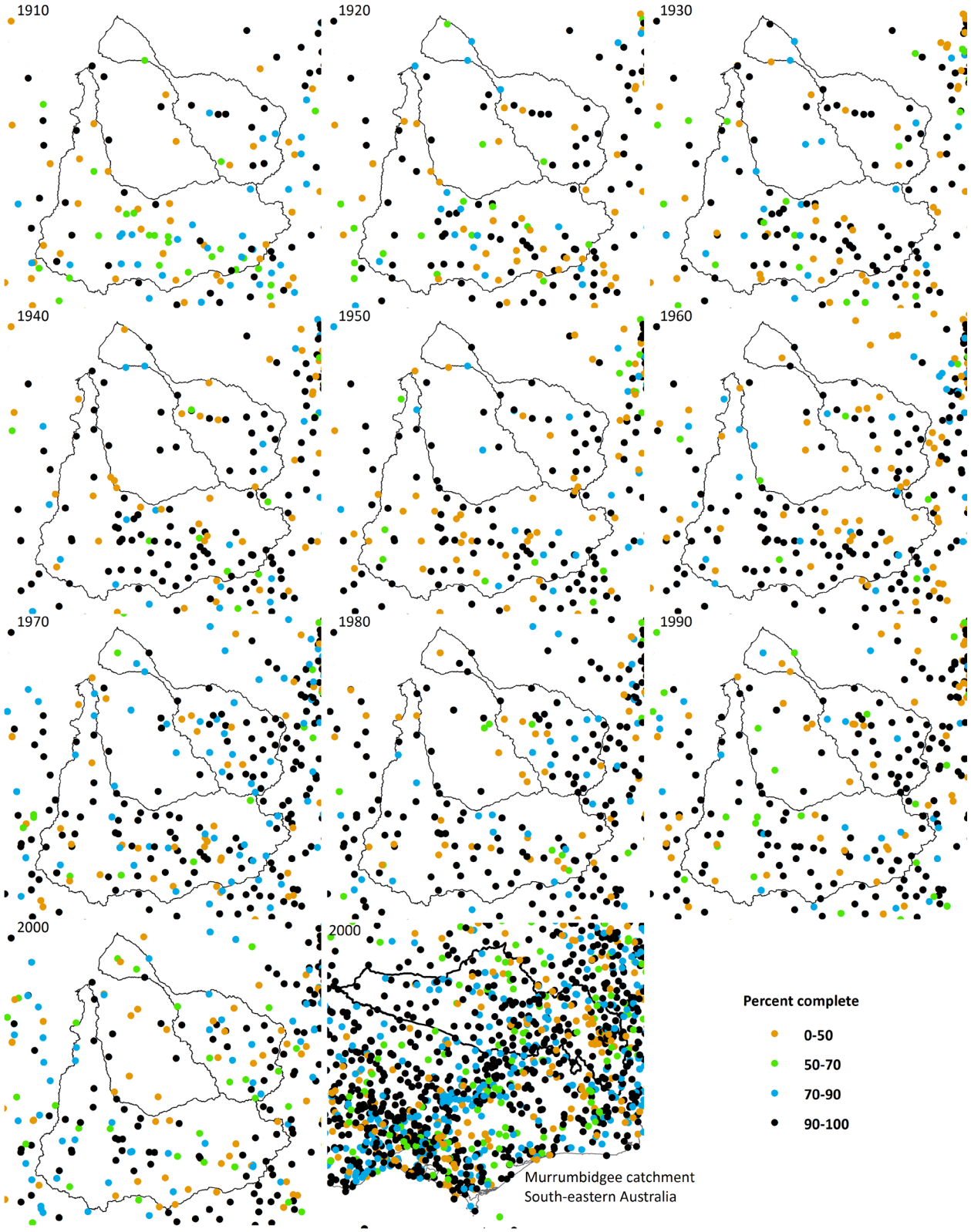

Figure 1.2 Decadal analysis of the location and completeness of Bureau of Meteorology stations measuring daily rainfall used in the SILO database. The decade labelled '1910' is defined from 1 January 1910 to 31 December 1919, and so on. At a station, a decade is 100% complete if there are observations for every day in that decade. The analysis for the decade starting in 2000 only extends to 2007. The last panel shows the availability of rainfall data in the vicinity of the Murrumbidgee catchment in south-eastern Australia

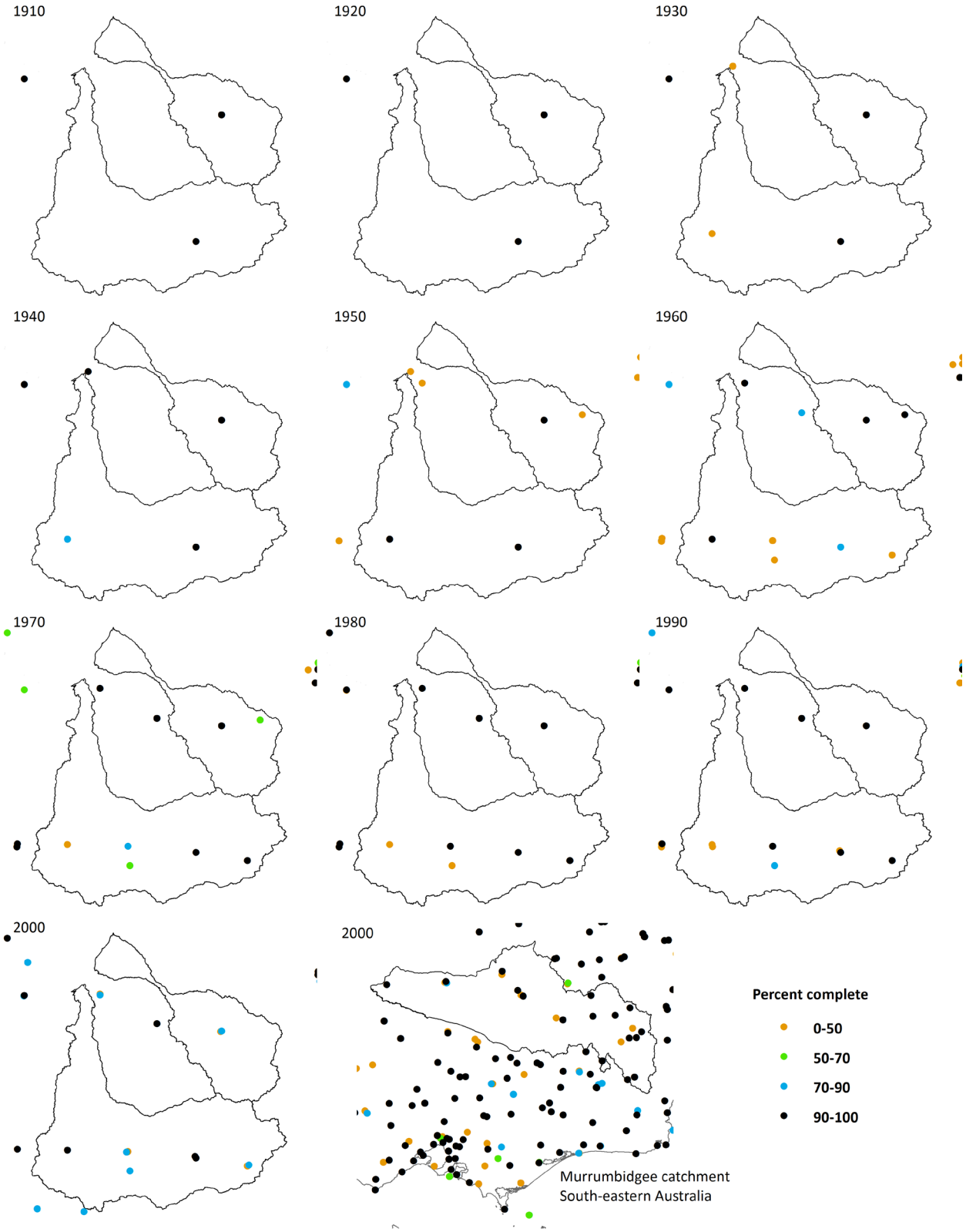

Figure 1.3 Decadal analysis of the location and completeness of Bureau of Meteorology stations measuring daily maximum air temperature used in the SILO database. The decade labelled '1910' is defined from 1 January 1910 to 31 December 1919, and so on. At a station, a decade is 100% complete if there are observations for every day in that decade. The analysis for the decade starting in 2000 only extends to 2007. The last panel shows the availability of maximum temperature data in the vicinity of the Murrumbidgee catchment in south-eastern Australia

Figure 1.2 and Figure 1.3 show there are considerably fewer stations measuring rainfall and maximum temperature in the Flinders and Gilbert catchments, compared to the Murrumbidgee catchment in south eastern Australia (~84,000 km^2). The Murrumbidgee catchment is a well known sub-catchment of the Murray-Darling Basin, and is comparable in size to the Flinders and Gilbert catchments.

1.2.1 SOURCE OF CLIMATE DATA

Spatially continuous datasets

This report and the reports dependent upon it are based on historical daily climate data derived from 0.05° x 0.05° (~ 5 km x 5 km) resolution grids, spanning the 121 year period 1 July 1890 to 30 June 2011. Data were sourced from the SILO data drill database, http://www.longpaddock.qld.gov.au/silo/ (Jeffrey et al., 2001). SILO provides surfaces of daily climate data interpolated and in-filled from point measurements made by the observation network developed and maintained by the Bureau of Meteorology. The variables used were rainfall, incoming shortwave solar radiation, vapour pressure, maximum air temperature, minimum air temperature and relative humidity. These data were used to produce the spatially continuous maps of climate surfaces in Section 2.

It is important to note that the gridded climate data are a modelled dataset (i.e. they are derived from observed data but do not contain the original observed data). Interpolation routines used on climate observations have been quality checked by the Bureau of Meteorology and have been subjected to additional error checking by the Queensland Government (Jeffrey et al., 2001). Data accuracy is expected to be lowest in areas where the observation density is low relative to the climate gradients and available for shorter time periods. Because rainfall has lower spatial and temporal auto-correlation than other climate variables, the Bureau of Meteorology has established a higher spatial density of observation stations for rainfall than other climate variables; all have generally increased in density over time, although there has been a slight reduction since the 1990s (Figure 1.2 and Figure 1.3).

In addition to daily rainfall data, the surface-water and ground-water models used in the Assessment require estimates of potential evaporation (PE). This represents the atmospheric demand for water under given meteorological conditions and provides an upper limit to the actual evaporation in the hydrological modelling. Morton's wet environment areal PE (APE)(Morton, 1983) was calculated for the daily 0.05° x 0.05° grids using the following SILO data: maximum and minimum air temperature; incoming solar radiation; atmospheric vapour pressure (converted to relative humidity using the SILO actual vapour pressure divided by the saturation vapour pressure at the daily air temperature extremes). This method is outlined in Li et al., (2009).

APE represents the evaporation that would take place from a continually saturated surface that is large enough to render the effects of any upwind boundary transitions negligible, thus integrating local variations to an areal average. In water-limited environments, daily hydrological modelling results are much less sensitive to errors in the PE data than they are to errors in the rainfall data (e.g. Andreassian et al., 2004). It is also easier to provide reliable PE data for the hydrological modelling, as PE has lower spatial variance with smaller day-to-day variation compared to rainfall (see Section 2).

Point datasets

In the figures in Section 2 where point data are displayed, these data were acquired from the SILO patch point dataset http://www.longpaddock.qld.gov.au/silo/ppd/index.php. Unlike the SILO data drill product (see previous section), these data contain real observations, gap filled where necessary using nearby stations. Seventy-one rainfall stations were selected for all of Australia on the basis that they had near continuous rainfall data from 1 July 1890 to 30 June 2011 (six stations were located in the Assessment area and an additional four stations were located within 100 km of the Assessment area).

1.3 Definition of water year and seasons

The Gulf region experiences a highly seasonal climate, where the majority of rain falls between December and March. Unless specified otherwise the wet season is defined as being the 6 month period from 1 November to 30 April, and the dry season as the 6 month period from 1 May to 31 October. All results in the Assessment will be reported over the water year, defined as the period 1 July to 30 June. The advantage of this is that it allows each individual wet season to be counted in a single 12 month period, rather than being split over two calendar years, i.e. counted as two separate seasons. This is much more satisfactory for reporting climate statistics and from a hydrological and agricultural assessment viewpoint.

1.4 Scenario definitions

Four scenarios will be evaluated in the Assessment, reflecting a combination of different levels of development and historical and future climates, much like those used in the Northern Australia Sustainable Yields Project (CSIRO, 2009a, b, c). In the Assessment the primary interest is in evaluating the scale of the opportunity under the current climate. Hence the future climate scenarios (scenarios C and D) are secondary in importance to scenarios A and B. This balance is reflected in the allocation of resources within the Assessment.

Scenario A

Scenario A is historical climate and current development. The historical climate series is defined as the observed climate (rainfall, temperature and potential evaporation for water years from 1 July 1890 to 30 June 2011). All results presented in this report are computed over this period unless specified otherwise. The current level of surface water, groundwater and economic development will be assumed (as at 1 July 2011). Scenario A will be used as the baseline against which assessments of relative change will be made. Historical tidal data will be used to specify downstream boundary conditions for the flood modelling.

Scenario B

Scenario B is historical climate and future development, as generated in the Assessment. Scenario B will use the same historical climate series as Scenario A. River inflow, groundwater recharge and flow, and agricultural productivity will be modified to reflect potential future development. The impacts of changes in flow due to this future development will be assessed, including impacts on:

- instream, riparian and near-shore ecology
- Indigenous water values
- economic costs and benefits
- opportunity costs of expanding irrigation
- institutional, economic and social considerations that may impede or enable adoption of irrigated agriculture.

Scenario C

Scenario C is future climate and current development. It will be based on a 121-year climate series (as in Scenario A) derived from a range of GCM projections for a 2 °C global temperature rise scenario. The range of GCM projections will encompass different GCMs for this single global warming scenario. The GCM projections will be used to modify the observed historical daily climate sequences. The current level of surface water, groundwater and economic development will be assumed. Tidal levels will be perturbed to reflect a ~2060 sea-level rise (i.e. the median date at which the GCMs reach a 2 °C global temperature rise).

Scenario D

Scenario D is future climate and future development. It will use the same future climate series as Scenario C. River inflow, groundwater recharge and flow, and agricultural productivity will be modified to reflect proposed future development, as in Scenario B.

2 Current climate of the lower Gulf region

There is no primary literature specifically on the meteorology or climatology of the Gulf region. Section 2.1 furnishes an overview of these topics, to provide context for the subsequent discussion of specific climatic variables.

2.1 Climate of northern Australia

2.1.1 KEY FACTORS CONTROLLING AUSTRALIA'S CLIMATE

The primary characteristics of Australia's climate are generally considered to be a consequence of four major inter-related factors (Hobbs, 1998):

1. Its location within the subtropical pressure zone. Australia's landmass is centrally located within the dry descending air of the Hadley cell circulation. This results in much of the continent being affected by large eastward travelling anti-cyclones (Figure 2-1). These high pressure systems, which may extend up to 4000 kilometres along their west-east axes, are responsible for the high temperatures and dryness that characterise much of the continent. Systems generating moisture occur either between individual anti-cyclones or to the north or south of them (Warner, 1986).
2. The size, shape and latitudinal range of the Australian continent. This has resulted in a broad range of climates.
3. The subdued relief (flatness) of the continent provides little obstruction to the controlling atmospheric systems. The exception is the Great Dividing Range along the east coast of Australia.
4. Australia's long coastlines and vast expanses of ocean to the east, west and south ensure that much of the continent is subject to maritime influences.

To these can be added factors such as the inter-annual variability of the Walker Circulation, the Inter-Tropical Convergence Zone (ITCZ) and the El Niño Southern Oscillation (ENSO) phenomenon. The net effect of these factors is the large semi-arid/arid zone, moderate to high seasonal variation and high inter-annual variability (Hobbs, 1998) for which Australia is renowned. To the south of the arid centre (Köppen class B) the climate is Mediterranean (Köppen class Cs); to the north the climate is tropical (Köppen class A) and is characterised by highly seasonal, summer dominated rainfall and year round high temperatures and potential evaporation rates (Köppen 1936).

Figure 2.1 Morning Glory cloud formation taken from a plane near Burketown. The southern Gulf of Carpentaria is the only location in the world where this rare meteorological phenomenon is known to occur on a semi-regular basis. Source: Mick Petrov

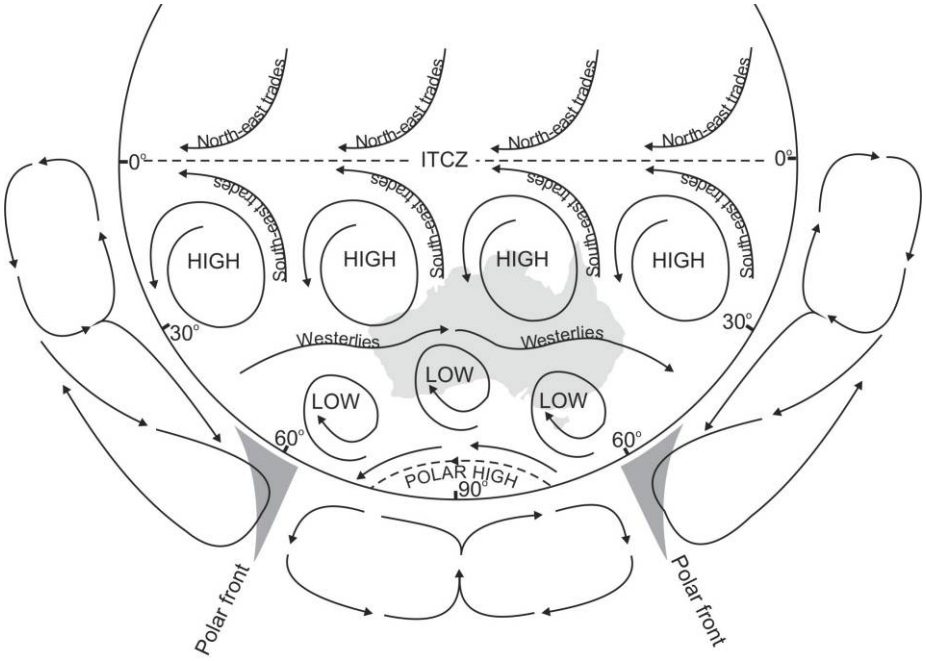

Figure 2.2 Three cell circulatory model (adapted from BoM 1989)

2.1.2 GENERAL CIRCULATION OVER NORTHERN AUSTRALIA

Between the months of December and April in the southern hemisphere, a broad area of low atmospheric pressure known as the ITCZ (also known as the monsoon, equatorial trough or thermal equator), moves south of the equator and intermittently crosses the northern shores of Australia (Figure 2.3). When this trough comes close to or crosses over land it brings humid conditions with showers, thunderstorms and widespread rain to northern Australia. The shallow and unstable air associated with the north-westerly monsoonal flow does not penetrate deep inland and generally favours the development of thunderstorms in inland areas. This can result in heavily localised rainfall and across most of northern Australia average rainfall declines away from the coast. Throughout the course of a wet season the location of the monsoon trough varies, and those periods where it temporarily retreats north of the Australian coastline are referred to as 'inactive' periods. Following a prolonged 'build-up' period, a typical northern wet season is comprised of two or three active/inactive cycles, each full cycle lasting between four to eight weeks (BoM, 1998). Inactive periods are usually of longer duration than active periods. The Madden-Julian Oscillation (MJO) provides a measure of the major fluctuations in tropical weather on weekly to monthly timescales.

The position and timing of the trough is highly variable from one wet season to another (Bonell et al., 1983). Monsoon circulation usually starts abruptly at any time from late November to mid-January. The season can last for as little as two weeks or as long as four months, with break periods in most seasons, when dry south-easterlies are temporarily re-established (Hobbs, 1998). In those years where the monsoonal trough does not extend over northern Australia, 'well organised rainfall' (i.e. widespread, as opposed to localised and spatially variable convective rainfall) does not occur. The monsoonal rains associated with the ITCZ are also supplemented by heavy and often widespread rainfall from tropical cyclones originating from the seas to the north and north-east of the Gulf region (Section 2.1.3). Tropical depressions and tropical cyclones are frequently associated with the active phase of the monsoon cycle. The mean withdrawal date of the summer monsoon is 7 March but has varied from 1 January to 6 April, and can be identified by an increase in low-level easterlies over northern Australia (Hobbs, 1988).

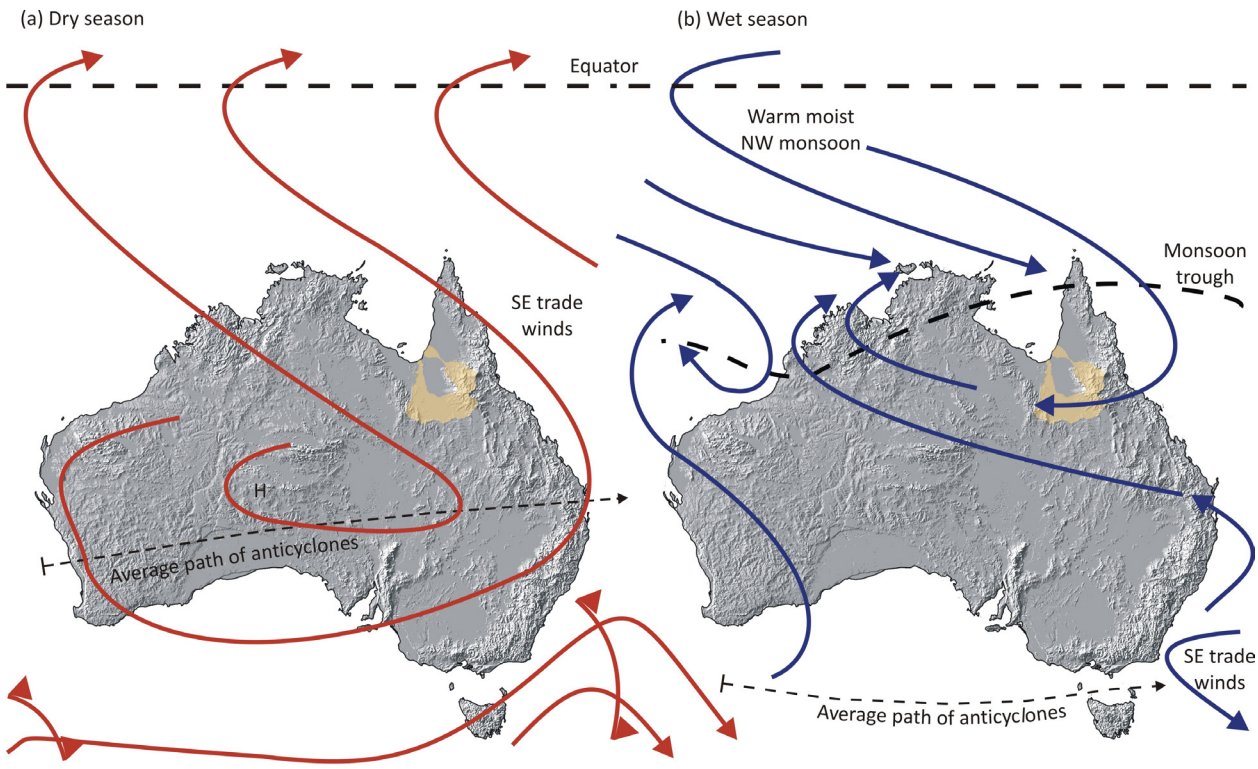

Figure 2.3 Typical synoptic systems during a) mid-dry season; and b) mid-wet season overlain on a shaded relief map of Australia. Flinders and Gilbert catchments shown by light brown shading. Adapted from BoM, 1998, Warner, 1986 and Petheram and Bristow, 2008.

During June to September the ITCZ follows the summer sun, moving north of the equator; high pressure cells also move northward (Figure 2.3). The withdrawal of the summer monsoon is associated with a reversal of the zonal wind direction (from westerly to easterly) and south-east trade winds gradually occupy tropical Australia. North of 30 degrees and south of 14 degrees (i.e. where the Great Dividing range lies adjacent to the Queensland coast), orographic uplift of the south-east trade winds results in year round rainfall and high rainfall totals along the north Queensland coast, particularly between Cardwell and Cooktown (Figure 2.3) where the ranges are very steep and fringe the coast (Sumner and Bonell, 1986). On the western side of the range there is a very steep declining rainfall gradient. In the Flinders and Gilbert catchments this results in the headwater catchments having slightly higher wet and dry season rainfall totals than the mid-catchment reaches. Having lost most of their moisture the trade winds then sweep across the rest of the Gulf region, resulting in mainly mild, dry south-easterlies over the Assessment area during the dry season.

2.1.3 TROPICAL CYCLONES AND TROPICAL DEPRESSIONS

The Bureau of Meteorology (BoM, 1978) defines a tropical cyclone as “a non-frontal synoptic scale, cyclonic rotational, low pressure system of tropical origin, in which ten minute mean winds of at least gale force (63 km/hr) occur, the belt of maximum winds being in the vicinity of the system’s centre”. By this definition many systems would not be classified as hurricanes or typhoons (wind speeds of 120 km/hr or greater), but rather as tropical or monsoonal depressions. The Bureau of Meteorology (BoM, 1972) definition of a tropical or monsoon depression is “a closed cyclonic rotational system of tropical origin in which mean winds at any point within the closed system do not exceed gale force”.

Tropical cyclones generally occur between latitudes 10°S and 25°S in the Southern Hemisphere, with 90% of cyclones occurring between 1 December and 30 April (Hobbs, 1998). The frequency of occurrence and tracks vary greatly from one year to the next (Figure 2.4) and the number of tropical cyclones in the Australian region is in part influenced by the ENSO. ENSO is caused by a complex and unstable interaction

between the ocean and atmosphere over the tropical Pacific Ocean (IPCC 2001), and influences climatic variation by irregularly oscillating between two modes, La Niña (Spanish for little girl) and El Niño (Spanish for little boy). Typically there are lower cyclone numbers during El Niño events. Figure 2.4 shows the average annual number of tropical cyclones in the Australian region in El Niño years and La Niña years (neutral years are not shown). For those systems affecting the Flinders and Gilbert catchments favoured regions for tropical cyclogenesis are in the Coral Sea and western Gulf of Carpentaria, though all tropical waters have the potential for tropical cyclone development (Figure 2.4).

Although cyclones are one of nature's most destructive phenomena, they rapidly weaken when they cross the coast from sea to land and become a rain depression. While this reduces the likely damage from strong winds, it does bring the risk of flood. While many tropical depressions along the north-east Queensland coast and in the Gulf of Carpentaria do not fully develop into tropical cyclones, they are typically accompanied by large-scale convection and heavy rain, which can make a significant contribution to wet season rainfall. It is rare that a storm crosses the Cape York Peninsula to enter the Gulf of Carpentaria (Hobbs, 1998).

The key regional centres in the Flinders catchment (i.e. Hughenden, Richmond, Julia Creek and Cloncurry) and Gilbert catchment (i.e. Georgetown, Einasleigh, Forsayth and Mount Surprise) are buffered to some extent from damaging winds by their distance from coast (Figure 2.4).

Potential changes in tropical cyclone numbers and intensity under possible future climates is discussed in CSIRO, 2007.

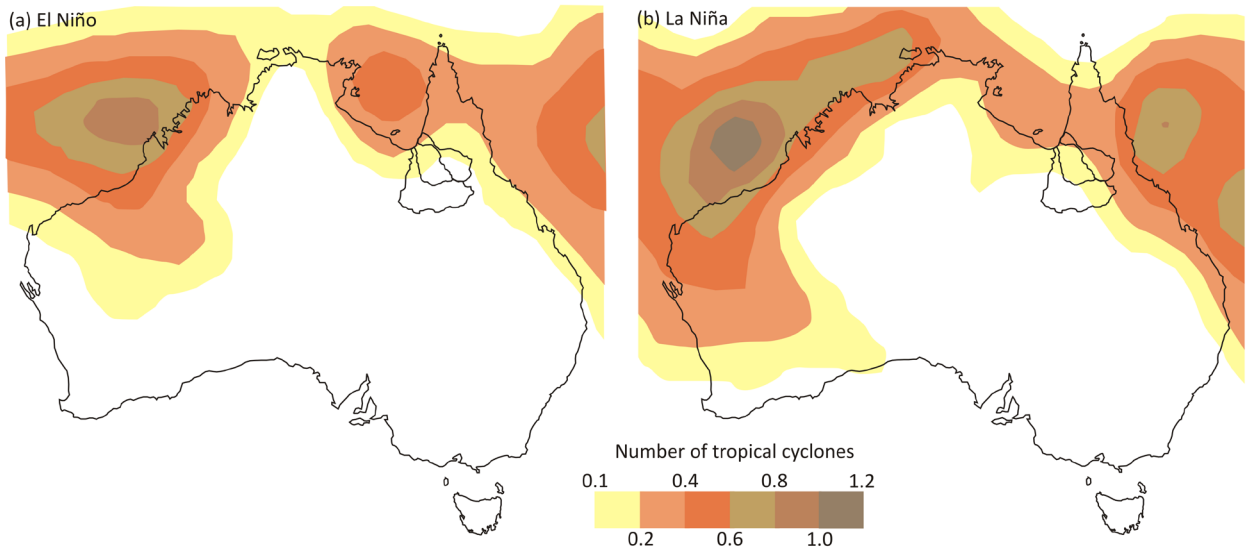

Figure 2.4 Average annual number of tropical cyclones in the Australian region in (a) El Niño years; (b) La Niña years. Adapted from Bureau of Meteorology cyclone maps http://www.bom.gov.au/jsp/ncc/climate_averages/tropical-cyclones/index.jsp

2.2 Rainfall

Over the historical period (i.e. 1 July 1890 to 30 June 2011) the mean annual rainfall spatially averaged across the Flinders and Gilbert catchments is 492 mm and 775 mm respectively. In the Flinders catchment mean annual rainfall varies from about 800 mm at the coast to about 350 mm in the south. In the Gilbert catchment mean annual rainfall varies from about 1050 mm at the coast to about 650 mm in the south-east of the catchment. As mean values can often be skewed by outlying values, it can be more informative to consider median values. In the Flinders and Gilbert catchments the spatially averaged median annual values of rainfall are 454 mm and 739 mm respectively.

In the Flinders catchment the low relief and low elevation mean that rainfall typically increases in a northerly direction (Figure 2.5), as the more northerly regions are more likely to be affected by the

monsoon trough and are closer to the coast. The exception is in the eastern headwaters of the Flinders catchment where modest topography corresponds with slightly elevated rainfall totals during the wet and dry season. This area also receives more rainfall from systems originating in the Coral Sea than the more westerly areas of the catchment. During the dry season rainfall generally decreases in a northerly direction because the south-east trade winds rapidly lose their moisture as they cross the Great Dividing Range and sweep across the Gulf (Figure 2.7).

Rainfall in the Gilbert catchment typically increases in a north-easterly direction i.e. towards the equator and the coast. The Gilbert catchment appears to have more complex rainfall patterns than the Flinders, probably due in part to the moderate relief causing local scale topographic effects.

Eighty-eight and ninety-three percent of rainfall in the Flinders and Gilbert catchments respectively falls during the wet season.

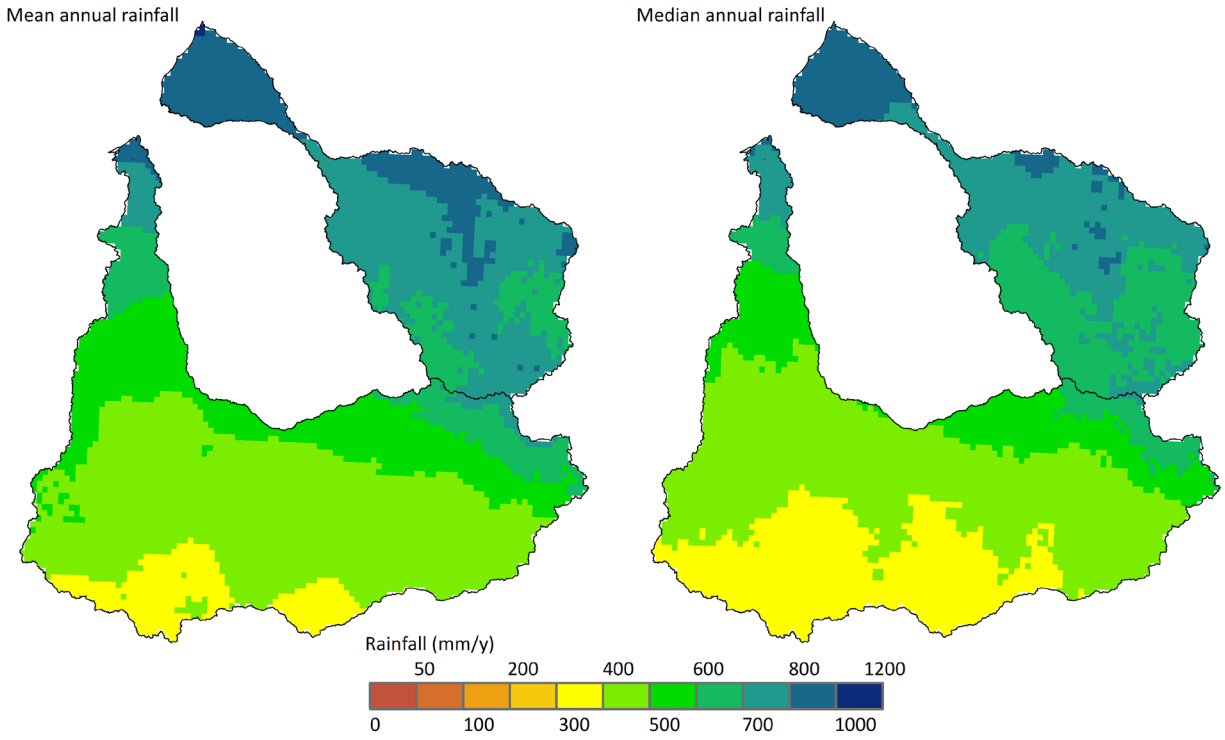

Figure 2.5 Historical mean annual rainfall (left) and median annual rainfall (right) in the Flinders and Gilbert catchments

Figure 2.6 Gilbert River during the dry season (Gilbert catchment). Source: CSIRO

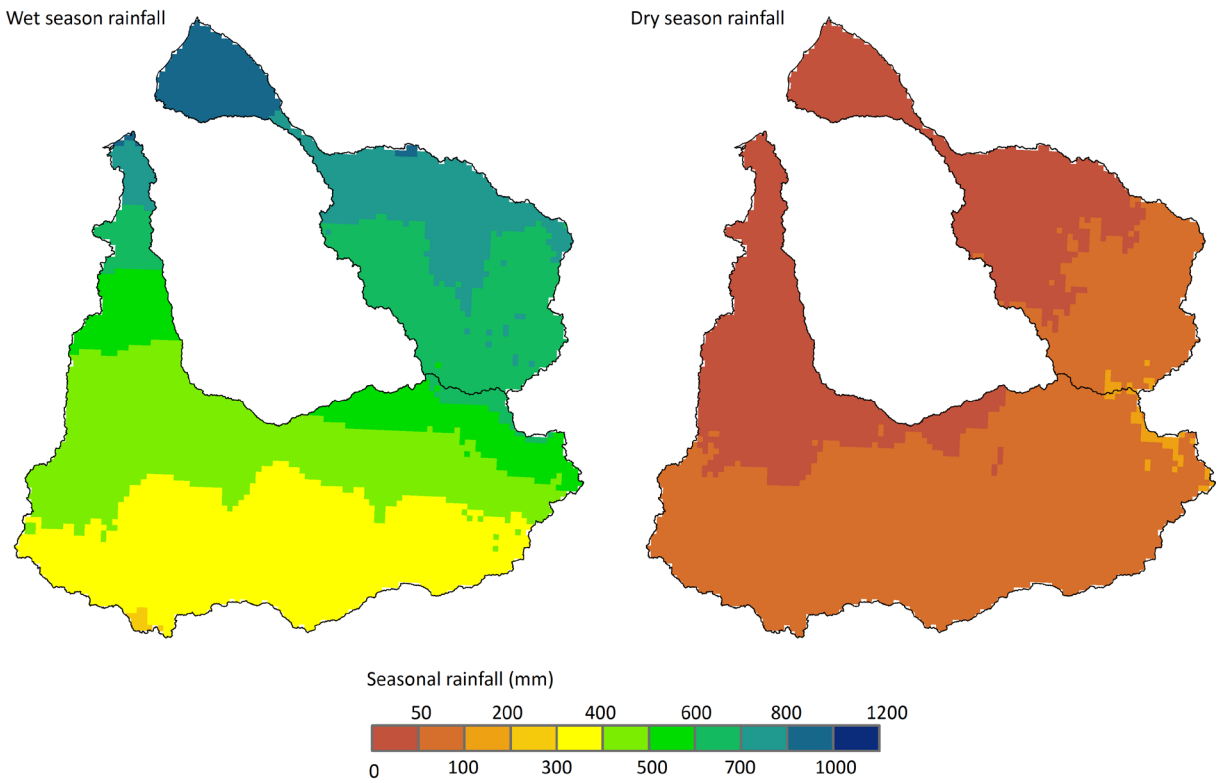

Figure 2.7 Historical mean wet season (left) and dry season (right) rainfall in the Flinders and Gilbert catchments

The highest median monthly rainfall in both the Flinders and Gilbert catchments occurs during January and February, which have median monthly values of about 100 and 200 mm respectively. The months with the lowest median rainfall are July and August, with about 0.5 mm across both catchments (Figure 2.8).

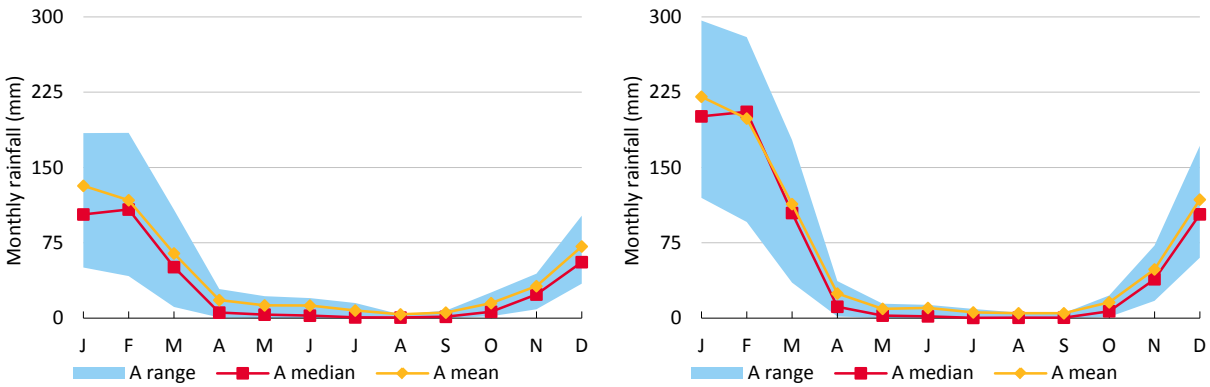

Figure 2.8 Historical monthly rainfall averaged over the Flinders (left) and Gilbert (right) catchments (A range is the 20th to 80th percentile monthly rainfall)

2.2.1 RAINFALL INTENSITY

Rainfall intensity (defined here as amount of rainfall per wet day) in northern Australia is considerably higher than in southern Australia (Leeper, 1970), and is considered very high on a global level. For example, Jackson (1986) found that for the whole of northern Australia, except the north-east coast, rainfall is more concentrated, with fewer rain days and higher mean daily intensities than one would predict from its monthly totals when compared to other tropical regions around the world. This is thought to be due to the importance of tropical cyclones to monthly rainfall for much of northern Australia. High intensity rainfall can have serious implications for the erosivity of rain events in an agricultural context. In the Flinders and

Gilbert catchments rainfall intensity typically increases towards the coast (Figure 2.9). Figure 2.9 shows the percent of days that daily rainfall is exceeded.

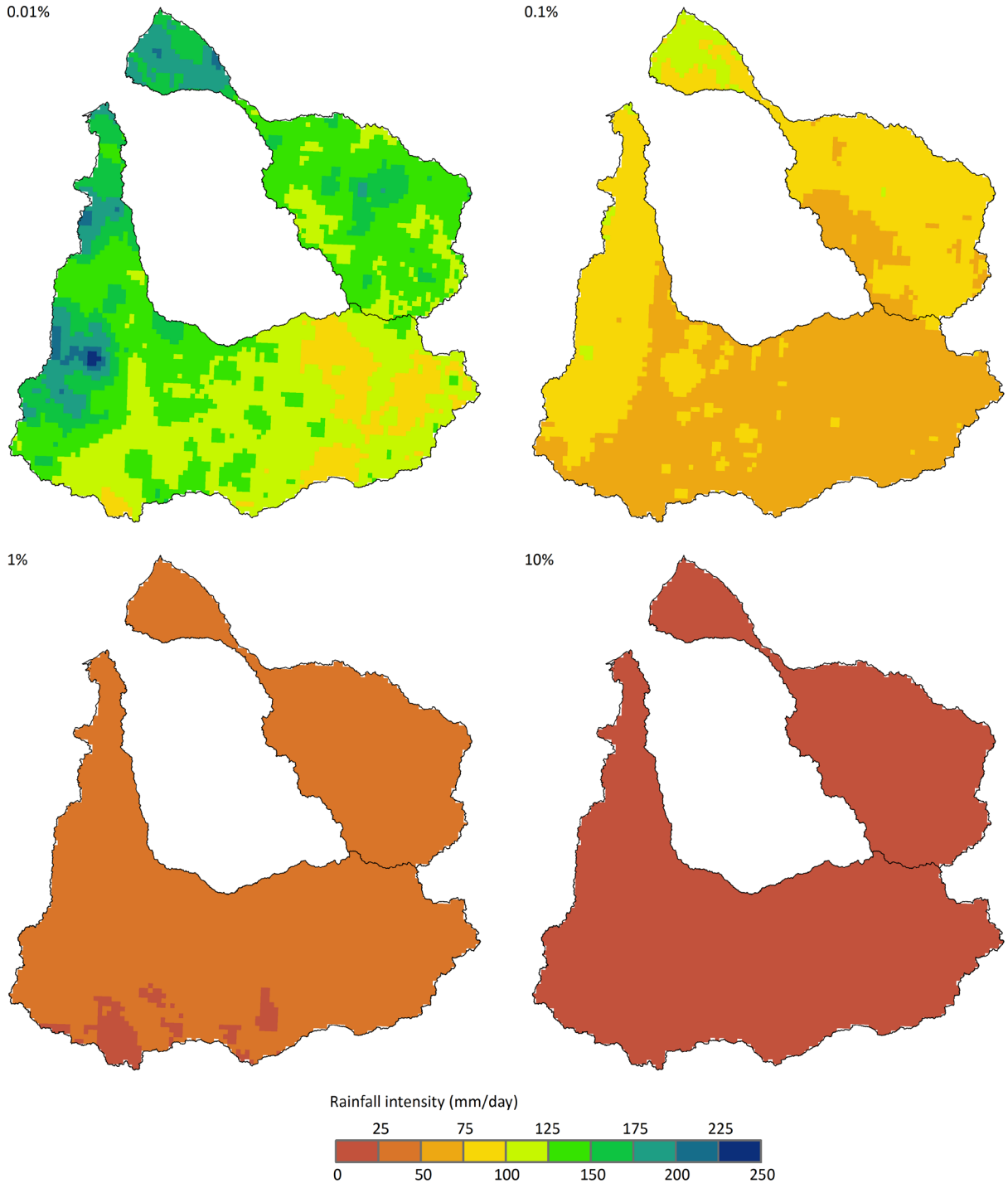

Figure 2.9 The daily rainfall that is exceeded in 0.01%, 0.1% 1% and 10% of days in the Flinders and Gilbert catchments

2.3 Seasonal, intra-decadal, inter-decadal variability and long term trends in rainfall

Climatic variability is a natural phenomenon that occurs at a variety of timescales, ranging from daily (e.g. diurnal variation in the weather) to intra-annual (e.g. seasonal variation), and even to many millennia (e.g. Milankovitch cycles caused by variations in the earth's orbit). A climatic trend is a long-term shift or change in climate after variability mechanisms operating at shorter time scales have been accounted for. They may be due to processes (that have always been present) that operate over very long time scales, or they may be the result of a 'changing' climate.

The variability in rainfall is one of the defining traits of the Australian climate and has been the source of much discussion (e.g. Leeper, 1970; McBride and Nicholls, 1983; Peel et al., 2002): it has even influenced popular folk literature such as that of Banjo Patterson and has been immortalised in the lyrics of songs and poems such as those by Dorothea Mackellar.

In this section a statistical method referred to as Ensemble Empirical Mode Decomposition (EEMD) (Peel et al., 2011a,b) was undertaken for the Assessment by Professor Tom McMahon and Dr Murray Peel of the University of Melbourne. The purpose was to examine the proportion of variance in the historical monthly time series of rainfall that is due to different frequency fluctuations and to evaluate whether there is a residual trend in rainfall. Here the method of Peel et al. (2011a) was applied to 121 years of monthly rainfall data from two stations in the Flinders catchment (i.e. Richmond and Cloncurry) and one station in the Gilbert catchment (i.e. Georgetown) and one station in the Norman catchment (i.e. Croydon).

2.3.1 ENSEMBLE EMPERICAL MODAL DECOMPOSITION

EEMD is an adaptive form of time-series decomposition for non-linear and non-stationary data, and is therefore appropriate for time-series of monthly and annual rainfall. It decomposes a time series into a set of Intrinsic Mode Functions (IMFs), which represent progressively lower frequency fluctuations within the time series, and a residual trend. EEMD analysis allows one to determine the average period (pseudo-cyclicity) for each IMF and the variance associated with each IMF (and the residual). If the IMFs and residual are summed they form the original time series.

Figure 2.10 shows the first six IMFs for the EEMD analysis of Richmond rainfall. These figures are representative of the IMFs from the other three stations.

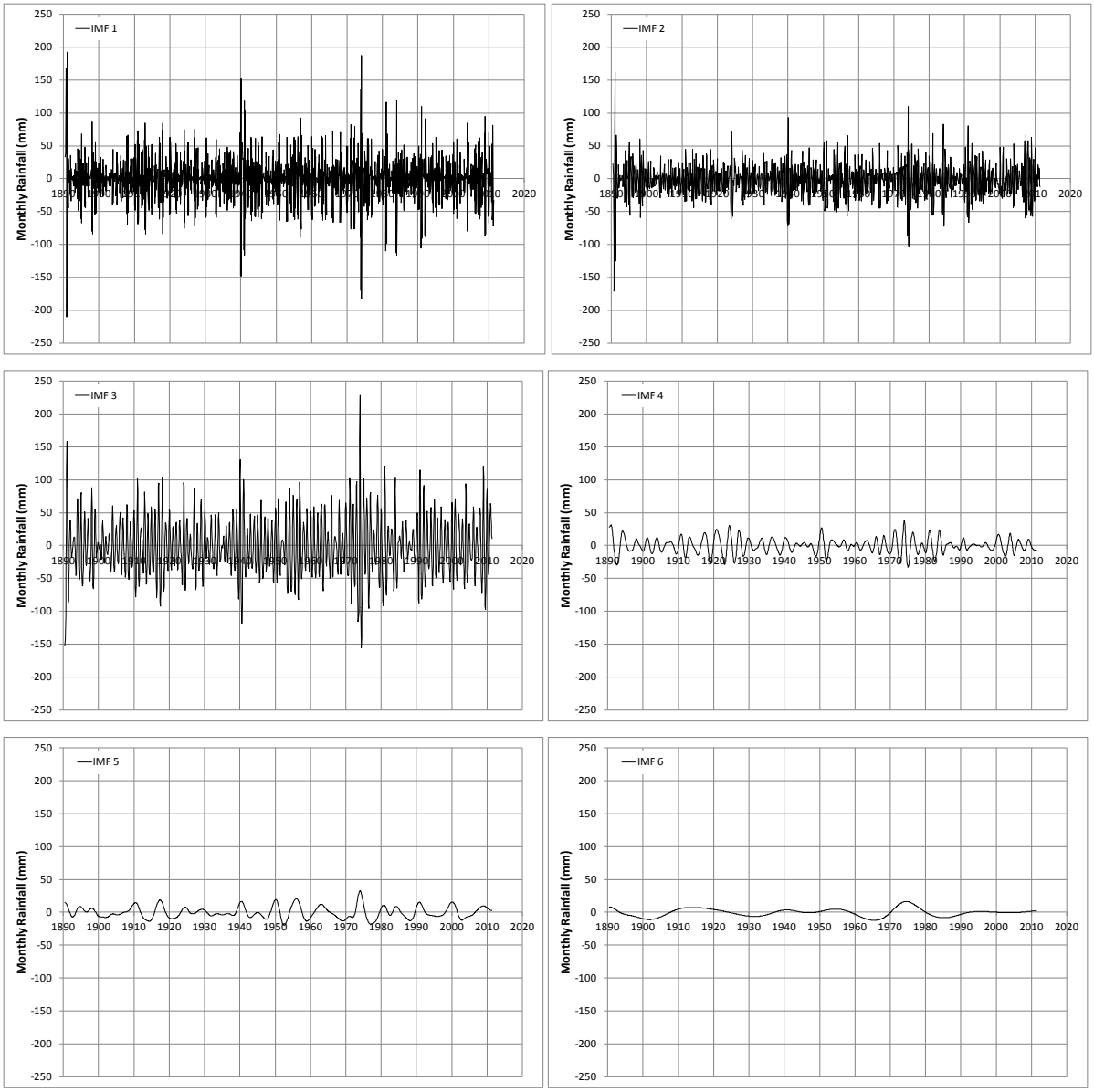

Figure 2.10 Monthly time series of EEMD IMFs for Richmond rainfall

Figure 2.11 shows the time series of raw monthly rainfall and EEMD residual (trend) for the four stations. All four stations show an increasing trend with time that varies from +4.5 to +14.5% over the length of the records. As can be seen in Table 2.1 the highest variance was observed in IMF3 which, at an average period of 12 months, is likely to be representative of the annual cycle.

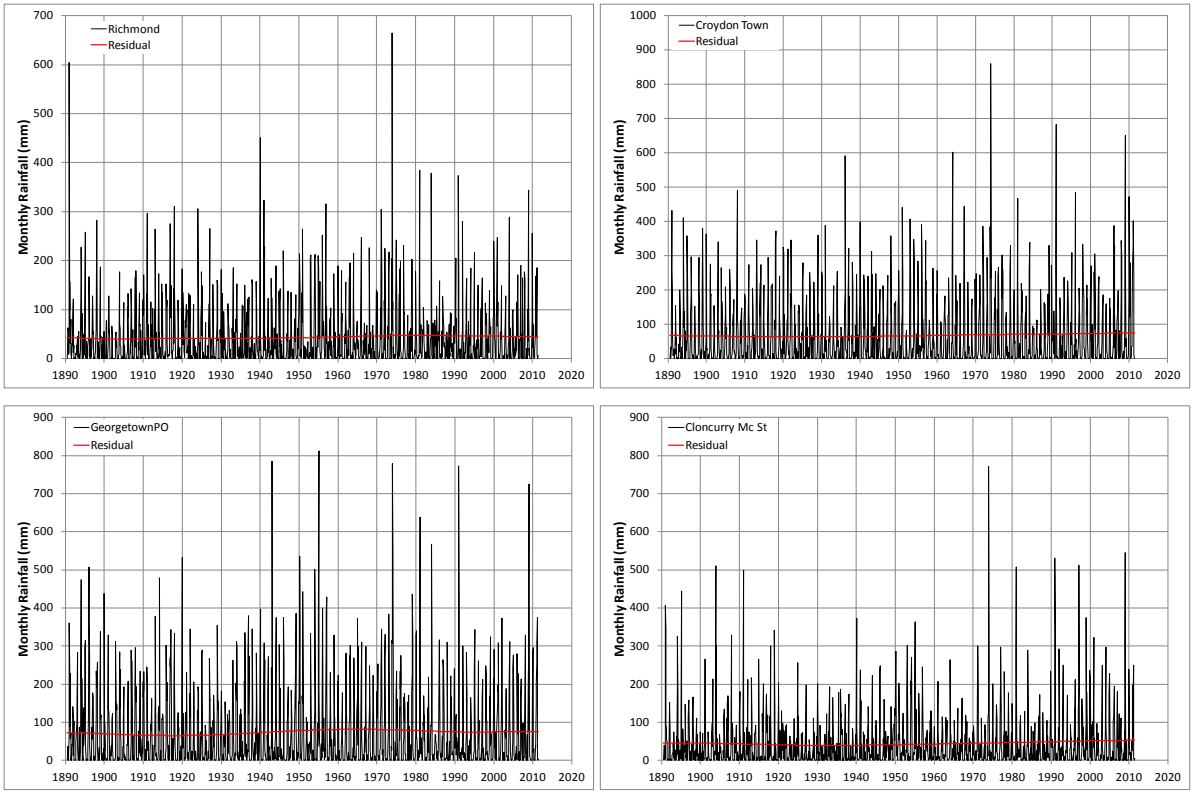

Figure 2.11 Monthly rainfall and residual trend at (clockwise from top left) Richmond, Croydon, Cloncurry and Georgetown.

Table 2.1 Average period (months) and monthly variance (mm2) of EEMD IMFs

STATION		IMF1	IMF2	IMF3	IMF4	IMF5	IMF6	IMF7	Residual
Richmond	Period	3.3	5.84	11.95	34.99	96.8	242		
	Var.	1246	564	1870	131	79	35		6
Croydon Town	Period	3.51	5.91	12.05	18.15	37.71	88	290.4	
	Var.	1849	1223	3783	445	212	164	62	11
Georgetown PO	Period	3.41	5.88	12.05	21.83	82.97	290.4		
	Var.	2377	1488	4435	1027	232	70		28
Cloncurry Mc St	Period	3.31	5.6	12.05	35.85	76.42	290.4		
	Var.	1476	712	2354	201	109	47		16

Collectively the first three IMFs accounted for between 85.9 to 93.6% of the variance within the four rainfall time series (Table 2.1). These IMFs represent the annual cycle and within year variability. Hence for these four stations multi-annual variability represents a small component of the total time series variability.

The resulting IMFs were compared against EMD decompositions of white noise replicates (not shown) of the same length and variance as the original rainfall time series in order to identify IMFs that are significantly different from a white noise process (see Peel et al. 2011b). At all four stations the only IMFs to be significantly different to white noise (i.e. from chance) are those representing the annual (12 month) cycle, which in each case was IMF 3.

In summary this analysis shows that the variability within the monthly rainfall time series is strongly dominated by the annual cycle. This analysis also indicated that over the last 121 years there has been a slightly increasing trend in rainfall.

2.3.2 INTER-ANNUAL VARIABILITY IN RAINFALL AND TEMPORAL PATTERNS IN RAINFALL

Although multi-annual variability represents a small component of the total monthly time series variability in the Gulf region (Section 2.3.1), the historical annual rainfall series for the Flinders and Gilbert catchments shows considerable variation between years (Figure 2.12). The highest catchment average annual rainfalls in the Flinders (1310 mm) and Gilbert (2187 mm) occurred in 1974, and were nearly three times the median annual rainfall values (i.e. 454 mm and 739 mm respectively). The ten year running mean provides an indication of the longer term variability. In the Flinders catchment the 10 year running mean annual rainfall varies from 367 mm to 629 mm. In the Gilbert catchment it varies from 631 mm to 1011 mm (Figure 2.12).

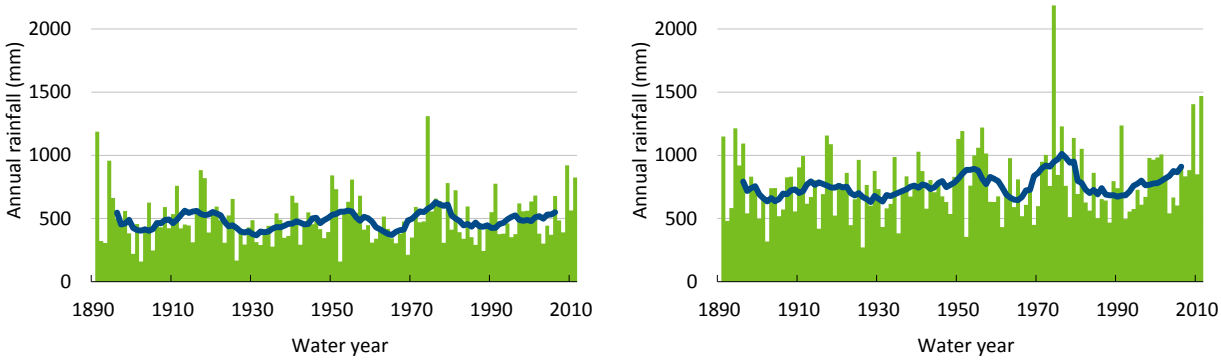

Figure 2.12 Historical annual rainfall averaged over the Flinders (left) and Gilbert (right) catchments. The low-frequency smoothed line is the 10 year running mean

The coefficient of variation (Cv) of annual rainfall (i.e. the standard deviation of mean annual rainfall divided by the mean annual rainfall) provides a measure of the temporal variability of annual rainfall. The larger the Cv value, the larger the relative variation in annual rainfall. Figure 2.13 shows that for a given mean annual rainfall the Cv of annual rainfall in the Flinders and Gilbert catchments is higher than most other rainfall stations around Australia with the same mean annual rainfall.

Further, Petheram et al., (2008) observed that for a given mean annual rainfall total, the inter-annual variability of rainfall in northern Australia is higher than that observed at rainfall stations from the rest of the world for the same Köppen climate types. In the Flinders and Gilbert catchments the Cv of annual rainfall is typically between 0.4 and 0.5, and between 0.3 and 0.4, respectively. Stations from the rest of the world of the same Köppen climate type and mean annual rainfall typically exhibit a Cv of annual rainfall between about 0.2 and 0.35.

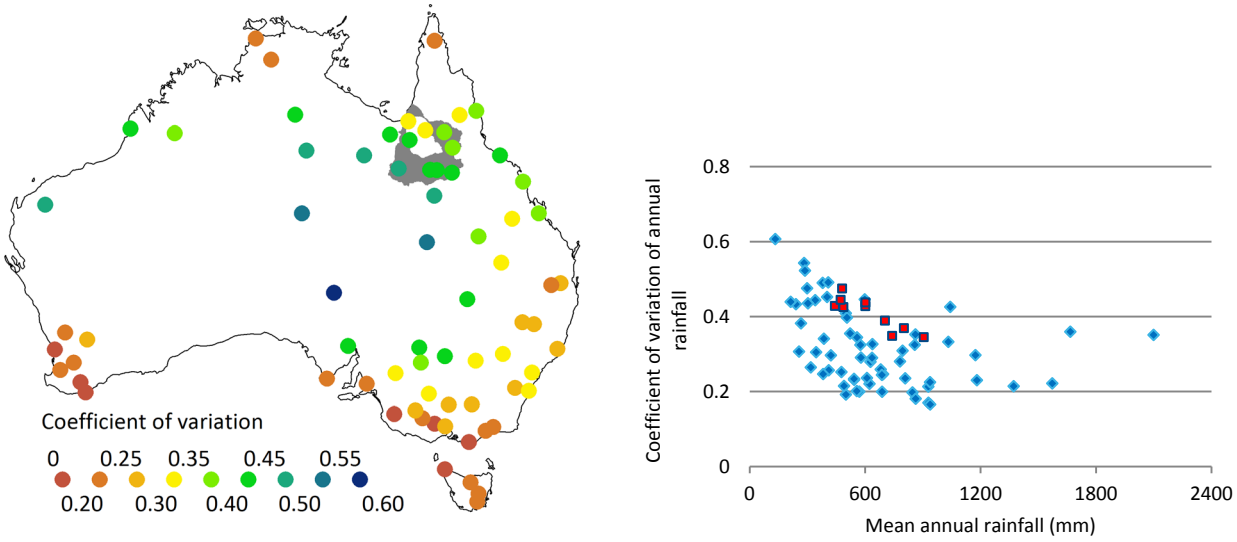

Figure 2.13 (Left) Coefficient of variation of annual rainfall for 71 rainfall station from around Australia. The grey polygons indicate the extent of the Flinders and Gilbert catchments. (Right) The coefficient of variation of annual rainfall plotted against mean annual rainfall for 71 rainfall stations from around Australia. Red squares indicate rainfall stations within 100km of the Flinders and Gilbert catchments

Values for the Cv of annual rainfall values across the Flinders and Gilbert catchments are shown in Figure 2.15a. Figure 2.15b shows the maximum number of consecutive years that rainfall was below the median value over the historical record.

Percent exceedance maps of annual rainfall for the Flinders and Gilbert catchment are shown in Figure 2.16 and demonstrate the large difference in the highest (10th percentile) and lowest (90th percentile) 10% of years. Additional annual rainfall percent exceedance maps are shown in Appendix B.

Figure 2.14 Einasleigh River downstream of Mount Adler (Gilbert catchment). Source: CSIRO

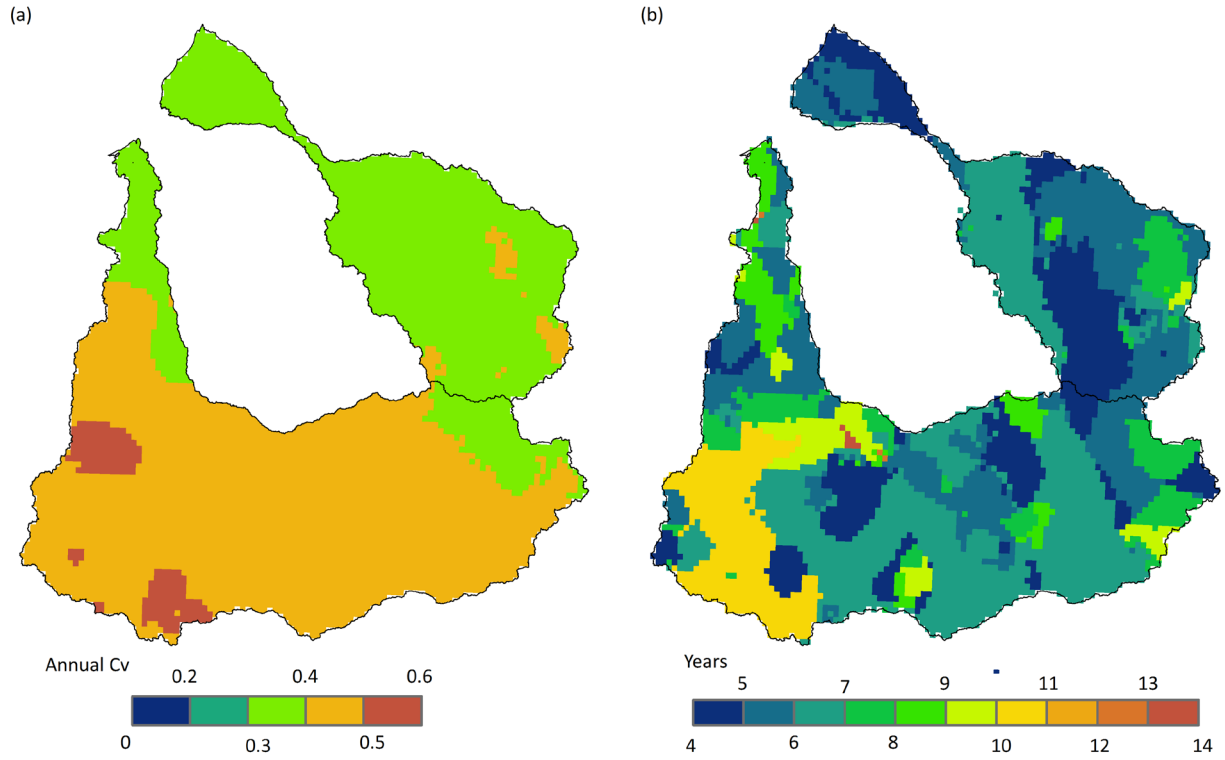

Figure 2.15 Historical (a) coefficient of variation of annual rainfall and (b) maximum number of consecutive years of below median rainfall for the Flinders and Gilbert catchments

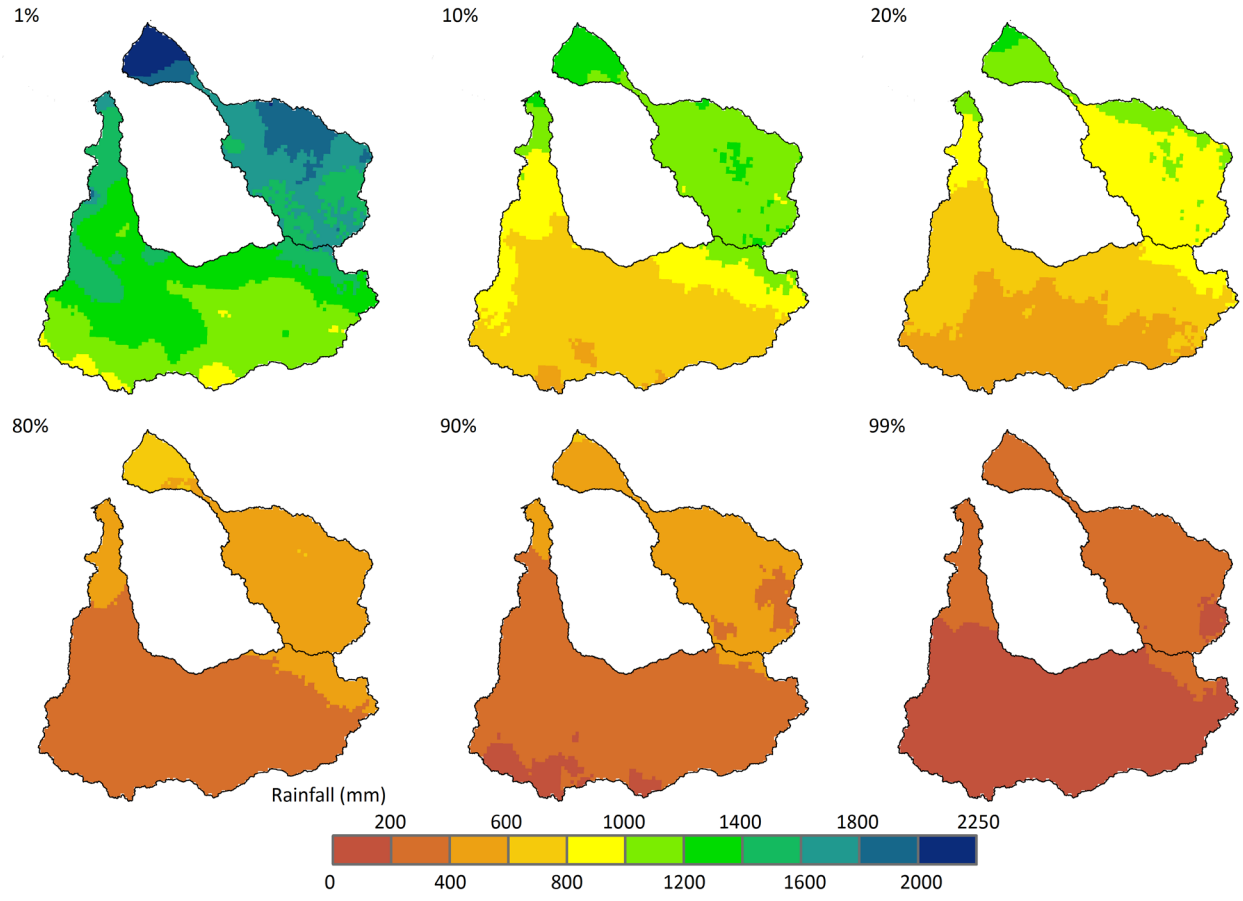

Figure 2.16 The annual rainfall that is exceeded in 1%, 10%, 20%, 80%, 90% and 99% of years in the Flinders and Gilbert catchments

There are several factors driving this high inter-annual variation in Australia's climate, including the El-Niño-Southern Oscillation (ENSO), the Indian Ocean Dipole, the Southern Annular Mode, the Madden-Julian Oscillation and the Inter-decadal Pacific Oscillation (IPO).

Of these influences, the ENSO is a phenomenon that is considered to be the primary source of global climate variability over the 2-6 year timescale (Rasmusson and Arkin, 1993) and is reported as being a significant cause of climatic variability for much of eastern and northern Australia. One of the modes of ENSO, El Niño, has come to be a term synonymous with drought in the western Pacific and eastern and northern Australia. Rainfall stations along eastern and northern Australia have been observed to have a strong correlation (0.5 – 0.6) with the Southern Oscillation Index (SOI) during spring (McBride and Nicholls, 1983). The implications of this are that rainfall stations that demonstrate a consistent relationship with ENSO have been found to have a higher inter-annual variability of rainfall than those with a poor relationship (Nicholls, 1988; Peel et al., 2002).

It should be noted, however, that for the four rainfall stations examined in Section 2.3.1, no statistically significant inter-annual or inter-decadal cycle was detected in the historical monthly rainfall record. This highlights one of the complexities of climate science; that the factors influencing climatic variability are inter-related and the net effect of their contribution is not simply the sum of their individual contributions. Rather they exhibit non-linear behaviour, where variation induced by one process may simultaneously cause and be a consequence of variation induced by another. For example, the association between ENSO and the Australian climate is modulated by the IPO, a climate index that describes long-term variability. Power et al., (1999) found a strong association between the magnitudes of ENSO impacts during negative IPO phases, while positive IPO phases showed a weaker relationship. More recently Micevski et al., (2006) examined streamflow data along the east coast of Australia and found that the IPO modulated the flood risk in New South Wales and southern Queensland, with flood quantiles being increased by a factor of approximately 1.7 during IPO negative periods. It should be noted, however, that the authors did not find an association between the IPO and ENSO in streamflow data north of the Tropic of Capricorn.

2.3.3 WET AND DRY SPELLS

The Flinders and Gilbert catchments are characterised by irregular periods of consistently low rainfall when successive wet seasons fail, as well as the typical annual dry season. Runs of wet and dry years, referred to here as wet and dry spells, are shown as annual differences from the median rainfall for the Flinders and Gilbert catchments in Figure 2.17 and Figure 2.18 respectively. A spell of consistently dry years may be associated with drought (though an agreed definition of drought continues to be elusive).

In these figures it can be seen that there were long runs of dry years centred around 1930 and 1960 in both catchments.

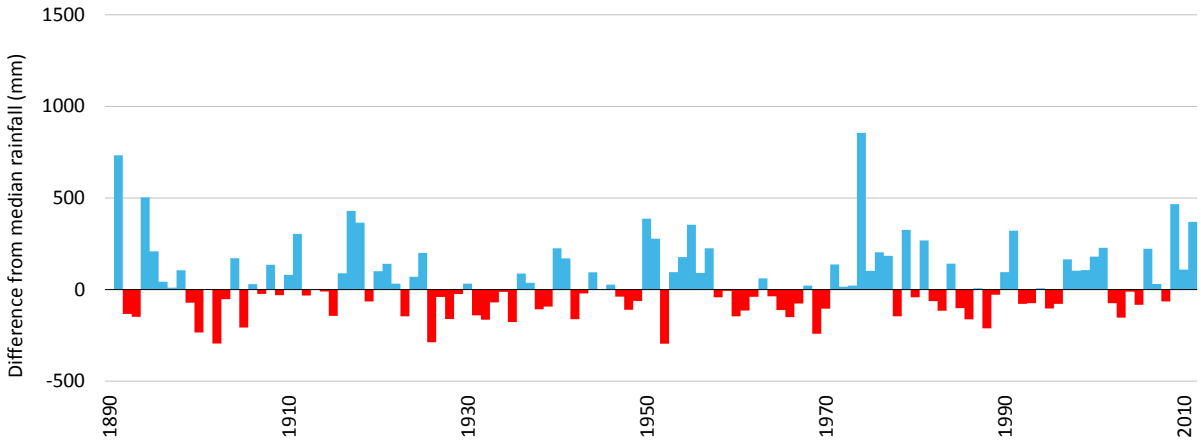

Figure 2.17 Runs of wet (blue columns) and dry (red columns) years in the Flinders catchment

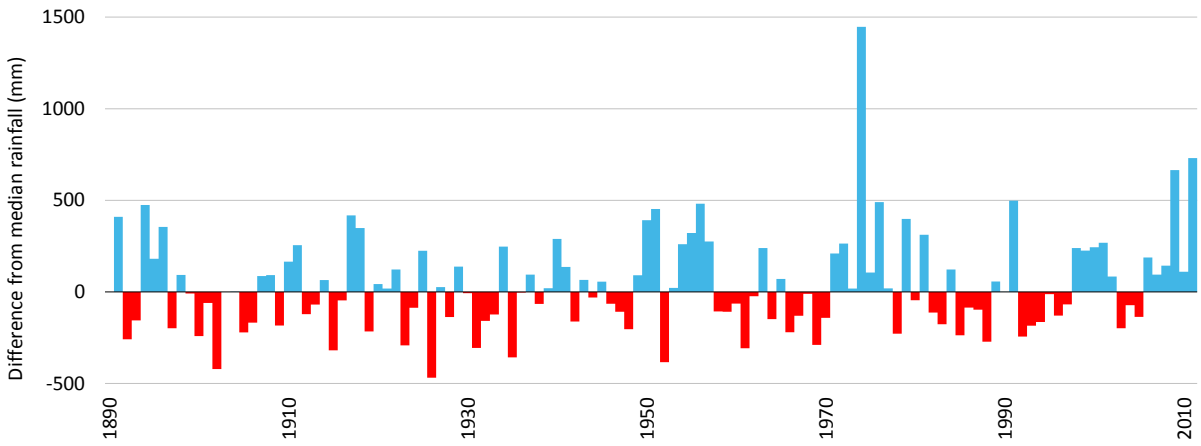

Figure 2.18 Runs of wet (blue columns) and dry (red columns) years in the Gilbert catchment

To enable the characteristics of wet and dry spells in the Flinders and Gilbert catchments to be compared to other parts of the country, the following sections examine the length, magnitude and severity of wet and dry spells for 71 rainfall stations across Australia (including six stations in the Flinders and Gilbert catchments). Rainfall stations were selected because each had near continuous data between 1890 and 2011. The run length and run magnitude of each rainfall station were summarised into a single number, to allow a simple comparison among stations.

Run length

Runs analysis, following the approach of Peel et al., (2004), is applied to annual rainfall data to describe and compare the length of wet and dry spells of rainfall stations in the Flinders and Gilbert catchments to stations elsewhere across Australia. In this analysis values that are equal to or below the median are defined as a dry year and values greater than the median are defined as a wet year. Run length is defined as a period of consecutive years of wet or dry.

Although the lag-one serial correlation (i.e. the correlation between consecutive values) is indicative of the run length behaviour of a time series, it does not completely determine run length behaviour. Peel et al., (2004) developed a metric (run length skewness (g)) that summarises the run length behaviour of a time series (Equation 1). This metric was calculated for each annual rainfall station for both wet (gwet) and dry (gdry) run lengths and provides a simple way of comparing rainfall stations in the Flinders and Gilbert catchments to rainfall stations elsewhere around Australia.

$$g = \frac{\sum_{i}^{j} a_i b_i^3}{N-1} \qquad (1)$$

where a_i is the frequency of run length b_i, j is the longest observed run length and N is the number of years.

The spatial distribution of run lengths for 71 long-term rainfall stations around Australia is plotted in Figure 2.19. In Figure 2.20 the run length behaviour is plotted against the lag-one serial correlation coefficient, with rainfall stations within 100 km of the Flinders and Gilbert catchments shown in red. The black lines in this figure indicate the 90% confidence interval, developed using a lag-one autoregressive (AR(1)) model as described by Peel et al., 2004. These confidence intervals provide an indication as to whether the run length skewness metric of a station is unusual given that stations lag-one serial correlation coefficient.

Based on the raw gwet and gdry values, the annual rainfall for stations in the Flinders and Gilbert tends to have equally long runs of dry and wet years and there is nothing unusual about their run length behaviour, i.e. the run lengths of rainfall stations in the Flinders and Gilbert catchments are well described by an AR(1) model (Figure 2.20). Figure 2.19 indicates that the run length of wet and dry years of rainfall stations in the Flinders and Gilbert catchments are comparable to rainfall stations along the east coast of Australia. Peel et

al., (2004) observed that for the two continents most affected by ENSO (Australia and South America), the ENSO-influenced rainfall stations displayed less bias towards longer runs than the non-ENSO-influenced stations. They concluded that stations influenced by ENSO are less likely to develop long runs equal to or below the median because ENSO variance is concentrated in the 2 to 6 year frequency band.

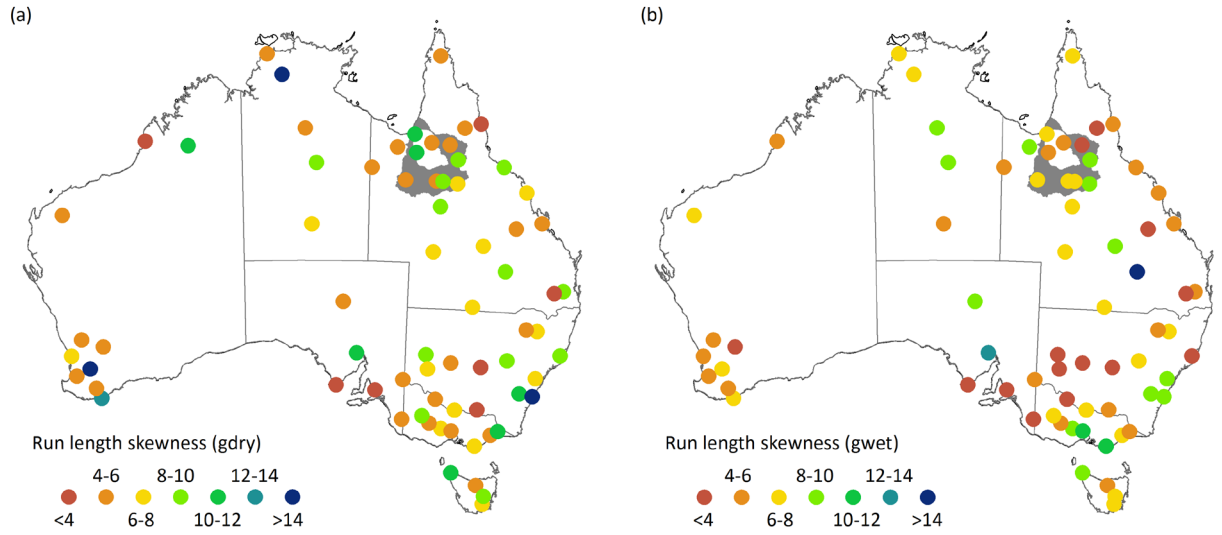

Figure 2.19 Run length skewness of dry and wet years for 71 rainfall stations around Australia

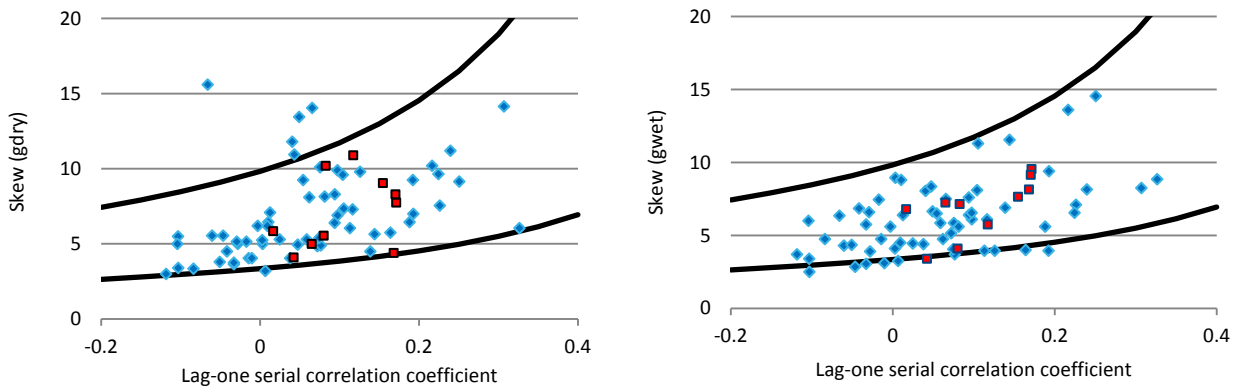

Figure 2.20 Run length of dry (left) and wet (right) years plotted against lag-one serial correlation coefficient for 71 rainfall stations around Australia. Red squares indicate rainfall stations within 100km of the Flinders and Gilbert catchments. The black lines indicate the 90% confidence limits developed by Peel et al., (2004)

Run magnitude

Run magnitude was assessed using the method of Peel et al., (2005), which utilises a measure of reservoir system vulnerability developed by Hashimoto et al., (1982), as a metric of run magnitude at each rainfall station. This metric is effectively the average of the largest negative deviation from the median in each run length event divided by the median annual rainfall. This metric has the useful feature of summarizing the run magnitude behaviour of all dry run lengths at a station into a single number ranging from 0 to 1, allowing simple comparison among stations.

The run magnitude of dry years at rainfall stations in the Flinders and Gilbert and the mid-latitudes of Australia appears to be generally larger than the run magnitude of dry years at most other rainfall stations in the south-east and south-west of Australia (Figure 2.21). This is expected, as run magnitude has been shown to be strongly correlated to the coefficient of variation of annual rainfall (Peel et al., 2005), and as shown in Figure 2.21.

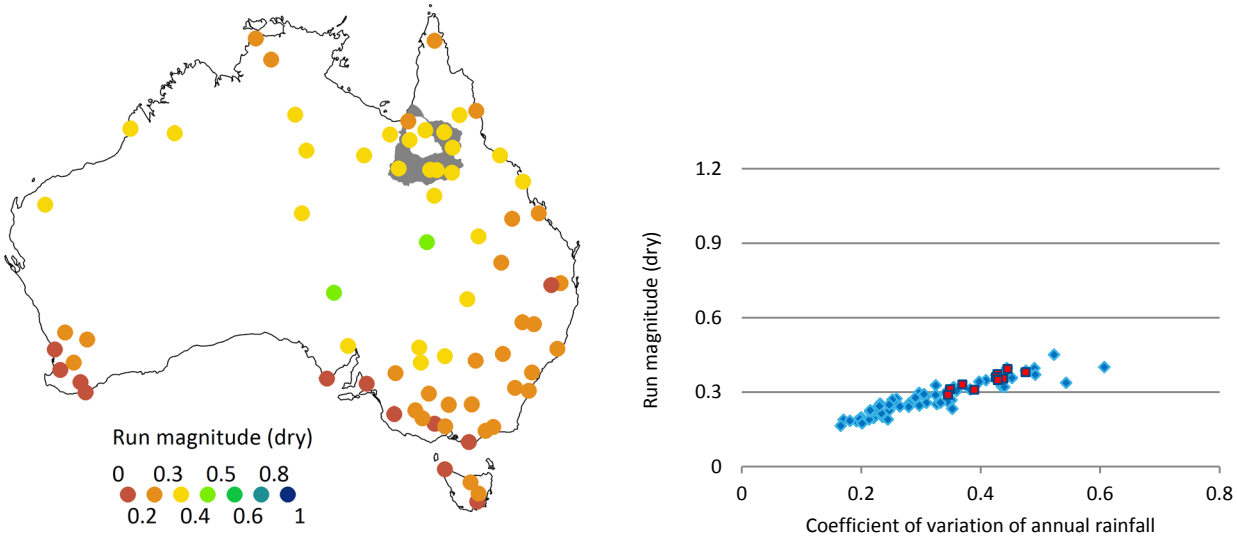

Figure 2.21 (Left) Run magnitude of dry spells for 71 rainfall stations around Australia. Grey shaded polygons illustrate the extent of the Flinders and Gilbert catchments. (Right) Run magnitude of dry spells plotted against the coefficient of variation of annual rainfall for 71 rainfall stations around Australia. Red squares indicate rainfall stations within 100 km of the Flinders and Gilbert catchments

Run severity

Run severity has been defined by Yevjevich (1967) and Dracup et al., (1980) as the sum of the negative deviations from a threshold (the median in this analysis) for a given length of negative deviations. They also noted that drought severity is the product of drought length (the period of negative deviations) and drought magnitude (the average of the negative deviations). Because the Flinders and Gilbert catchments had a normal dry run length and high dry run magnitude, the run severity of dry periods was also found to be high.

In other words, the Flinders and Gilbert catchments are likely to experience dry periods of greater severity than many centres in the south-east and south-west of Australia.

2.3.4 SPATIAL AND TEMPORAL CORRELATION OF RAINFALL ACROSS AUSTRALIA

It is unusual for the whole country to experience very high or very low rainfalls at the same time, with the possible exception of flood years like 1955 and 1974 and drought years like 1897, 1902 and 1905 (Hobbs, 1998). There are, however, numerous occasions in the instrumental record where one part of the country has experienced above average rainfall, and another sometimes adjacent region has experienced drought. From a national perspective, this regional 'climatic compensation' can help to mitigate national agricultural production risks.

Here the extent to which agricultural production in the Flinders and Gilbert catchments may help to mitigate the risk of low rainfall elsewhere in Australia is examined. The analysis for this is complex, but here we undertake a simple correlation analysis of annual rainfall mass residual curves (i.e. the cumulative sum of deviations from the median annual rainfall) to get an indication for how well stations around Australia are correlated to long term patterns in rainfall at Richmond in the Flinders catchment (Figure 2.22a) and to Georgetown in the Gilbert catchment (Figure 2.22b).

The results shown in Figure 2.22 indicate that the annual rainfall mass residual curves at stations in eastern and northern Australia are weak to moderately correlated, not unexpected given the moderately strong correlation of rainfall stations in eastern and northern Australia to ENSO (Section 2.3.2). Consequently, additional agricultural production potential in northern Australia will have a somewhat limited capacity at reducing agricultural production variations arising from drought in south eastern Australia.

An interesting observation is that annual rainfall patterns at Normanton (yellow circle in Gulf region, Figure 2.22) are not correlated to annual rainfall patterns measured at other rainfall stations in the Assessment area.

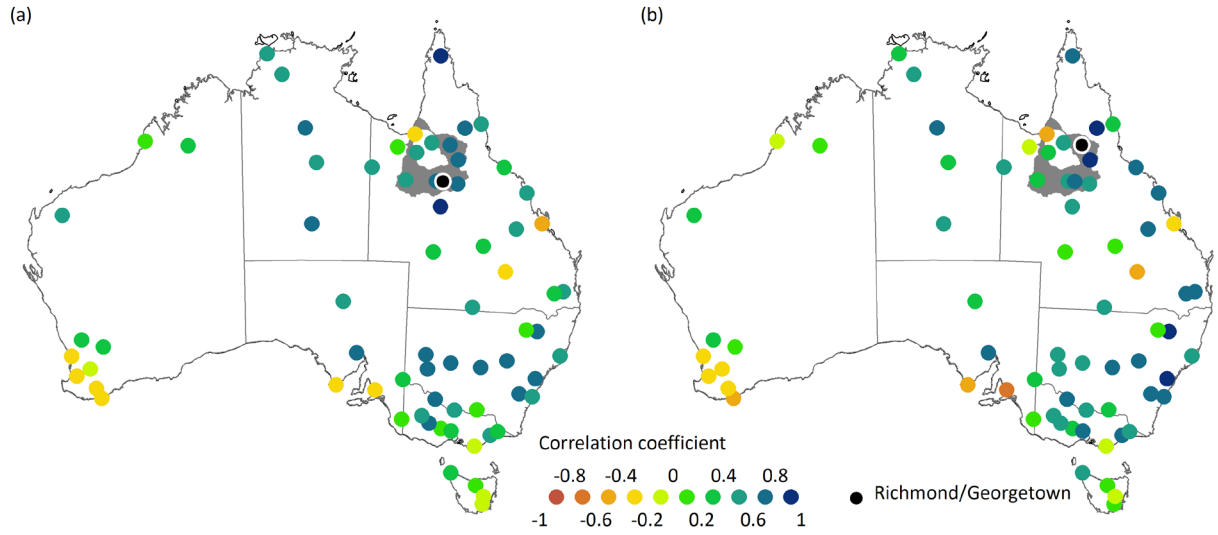

Figure 2.22 Temporal correlation of annual rainfall mass residual curves for 70 rainfall stations around Australia to the annual rainfall mass residual curves at (a) Richmond (black circle with halo on left); and (b) Georgetown (black circle with halo on right). The grey shaded polygons indicate the extent of the Flinders and Gilbert catchments

2.4 Other climatic parameters

Of all the climatic parameters affecting hydrology and agriculture, rainfall is usually the most important. Rainfall is the main determinant of runoff and recharge and is a fundamental requirement for plant growth. For this reason, reporting of climatic parameters is heavily biased towards rainfall data. Nevertheless other climatic parameters are important in agriculture. Prior to 1957 the SILO climate dataset used a variety of algorithms to synthetically generate non-rainfall parameter values based on the observed climate statistics between 1957 and current time (Jeffery et al., 2001). For this reason we selected historical plots and maps for non-rainfall parameter values between 1965 to current (unless specified otherwise), though the hydrological and agricultural modelling period remains as specified in Section 1.4 (i.e. 1 July 1890 to 30 June 2011). It should be noted that the inter-annual variability of the non-rainfall parameters is considerably less than that of rainfall, and not simply because the record is shorter. Non-rainfall parameters have higher spatial and temporal auto-correlation than rainfall. Annual areal potential evaporation, for example, varied by ~10% between 1965 and 2010 (Figure 2.23). The Cv of annual potential evaporation for both the Flinders and Gilbert catchments is 0.09, about three to four times lower than that for rainfall. When examining the maps of non-rainfall parameters the reader should consider the sparsity of measurement stations (i.e. Figure 1.3). Percent exceedance maps for monthly rainfall, potential evaporation, mean daily maximum temperature, mean daily minimum temperature and mean daily relative humidity are provided in Appendix C. The agrometerology aspects of crop production in the Flinders and Gilbert catchment will be discussed in more detail in the Agricultural productivity technical report.

2.4.1 EVAPORATION

Evaporation is “the rate of liquid water transformation to vapour from open water, bare soil, or vegetation with soil beneath”, while transpiration is “that part of the total evaporation that enters the atmosphere from the soil through the plants” (Shuttleworth, 1993).

There are three major ways in which evaporation (Ea) affects a region’s potential for irrigation. The first is through the catchment wide losses by evaporation that determine runoff (R) and drainage (D) or the

'excess water' (R + D), which forms the basis of the potentially exploitable resource. This is evaluated in the companion technical report about river modelling calibration.

$$R + D = P - Ea \quad (1)$$

The second major way in which evaporation affects irrigation potential is through evaporative losses from water storages. This is examined in the companion technical report about water storage.

The third way in which evaporation affects irrigation potential is via its influence on the crop water requirement. This is discussed in the companion technical report about agricultural productivity.

Figure 2.23 shows the annual areal potential evaporation averaged over the Flinders and Gilbert catchments. The Flinders and Gilbert catchments have a similar mean annual areal potential evaporation, 1862 mm and 1868 mm respectively. Patterns of annual areal potential evaporation are similar in both catchments. Mean wet season areal potential evaporation in the Flinders and Gilbert catchments is 1115 mm and 1067 mm respectively. Mean dry season areal potential evaporation in the Flinders and Gilbert catchments is 762 mm and 815 mm respectively.

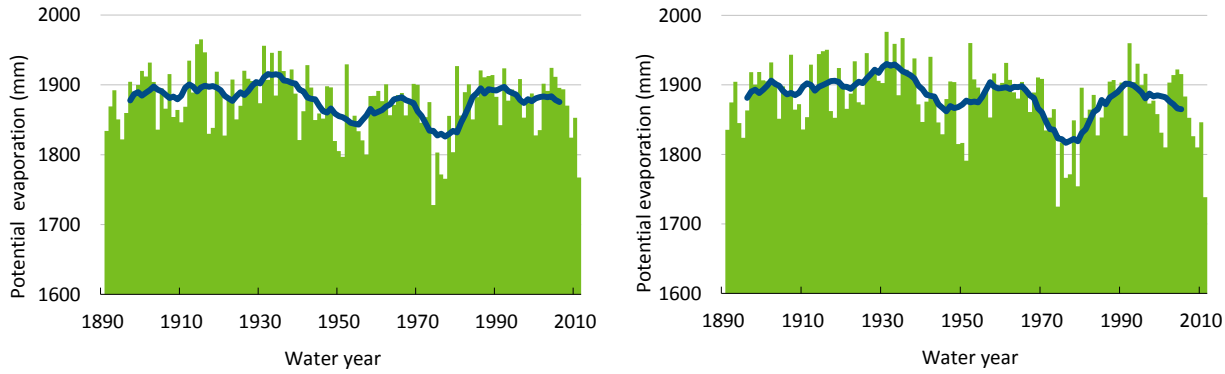

Figure 2.23 Historical annual areal potential evaporation averaged across the Flinders (left) and Gilbert (right) catchments. It should be noted, however, that observations of parameters used to compute areal potential evaporation were only available after 1957

Figure 2.24 shows monthly areal potential evaporation averaged across the Flinders and Gilbert catchments between 1965 and 2011. The temporal pattern and magnitude of areal potential evaporation in the two catchments are similar. Areal potential evaporation exceeds 180 mm per month in most years between October and January. Areal potential evaporation is at its lowest in June. Months where areal potential evaporation is high correspond to those months where the demand for water by plants is also high.

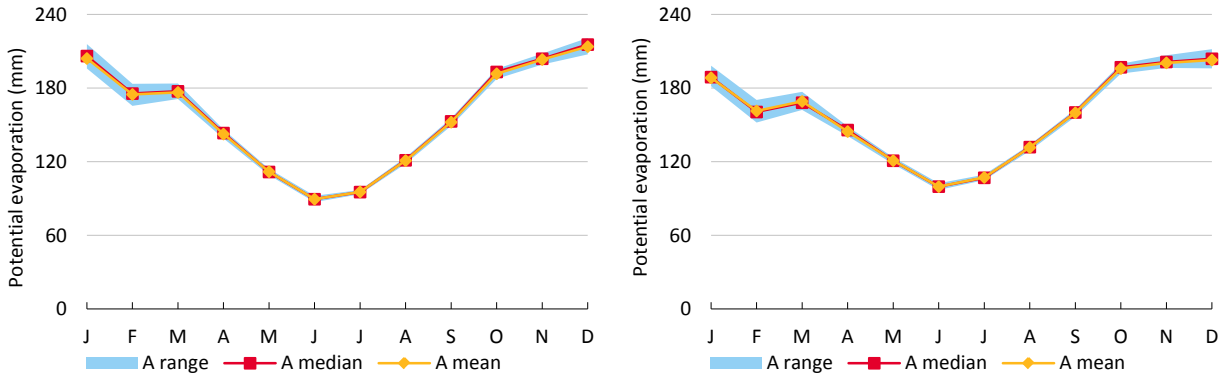

Figure 2.24 Monthly potential areal evaporation averaged over the Flinders (left) and Gilbert (right) catchments between 1965 and 2011 (A range is the 20th to 80th percentile monthly potential areal evaporation)

Mean annual (seasonal) rainfall (Figure 2.26) minus mean annual (seasonal) areal potential evaporation (Figure 2.27) is referred to as the mean annual (seasonal) rainfall deficit (Figure 2.28), a general measure of water availability. This metric is sometimes used as a first-cut assessment of the mean annual irrigation

demand and net evaporation from water storages. To refine this estimate the water balance needs to be calculated at shorter time intervals so that the intra-annual variability in precipitation and evaporation can be accounted. This process is detailed in the companion technical report about agricultural productivity.

The spatial distribution of annual, wet season and dry season rainfall, areal potential evaporation and rainfall deficit are shown in Figure 2.26, Figure 2.27 and Figure 2.28.

Figure 2.25 Cotton near Richmond in the Flinders catchment. Source: CSIRO

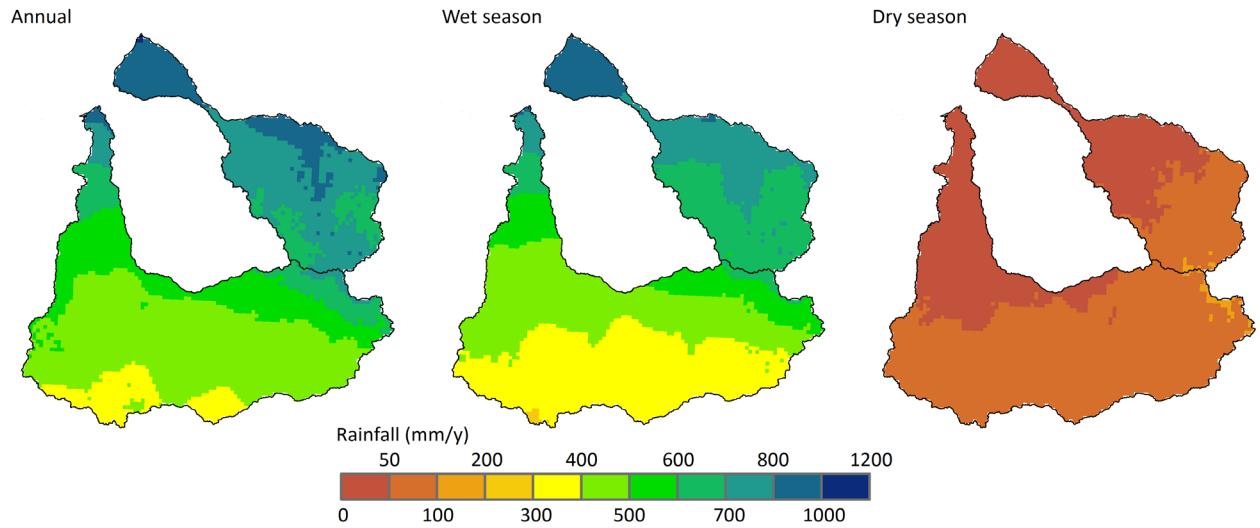

Figure 2.26 Historical mean annual, mean wet and mean dry season rainfall for the Flinders and Gilbert catchments

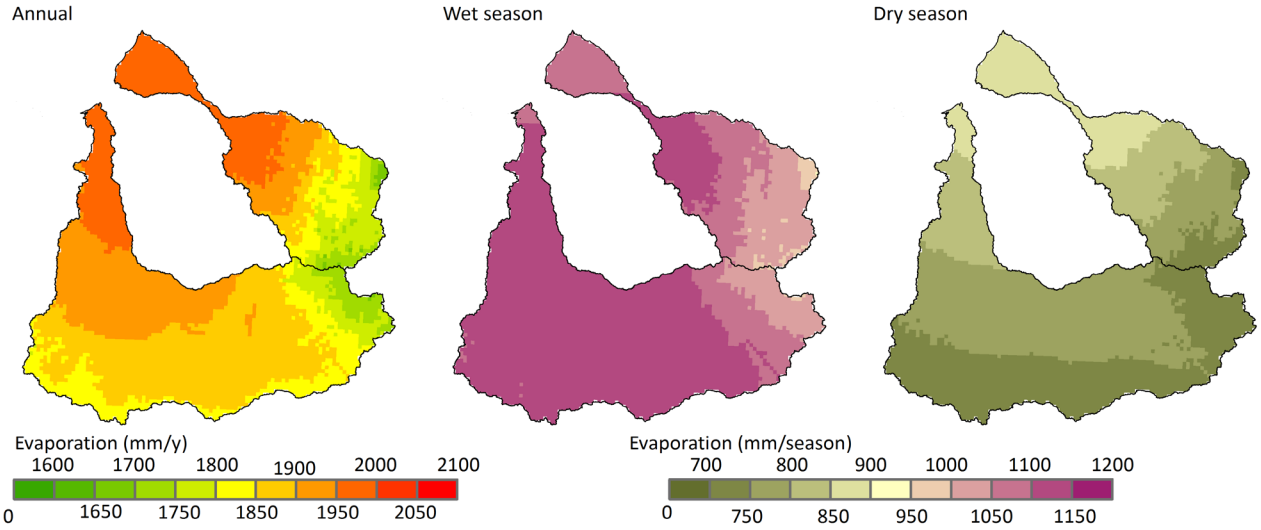

Figure 2.27 Historical mean annual, mean wet and mean dry season potential evaporation for the Flinders and Gilbert catchments

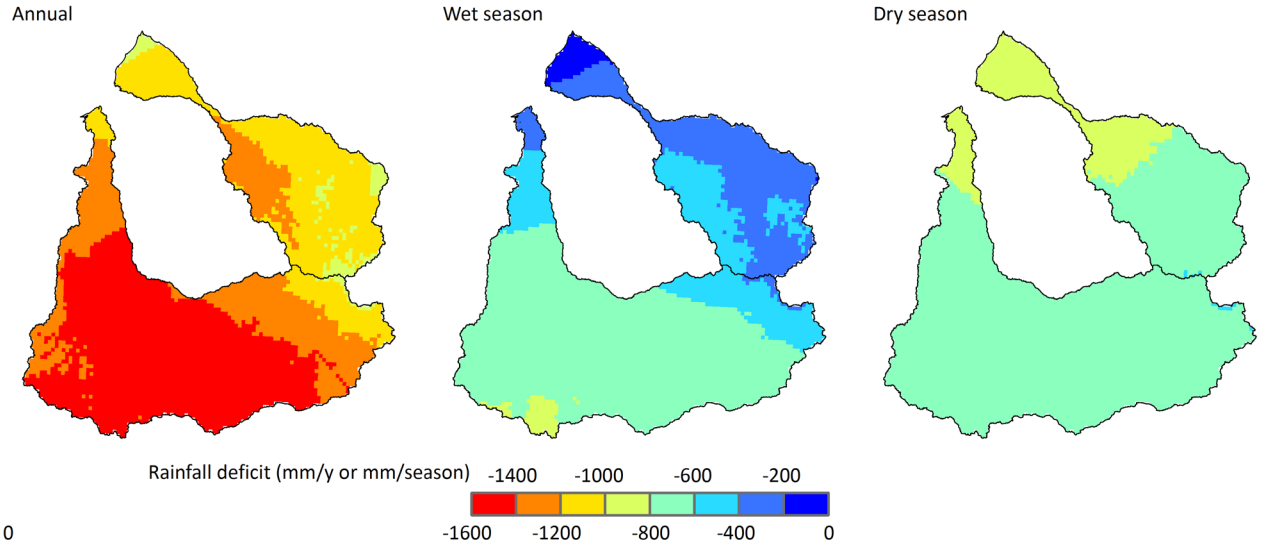

Figure 2.28 Historical mean annual, mean wet and mean dry season rainfall deficit for the Flinders and Gilbert catchments

Köppen classification and aridity index

The amount and temporal distribution of precipitation and potential evaporation do much to characterise climates, particularly in northern Australia where temperatures are uniformly high. Two common methods for characterising climates are presented. These are the Köppen-Geiger classification (Köppen, 1936) and the UNEP aridity index.

The Köppen-Geiger classification as redefined by Peel et al., (2007) divides the world into 30 climate types, of which four are represented in the Flinders and Gilbert catchments (Figure 2.29). These are the tropical savanna Aw, arid hot steep BSh, arid hot desert BWh, and temperate dry winter, hot summer CWa.

The UNEP aridity index is computed by dividing rainfall by potential evaporation. Under this classification, the majority of the two catchments are categorised as semi-arid. In southern Australia, where potential evaporation rates are typically lower, semi-arid landscapes occur around the 400 mm rainfall isohyet. The high seasonality of rainfall and high rates of potential evaporation in the Flinders and Gilbert catchments mean that they are largely classified as semi-arid despite receiving an average of almost 500 and 800 mm rainfall respectively.

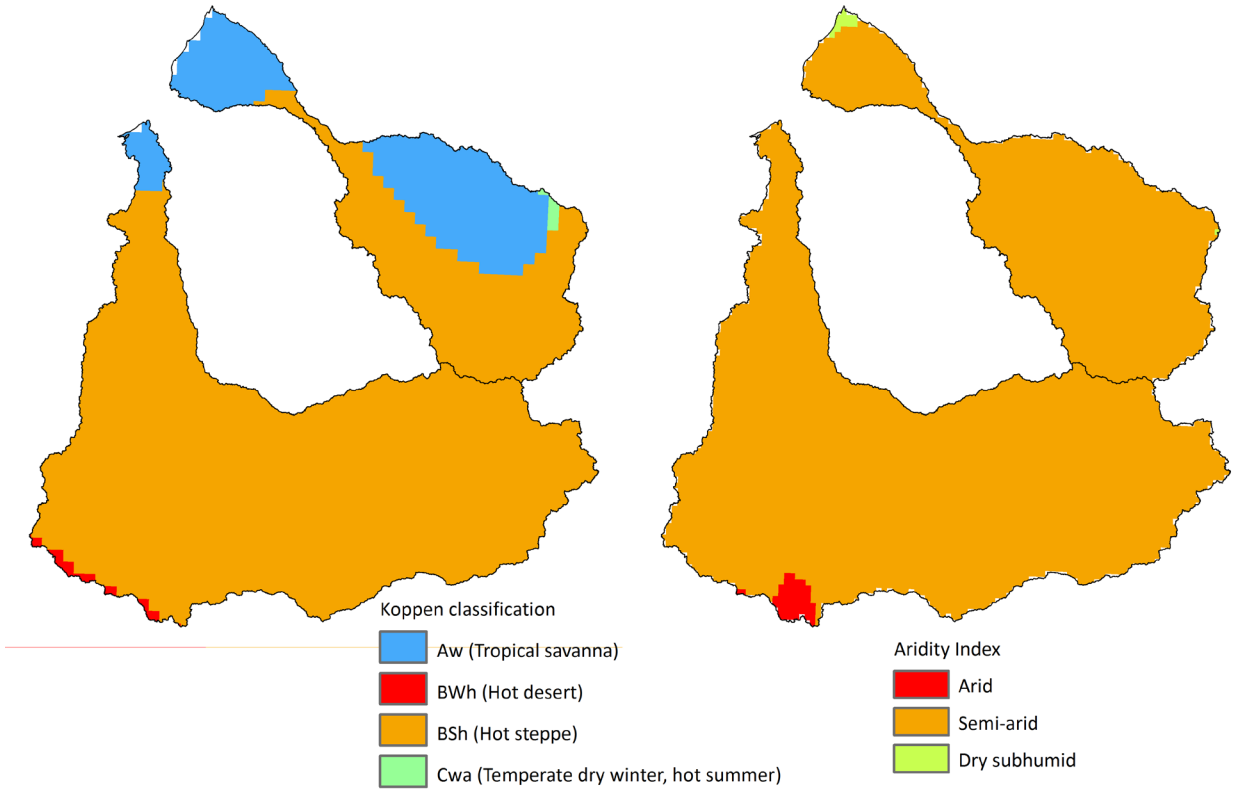

Figure 2.29 Köppen classification and UNEP aridity index for the Flinders and Gilbert catchments

2.4.2 AIR TEMPERATURE

Plants are sensitive to air temperature, where temperature is an important factor controlling changes in development from germination, through vegetative growth to floral initiation and reproductive growth, though not all stages of development are equally sensitive to temperature. Plant growth is at its maximum at an optimal temperature. Above or below the optimal temperature plant growth is reduced. Below a certain minimum temperature or above a certain maximum temperature, plants will not grow.

By integrating temperature measurements and time (i.e. referred to as degree days) the timing of cardinal stages of plant development can be predicted. Hence mean monthly air temperatures, which take into account seasonal changes, are generally much more relevant to plant growth than mean annual values.

Monthly mean maximum temperature and monthly mean minimum temperature averaged across the Flinders and Gilbert catchments are shown in Figure 2.30 and Figure 2.31 respectively. The Flinders catchment exhibits higher high temperatures and lower low temperatures than the Gilbert catchment. The highest temperatures occur in October to February and the lowest temperatures occur in June and July.

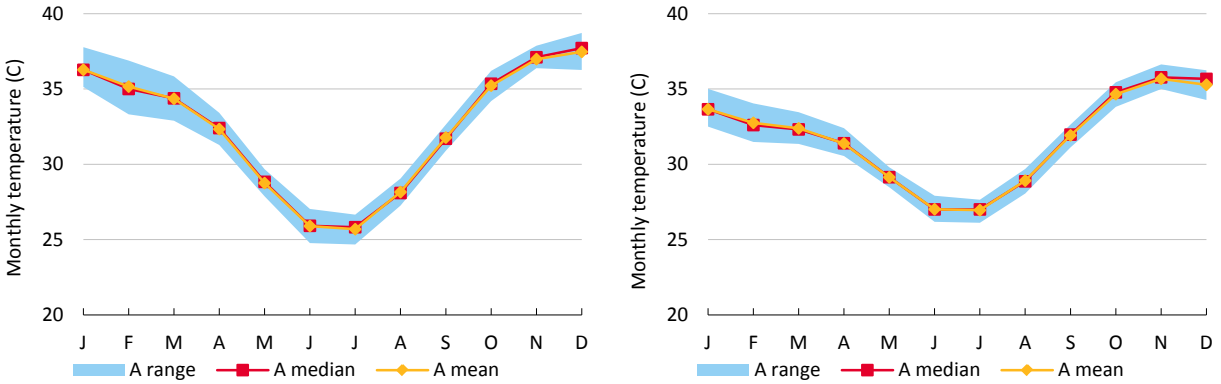

Figure 2.30 Mean daily maximum monthly temperature averaged over the Flinders (left) and Gilbert (right) catchments between 1965 and 2011 (A range is the 20th to 80th percentile mean daily maximum monthly temperature)

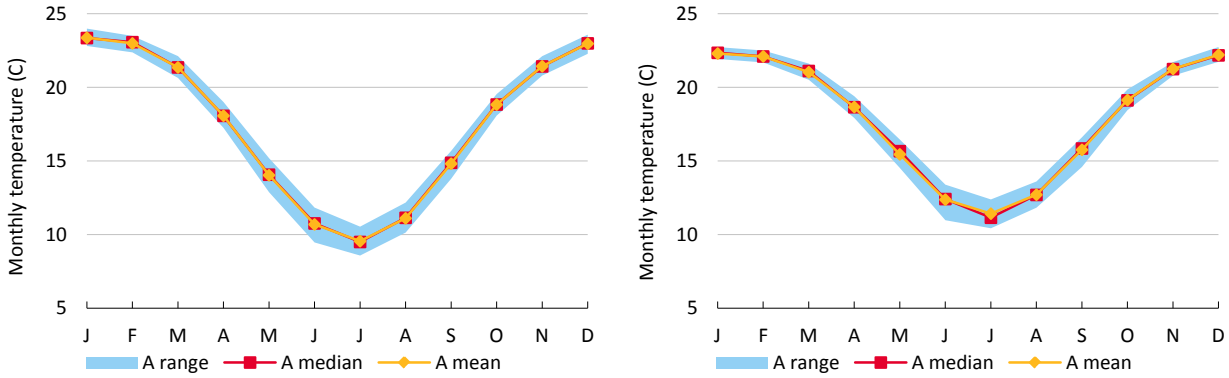

Figure 2.31 Mean daily minimum monthly temperature averaged over the Flinders (left) and Gilbert (right) catchments (between 1965 and 2011 (A range is the 20th to 80th percentile mean daily minimum monthly temperature)

When considering the effect of temperature on yield, it is also important to take extreme conditions into account, particularly at sensitive stages of growth. Figure 2.32 shows the maximum annual temperature that is exceeded in 20%, 50% and 80% of years. Figure 2.33 shows the minimum annual temperature that is exceeded in 20%, 50% and 80% of years. Temperatures in both catchments are lowest in the east. In the Flinders catchment temperatures are highest in the south, while in the Gilbert temperatures are typically highest in the central reaches of the catchment.

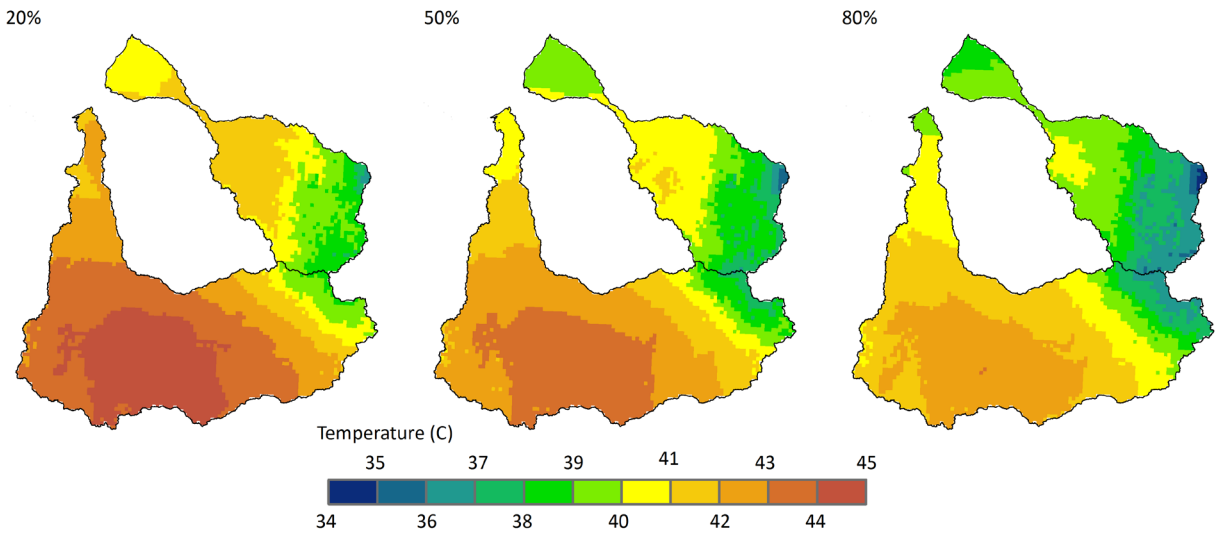

Figure 2.32 The maximum annual temperature that is exceeded in 20%, 50% and 80% of years in the Flinders and Gilbert catchments

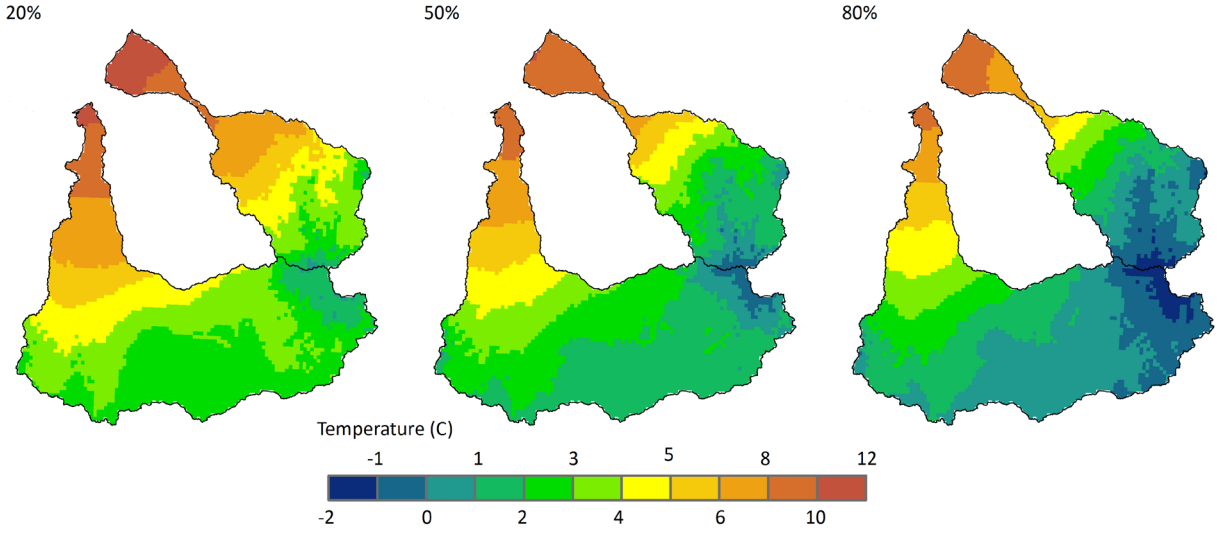

Figure 2.33 The minimum annual temperature that is exceeded 20%, 50% and 80% of years in the Flinders and Gilbert catchments

2.4.3 SHORT WAVE RADIATION

Incoming short wave radiation, commonly referred to as sunlight, is used by most land plants for photosynthesis, the process by which plants capture carbon dioxide from the atmosphere and convert it into carbohydrates. In general higher crop yields are achieved by harvesting more short wave radiation. This is commonly achieved through management practises such as optimising the time of sowing, optimising plant populations, strategic application of fertilizers and irrigation management. These will be discussed in context to the Flinders and Gilbert catchments in the companion technical report about agricultural productivity.

Monthly radiation averaged across the Flinders and Gilbert catchments is shown in Figure 2.34. Radiation values are relatively high in all months and peak in October, before the onset of the monsoon. Figure 2.35 shows the percent of years that annual shortwave radiation is exceeded. Annual radiation typically increases in an easterly direction.

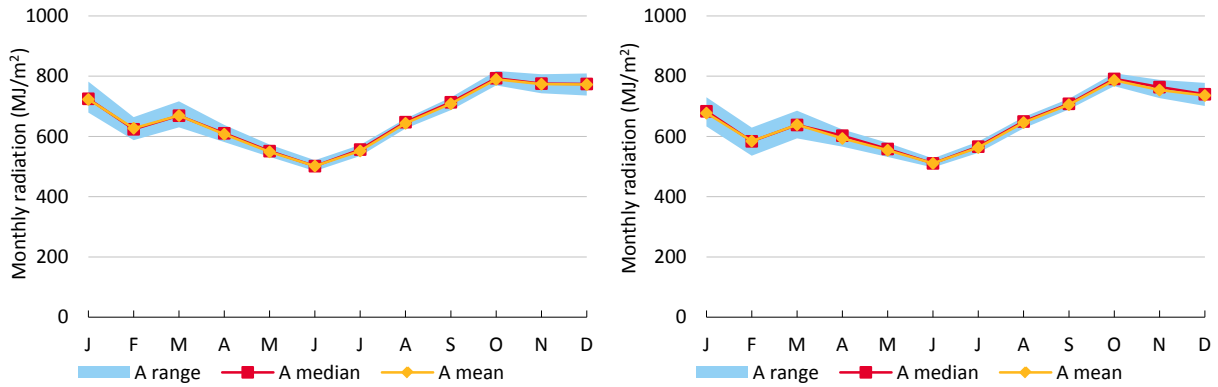

Figure 2.34 Monthly radiation for the Flinders (left) and Gilbert (right) catchments between 1965 and 2011 (A range is the 20th to 80th percentile monthly radiation)

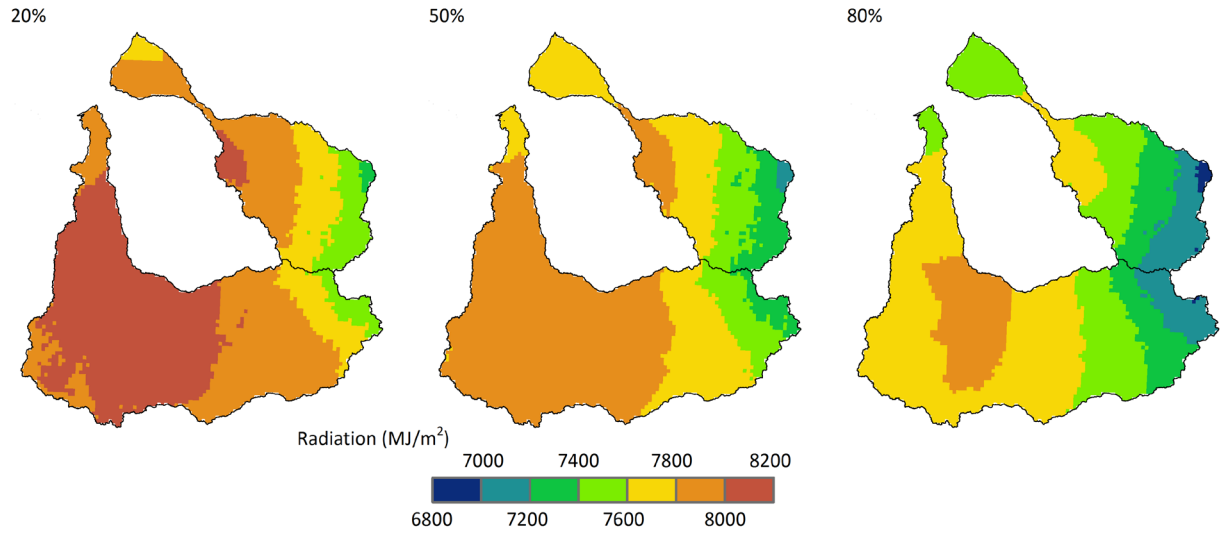

Figure 2.35 The annual shortwave radiation that is exceeded in 20%, 50% and 80% of years in the Flinders and Gilbert catchments

2.4.4 RELATIVE HUMIDITY

Relative humidity is the ratio of actual water vapour content to the saturated water vapour content at a given temperature and pressure expressed in percentage. Relative humidity can affect the economic yield of crop production through its influence on plant water usage, photosynthesis, leaf growth, pollination and disease. Relative humidity is also an important parameter in terms of human comfort, because it affects the way that humans perceive heat.

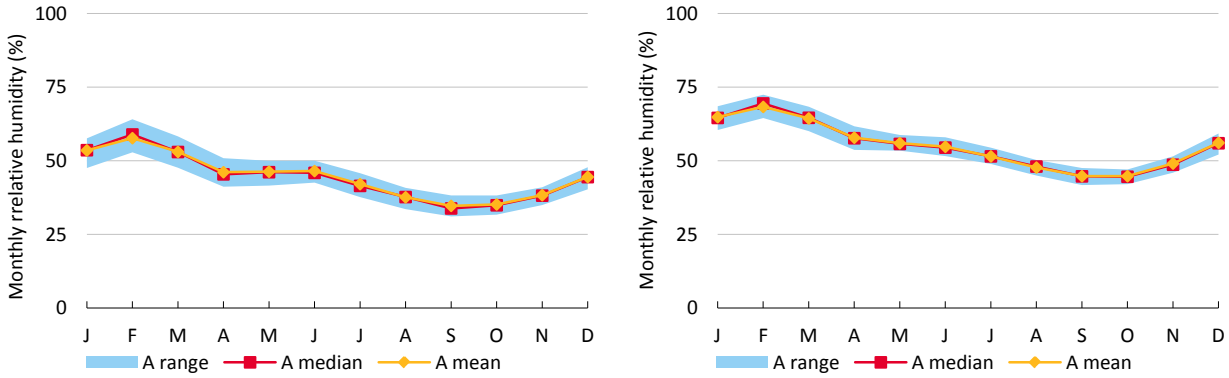

Figure 2.36 Monthly relative humidity averaged across the Flinders (left) and Gilbert (right) catchments between 1965 and 2011 (A range is the 20th to 80th percentile monthly relative humidity)

3 Methods

3.1 Generation of future climate data

Global climate models (GCMs) are an important tool for simulating global and regional climate. The climate activity will provide variants of 121 years of daily climate series for a 2 °C global temperature rise relative to ~1990, guided by GCMs from the Intergovernmental Panel for Climate Change (IPCC) Fourth Assessment Report (AR4). However, GCMs provide information at a resolution that is too coarse to be used directly in catchment-scale hydrological modelling, which can contribute, for example, to rainfall being generated too often and at too low intensity (Stephens et al., 2010). This is particularly important in tropical regions where even high resolution coupled climate models simulate tropical cyclones to be weaker and larger in spatial extent than those observed (IPCC, 2007). Hence, an intermediate step is generally performed: the broad-scale GCM outputs are transformed to catchment-scale variables.

Two fundamental approaches exist for downscaling broad-scale GCM output to a finer spatial resolution: dynamic downscaling and statistical downscaling (Fowler et al., (2007) and references therein). Dynamic downscaling is computationally very intensive, however, and there are limited archived future sub-daily GCM outputs from which to downscale, while sophisticated statistical downscaling methods (e.g. regression models, weather typing schemes and weather generators) are laborious. Recent studies, however, also suggest that no single downscaling method is superior across a range of hydrological metrics (Mitchell, 2003; Whetton et al., 2005; Prudhomme and Davies, 2009; Chiew et al., 2010; Segui et al., 2010). In a comparative assessment of scaling methods in an area dominated by large-scale storm events, Salathé (2003) found simple scaling methods to be effective in simulating hydrological systems. For these reasons, and because climate change assessment is of secondary importance in the Assessment, a simple scaling technique, the empirical scaling method (Chiew et al., 2009a), was employed. Although similar to pattern scaling (Whetton et al., 2000; Todd et al., 2011), the empirical scaling method used here takes into account changes in daily distribution of rainfall as well as changes in seasonal means.

The rest of this section is organised as follows. First the justification for using GCM data from the fourth assessment report to inform the empirical scaling method is provided. Next the GCM selection process is outlined. This is followed by a brief summary of the empirical scaling method. For a detailed description of the empirical scaling method refer to Li et al., (2009) or Chiew et al., (2009a).

Comparison of AR4 and AR5 GCM runs

It is generally accepted that the uncertainty in predicting climate change impact on water is dominated by the uncertainty in the GCM projections (e.g. Petheram et al., 2012). Hence there is considerable interest in determining whether the AR5 GCMs simulations produce wider or a smaller range of rainfall projections than the previously available data from the AR4 GCMs. However, AR5 GCM runs are currently being archived and the full set of AR5 GCMs and runs will only become available from mid 2013. Up until that time contributing climate modelling groups are able to modify their archived datasets. This makes current usage of the AR5 GCM runs problematic, as it may not be possible to reproduce results.

In a preliminary study by Teng et al., (2012), future runoff projections across Australia, informed by 19 AR5 and 19 AR4 GCM were compared. It was found that the range of uncertainty in the projections was similar, with both sets of models exhibiting about a 50% difference between the 10^{th} and 90^{th} percentile projections. Use of only the better GCM selected, based on their ability to reproduce the observed historical mean annual rainfall, reduced the range of uncertainty in the runoff projections by about 20% in both the AR5 and AR4 GCMs. For northern Australia specifically little change in median annual rainfall was observed. Hence output from the AR4 GCMs used in this study are likely to produce a similar range of results to that based on output from the AR5 GCMs.

Due to the preliminary nature of the currently archived AR5 GCM data, a pragmatic decision was made to use the AR4 model runs. Having decided to select GCM model runs from the AR4 dataset, the next step is to select the global climate models to use in the Assessment.

Selection of global climate models

A commonly held premise of hydrological prediction is that models that are better able to simulate the past are more likely to accurately simulate the future. In an Australia-wide assessment of rainfall simulations using 23 GCMs, Chiew et al., (2009b) found that there was no clear difference in future rainfall projections across northern Australia between the better and poorer performing GCMs and that the use of weights to favour the better GCMs gave similar rainfall results to modelling using all the 23 GCMs. The use of palaeo-observations to determine which, if any, GCMs have the proper sensitivity in tropical regions is also of little value because tropical oceanic and terrestrial palaeo-climate proxies are conflicting (Rind, 2008).

To assess the uncertainty and simulate the range of future runoff predictions, future climate projections from a large range of archived GCM simulations were downloaded from the Program for Climate Model Diagnosis and Intercomparison (PCMDI) website <http://www-pcmdi.llnl.gov>. Of the 23 GCMs examined by Chiew et al., (2009b), 15 have readily available daily rainfall data. These 15 GCMs were used in the Assessment (Table 3.1).

Scaling method

The empirical scaling method employed in the Assessment used output from the 15 GCMs listed in Table 3.1 to scale the 121 years of historical daily rainfall and PE sequences, to construct the 15 by 121-year sequences of future daily rainfall and PE. The method comprised two broad steps: the first considered changes in the mean 'seasonal' values of rainfall and PE, and the second considered changes to the daily distribution of rainfall within each 'season'. An overview of the method is provided below.

The first step involved estimating the seasonal scaling factors for four 3-month blocks (December to February, March to May, June to August and September to November) as first described by Mitchell (2003). Using the archived monthly simulations for each of the 15 GCMs, simulated rainfall was plotted against simulated global average surface air temperature, for each season and each GCM grid point. A percentage change in rainfall per degree global warming relative to the GCM modelled baseline was computed by fitting a linear regression. The scaling factors were applied for a 2 °C global warming scenario, roughly in line with the IPCC (2007) projected median warming by ~2060 relative to ~1990.

The second step accounted for changes to the distribution of daily rainfall. This is potentially important because many GCMs indicate that future extreme high rainfall is likely to be more intense, even in regions where a decrease in mean seasonal or annual rainfall is expected. For each season, daily scaling factors were computed for different rainfall percentile ranges (i.e. zero to 2.5, 2.5 to 7.5, 7.5 to 12.5% and so forth, until the observed grid cell rainfall is less than 1 mm) by comparing daily rainfall simulations from the 15 GCMs for a single Special Report on Emissions Scenarios (SRES) A1B run for two 20-year time periods, 2046 to 2065 and 1981 to 2000. Daily scaling factors were obtained for all rainfall percentiles by interpolating between the values for each of the rainfall percentile ranges. To ensure compatibility with the seasonal scaling factors, the changes for the different rainfall percentiles were expressed as a percentage change per degree of global warming. The above daily scaling factors were then be used to scale the 121-year historical rainfall sequences from each 0.05 degree grid cell that fell within the GCM grid cell. The entire series were scaled so that the future mean rainfalls in the four seasons were the same as those estimated using the seasonal scaling factors. This step was necessary because the daily scaling factors were available only for two time periods from a single modelling run, whereas the seasonal scaling factors were determined using a large number of data points from several ensemble runs with more than 100 years of continuous monthly simulations archived for each GCM. This process was repeated for each GCM, for each season and for each GCM grid cell. The method of using an empirical scaling method to transform broad-scale GCM outputs to catchment scale variables is herein denoted 'GCM-ES'.

Table 3.1 Global climate models, their founding institution and model resolution

GLOBAL CLIMATE MODEL	INSTITUTION	APPROXIMATE MODEL RESOLUTION (degrees)
CCCMA CGM3.1 T47	Canadian Climate Centre, Canada	3.8 x 3.7
CCCMA CGM3.1 T63	Canadian Climate Centre, Canada	2.8 x 2.8
CNRM CN3	Meteo-France, France	2.8 x 2.8
CSIRO MK3.0	CSIRO, Australia	1.9 x 1.9
GFDL-CM2.0	Geophysical Fluid, Dynamics Lab, United States	2.5 x 2.0
GISS AOM	NASA/Goddard Institute for Space Studies, United States	4.0 x 3.0
IAP FGOALS-g1.0	LASG/Institute of Atmospheric Physics, China	2.8 x 2.8
INM CM3.0	Institute of Numerical Mathematics, Russia	5.0 x 4.0
IPSL CM4	Institute Pierre Simon Laplace, France	3.8 x 2.5
MIROC3.2-M	Centre for Climate Research, Japan	2.8 x 2.8
MIUB ECHO-G	Meteorology Institute of the University of Bonn, Germany, and Meteorological Research Institute of KMA, Korea	3.8 x 3.7
MPI ECHAM5	Max Planck Institute for Meteorology DKRZ, Germany	1.9 x 1.9
MRI CGCM2.3.2	Meteorological Research Institute, Japan	2.8 x 2.8
NCAR CCSM3	National Center for Atmospheric Research, United States	1.4 x 1.4
NCAR PCM1	National Center for Atmospheric Research, United States	2.8 x 2.8

Figure 3.1 Upper Cloncurry River during dry season (Flinders catchment). Source: CSIRO

4 Results

4.1 Projected future climate statistics

Rainfall

As rainfall is a key control on hydrology processes and agricultural productivity, we characterise changes in rainfall that are simulated by 15 GCM-ESs' for a 2 °C increase in global average surface air temperature relative to ~1990 global average surface air temperature.

Figure 4.1 and Figure 4.2 show appreciable scatter in the simulated changes in mean annual rainfall that are projected to occur over the Finders and Gilbert catchments under Scenario C. These results are summarised in Figure 4.3 and Figure 4.4 where, for each SILO grid cell in the Flinders and Gilbert catchments, the 10th, 50th and 90th percentile mean annual rainfall values from the 15 GCM-ESs' were selected. The 10th, 50th and 90th percentile mean annual rainfall values constitute the Cwet, Cmid and Cdry mean annual rainfall respectively.

In Figure 4.5 and Figure 4.6 15 GCM-ESs' rainfall and PE projections have been spatially averaged across the Flinders and Gilbert catchments respectively and the GCM-ESs' ranked in order of increasing mean annual rainfall. From these figures it can be seen that about half the GCM-ESs' projections indicate an increase in mean annual rainfall and half indicate a decrease in mean annual rainfall. However, it should be noted that about 60% of GCM-ESs' mean annual rainfall projections are within ±10% of the historical mean. It is possible for small trends in rainfall to be generated by internal variability modelled by the GCMs (Cai et al., 2010, Cai et al., 2011). Hence one could argue that the consensus result is that mean annual rainfall will not change into the future.

Clearly there are some deficiencies in the GCM-ESs' and we are not sure how this may impact on trends in mean annual rainfall. The lack of consensus in future trends over the Flinders and Gilbert catchments and the eastern half of northern Australia in general (Li et al. 2009) is in part because under a warming climate it is not clear how the phase, intensity and amplitude of the ENSO will change (Collins et al., 2010). While ESNO is considered to be the primary source of global climate variability over the 2-6 year timescale, it has its largest influence on weather patterns and climate variability over the tropical Pacific and the continental landmasses on either side, i.e. coastal regions of South American, South East Asia and north and eastern Australia (Philander, 1989). In these areas rainfall teleconnections with ENSO are not well simulated and there is a large spread among models (Cai et al., 2009, Cai et al., 2011).

Figure 4.7 and Figure 4.8 illustrate the range in monthly GCM-ES rainfall and PE projections respectively. In Figure 4.7 C range is the difference between the 10th and 90th percentile spatially averaged GCM-ES mean monthly rainfall. This is computed for each month.

Potential evaporation

Figure 4.5 and Figure 4.6 of the resultant mean annual changes in GCM-ES PE show, using Morton's formulation, projected APE increases by between about 3 to 9%. This change has been predominantly driven by the increase in air temperature, which affects Morton's wet area potential both directly via its influence on surface temperature and indirectly via its effect on vapour pressure and on long-wave radiation. However, Morton's formulation of APE does not incorporate the effects of wind speed, even though wind speed is a key variable in the aerodynamic component of evaporation. Recently (McVicar et al., 2008) showed that all of northern Australia has experienced declines in wind speed of approximately 0.01 m/second/year over the last 30 years, and this has been shown to be the primary factor driving the observed decreases of pan evaporation across much of Australia, including northern Australia, over the same time period (Roderick et al., 2007). The effect of decreasing wind speed is to moderate the effect rising temperatures will have on potential evaporation rates. If decreasing wind speeds were to hold into

the future, the projections of APE here (i.e. using Morton's wet area potential formulation) will be higher than they would be if a fully physical potential formation were to be used (that is, one that incorporates net radiation, humidity, wind speed and temperature).

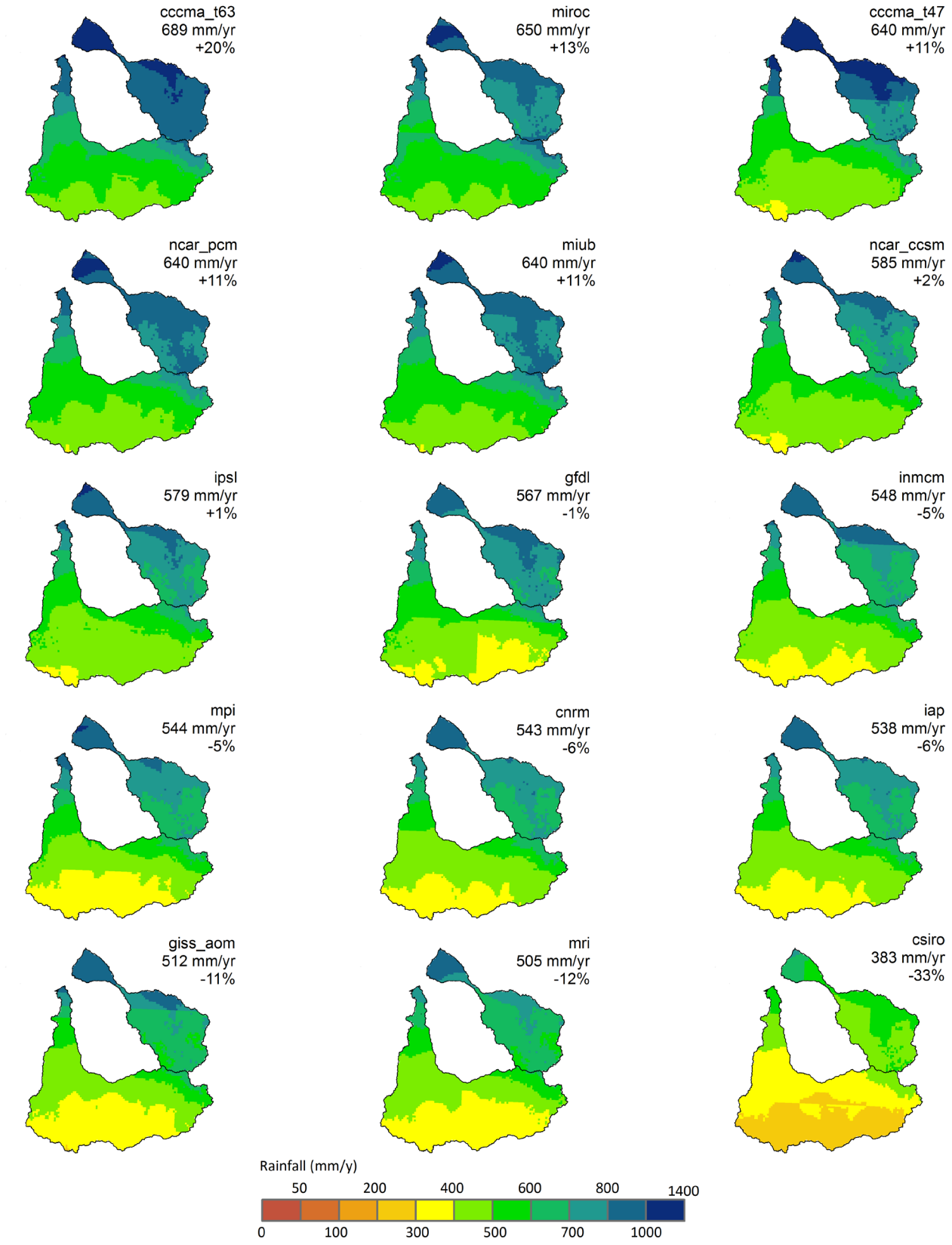

Figure 4.1 Modelled future mean annual rainfall using future climate series informed by 15 GCM-ESs' for a 2 °C increase in global average surface air temperature. The plots are positioned from wettest (top left) to driest (bottom right), based on mean annual rainfall averaged across both the Flinders and Gilbert catchments

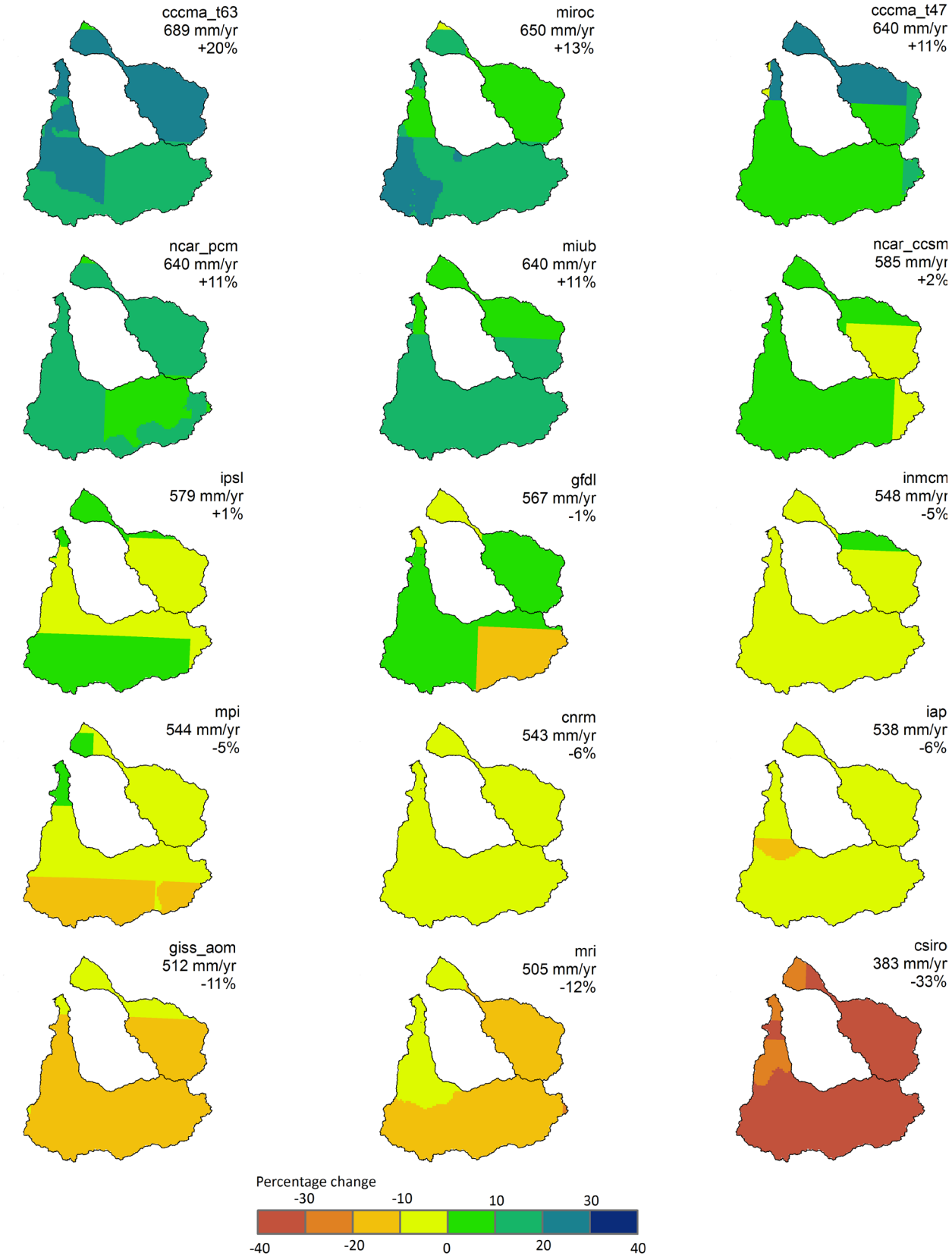

Figure 4.2 Percentage change in modelled future mean annual rainfall using future climate series informed by 15 GCM-ESs' for a 2 °C increase in global average surface air temperature. The plots are positioned from wettest (top left) to driest (bottom right), based on mean annual rainfall averaged across both the Flinders and Gilbert catchments

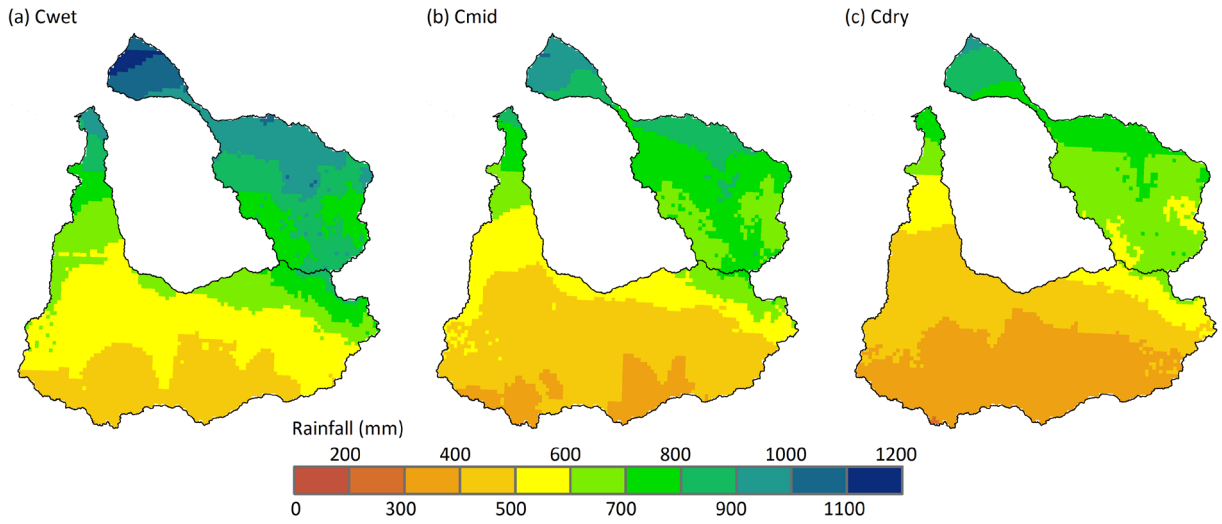

Figure 4.3 Spatial distribution of mean annual rainfall across the Flinders and Gilbert catchments under scenarios Cwet, Cmid and Cdry

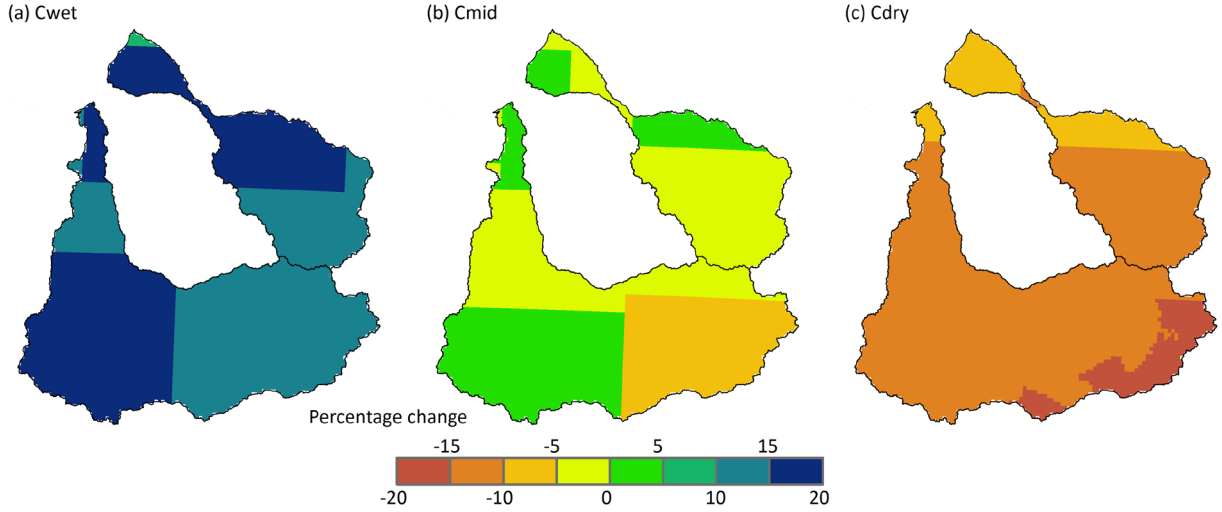

Figure 4.4 Spatial distribution of mean annual rainfall under scenarios Cwet, Cmid and Cdry relative to Scenario A

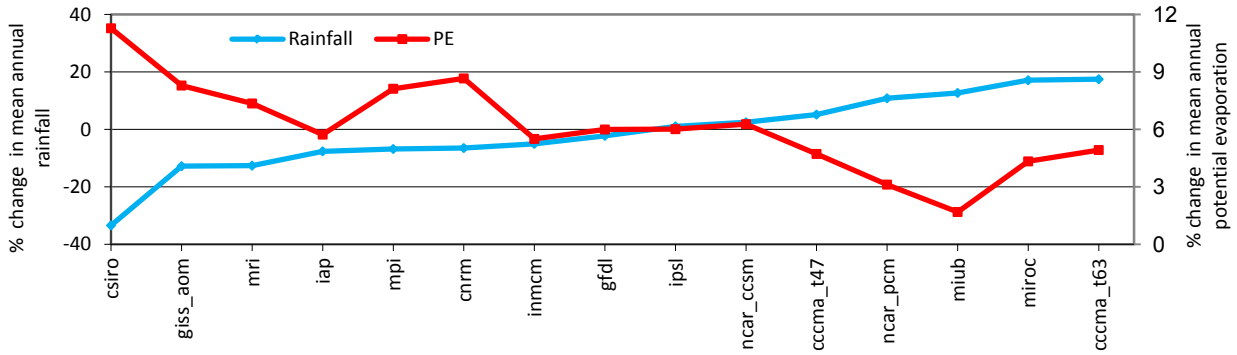

Figure 4.5 Percentage change in mean annual rainfall under the 15 Scenario C simulations relative to Scenario A mean annual rainfall (blue line) and PE (red line) for the Flinders catchment. GCM-ESs' ranked by increasing rainfall

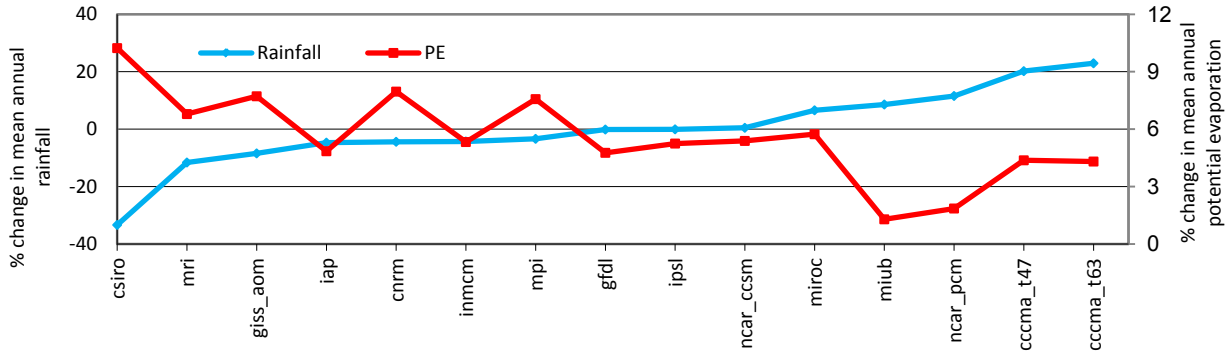

Figure 4.6 Percentage change in mean annual rainfall under the 15 Scenario C simulations relative to Scenario A mean annual rainfall (blue line) and PE (red line) for the Gilbert catchment. GCM-ESs' ranked by increasing rainfall

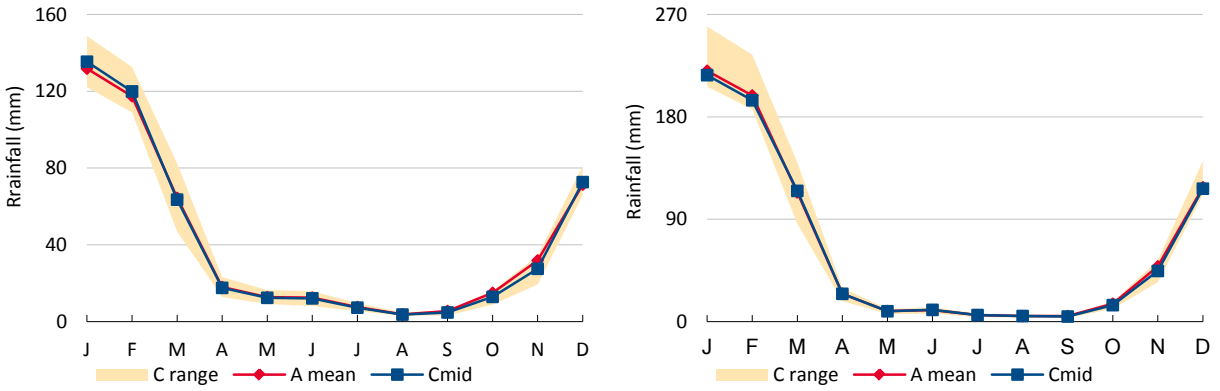

Figure 4.7 Mean monthly rainfall for the Flinders (left) and Gilbert (right) catchments under scenarios A and C. (C range is based on the computation of the 10 and 90th percentile rainfall for each month separately – the lower and upper limits in C range are therefore not the same as scenarios Cdry and Cwet)

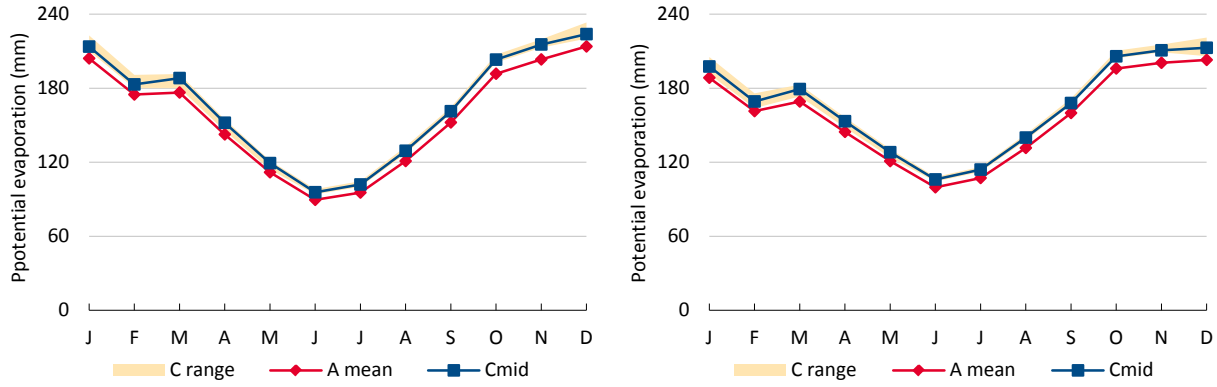

Figure 4.8 Mean monthly potential evaporation for the Flinders (left) and Gilbert (right) catchments under scenarios A and C. (C range is based on the computation of the 10 and 90th percentile potential evaporation for each month separately – the lower and upper limits in C range are therefore not the same as scenarios Cdry and Cwet)

In addition to rainfall amounts, rainfall characteristics such as rainfall intensity are important elements governing the amount of runoff generated for a certain amount of rainfall. With the exception of the lower Gilbert, which had a modelled increase in 1 and 5 percentile daily rainfall values, the majority of the Assessment area does not show an increase in rainfall intensity (Figure 4.9). The lower Gulf region appears to be anomalous in this regard across northern Australia. Petheram et al. (2012) showed that the overwhelming majority of GCM-ESs' simulate increases in the most intense 1% of rainfall across northern Australia relative to Scenario A.

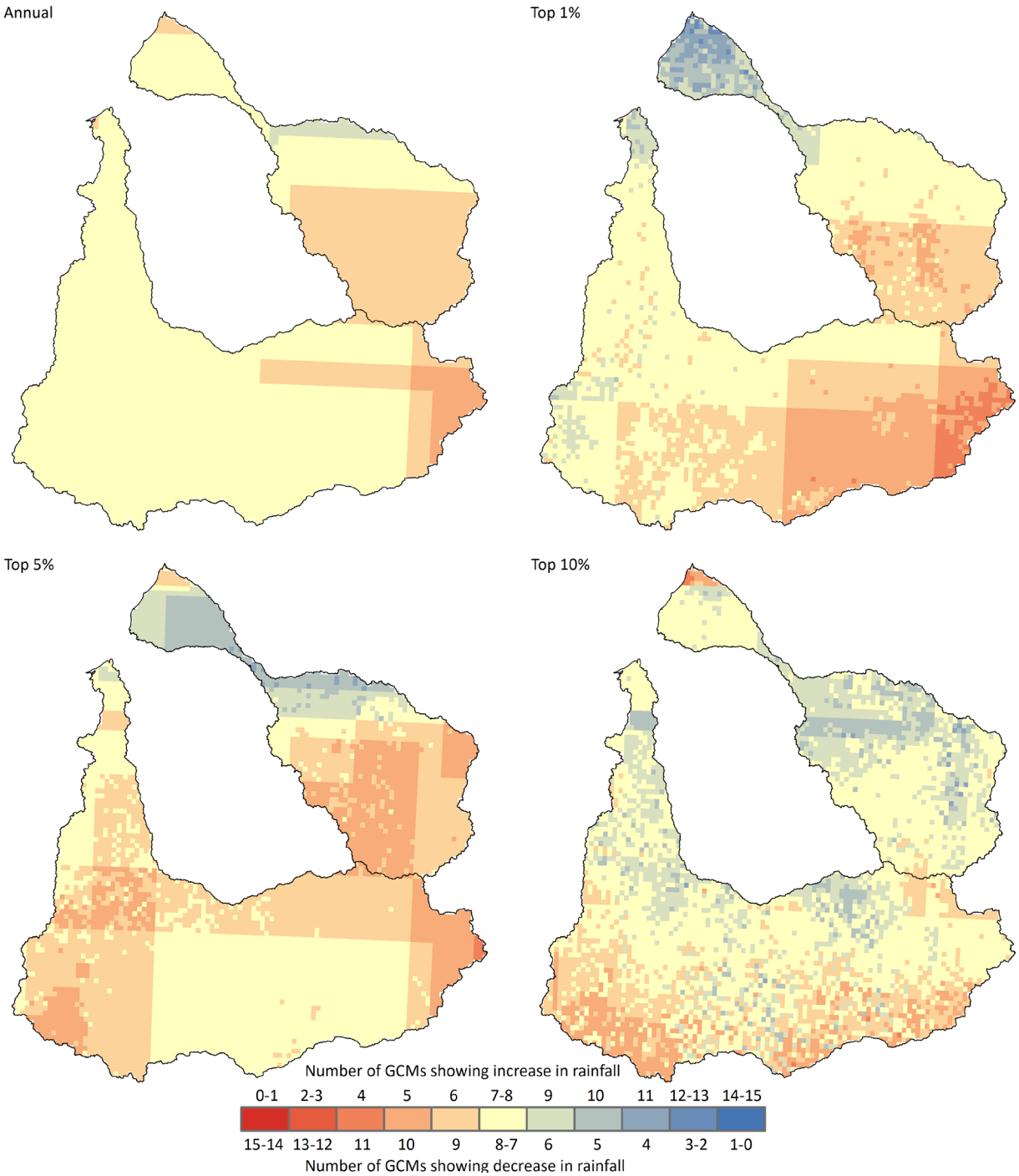

Figure 4.9 Number of GCM-ESs' (out of 15) showing a decrease (or increase) in future mean annual rainfall, 1st, 5th and 10th percentile daily rainfall (i.e. daily rainfall that is exceeded 1%, 5% and 10% of the time) for a 2 °C increase in global average surface air temperature relative to ~1990 global air temperatures

5 Conclusions

The mean annual rainfall, averaged over the 121-year historical period (1890 to 2011) and across the Flinders and Gilbert catchments was 492 mm and 775 mm respectively. Eighty-eight and ninety-three percent of rainfall in the Flinders and Gilbert catchments, respectively, fell during the wet season. There is a predominant north-south rainfall gradient over much of the area, and mean annual rainfall is typically higher near coastal areas and northern parts of the catchments.

The highest monthly rainfall in both the Flinders and Gilbert catchments occurs during January and February, with a median monthly value of about 100 and 200 mm respectively. The months with the lowest median rainfall are July and August, about 0.5 mm in each of the Flinders and Gilbert catchments.

Approximately 90% of the variance in the historical monthly time series of rainfall was due to the annual cycle and within year variability. The remaining 10% was attributed to inter-annual variability in rainfall. An increasing trend in rainfall of between +4 and +14.5% was computed over the length of the historical period.

Although the majority of the variation in the historical monthly rainfall record was attributed to the annual cycle and within year variability, rainfall in the Flinders and Gilbert catchments nevertheless shows considerable variation from one year to the next. The highest catchment average annual rainfall in the Flinders (1310 mm) and Gilbert (2187 mm) occurred in 1974, nearly three times the median annual rainfall. The coefficient of variation of annual rainfall (i.e. the standard deviation of mean annual rainfall divided by the mean annual rainfall) in the Flinders and Gilbert catchments is typically between 0.4 and 0.5 and 0.3 and 0.4 respectively. This is high relative to other rainfall stations around the world of similar mean annual rainfall and similar climate type and high compared to rainfall stations in south-eastern and south-western Australia. The length of dry spells in the Flinders and Gilbert catchments are comparable to other areas of eastern Australia and are not unusual in any way. However, the magnitude of dry spells in the Flinders and Gilbert catchments appear to be larger than the majority of the stations examined in the eastern half of Australia.

Potential evaporation is high, exceeding 1800 mm in both catchments in most years. Potential evaporation exhibits a strong seasonal pattern, typically ranging from 200 mm per month during the build up and the wet season to about 100 mm per month during the middle of the dry season (June to July). The high evaporation rates and relatively low rainfall result in a large annual rainfall deficit across most of the Assessment area. Consequently most of the area of both catchments is classified as having a semi-arid climate.

Approximately half the global climate models empirically scaled to transform broad GCM outputs to catchment scale variables (designated GCM-ES) used here, resulted in a spatially averaged increase in mean annual rainfall, and half resulted in a decrease. The increases were up to 17% in the Flinders and 22% in the Gilbert, while the decreases were up to 33% (in both the Flinders and Gilbert), relative to the 1890 to 2011 average. However, approximately 60% of the GCM-ESs' differed by less than ±10% from the historical rainfall (1890 to 2011). With the exception of the lower Gilbert, which had a modelled increase in 1 and 5 percentile daily rainfall values, the majority of the Assessment area does not show an increase in rainfall intensity. Hence the consensus result from the 15 global climate models is that the impacts on mean annual rainfall of a 2 °C increase in global temperatures relative to ~1990 is not likely to be major in either the Flinders or Gilbert catchments.

References

Andreassian V, Perrin C and Michel C (2004) Impact of imperfect potential evapotranspiration knowledge on the efficiency and parameters of watershed models. Journal of Hydrology 286(1-4), 19-35. DOI: DOI 10.1016/j.jhydrol.2003.09.030.

BoM (1972) Tropical Cyclone Warning Service, Australia, Directive Part 1: Glossary. Bureau of Meteorology, Melbourne.

BoM (1978) Australian Tropical Cyclone Forecasting Manual. Bureau of Meteorology, Melbourne.

BoM (1989) Climate of Australia. Bureau of Meteorology. Morphet Press Type Ltd 49pp.

BoM (1998) Climate of the Northern Territory. Bureau of Meteorology. June 1998.

Bonell M, Gilmour DA, Cassells DS (1983) Runoff generation in tropical rainforests of northeast Queensland, Australia, and the implications for land use management. In 'Hydrology of Humid Tropical Regions' (Ed Reiner Keller). IAHS Publication No. 140.

Cai W, Cowan, T, Sullivan J, Ribbe AJ and Sh G (2011) Are anthropogenic aerosols responsible for the northwest Australian summer rainfall increase? Journal of Climate 23, 12.

Cai W, Sullivan A. and Cowan T (2009) Rainfall teleconnections with Indo-Pacific variability in the IPCC AR4 models. Journal of Climate 22, 26.

Cai W, van Rensch P, Cowan T and Sullivan A (2010) Asymmetry in ENSO teleconnection with regional rainfall. Its multidecadal variability and impact. Journal of Climate, 23, 4944-4955.

Chiew FHS, Kirono DGC, Kent DM, Frost AJ, Charles SP, Timbal B, Nguyen KC and Fu G (2010) Comparison of runoff modelled using rainfall from different downscaling methods for historical and future climates. Journal of Hydrology 387(1–2), 10–23.

Chiew FHS, Teng J, Vaze J and Kirono DGC (2009b) Influence of global climate model selection on runoff impact assessment. Journal of Hydrology 379(1-2), 172-180. DOI: DOI 10.1016/j.jhydrol.2009.10.004.

Chiew FHS, Teng J, Vaze J, Post DA, Perraud JM, Kirono DGC and Viney NR (2009a) Estimating climate change impact on runoff across southeast Australia: Method, results, and implications of the modelling method. Water Resources Research 45(W10414), 1-17. DOI: Artn W10414

Collins M, An SI, Cai WJ, Ganachaud A, Guilyardi E, Jin FF, Jochum M, Lengaigne M, Power S, Timmermann A, Vecchi G and Wittenberg A (2010) The impact of global warming on the tropical Pacific ocean and El Nino. Nature Geoscience 3(6), 391-397. DOI: Doi 10.1038/Ngeo868.

CSIRO (2007) Climate change in Australia. ISBN 97819123947. http://www.climatechangeinaustralia.gov.au/technical_report.php

CSIRO (2009a) Water in the Gulf of Carpentaria Drainage Division. A report to the Australian Government from the CSIRO Northern Austrlaia Sustainable Yields Project. CSIRO Water for Healthy Country Flagship, Australia.

CSIRO (2009b) Water in the Timor Sea Drainage Division. A report to the Australian Government from the CSIRO Northern Austrlaia Sustainable Yields Project. CSIRO Water for Healthy Country Flagship, Australia.

CSIRO (2009c) Water in the northern North-East Coast Drainage Division. A report to the Australian Government from the CSIRO Northern Austrlaia Sustainable Yields Project. CSIRO Water for Healthy Country Flagship, Australia.

Dracup JA, Lee KS and Paulson Jr EG (1980) On the definition of droughts. Water Resources Research, 16(2): 297–302.

Fowler HJ, Ekstrom M, Blenkinsop S and Smith AP (2007) Estimating change in extreme European precipitation using a multimodel ensemble. Journal of Geophysical Research-Atmospheres 112(D18). Doi: Artn D18104.

Hashimoto T, Stedinger JR and Loucks DP (1982) Reliability, resiliency and vulnerability criteria for water resource system performance evaluation. Water Resources Research, 18(1): 14–20.

Hennessy K, Fitzharris B, Bates BC, Harvey N, Howden SM, Hughes LSJ and Warrick R (2007) Australia and New Zealand. In Climate Change 2007 – Impacts, Adaptation and Vulnerability –Contributions of Working Group II to the Fourth Assessment Report of the International Panel on Climate Change. (Eds ML Parry, OF Canziani, JP Palutikof, PJ van der Linden, CE Hanson) pp. 507-540. Cambridge University Press, Cambridge.

Hobbs J (1998) Present climates of Australia and New Zealand. In: JE Hobbs JL, HA Bridgman (ed.) Climates of the Southern Continents: Present, Past and Future. John Wiley & Sons Ltd.

IPCC (2007) Climate Change 2007: The Physical Basis. Contributions of Working Group 1 to the Fourth Assessment Report of the Intergovernmental Panel on Climate Change. <http://www.ipcc.ch accessed 2 May 2011>.

Jackson IJ (1986) Relationships between rain days, mean daily intensity and monthly rainfall in the tropics. Journal of climatology 6:117-134.

Jeffrey SJ, Carter JO, Moodie KM and Beswick AR 2001 (2001) Using spatial interpolation to construct a comprehensive archive of Australian climate data. Environmental Modelling and Software 16(4), 309-330.

Köppen, W. (1936) Das geographisca System der Klimate, in: Handbuch der Klimatologie, edited by: Köppen, W. and Geiger, G., 1. C. Gebr, Borntraeger, 1–44, 1936

Leeper, G. W. (1970). The Australian environment. Melbourne, CSIRO and Melbourne University Press.

Li L, McVicar, TR, Donohue RJ, Van Niel TG, Teng J, Potter NJ, Smith IN, Kirono DGC, Bathols JM, Cai WJ, Marvanek SP, Chiew FHS and Frost AJ (2009) Climate data and their characterisation for hydrological scenario modelling across northern Australia: a report to the Australian Government from the CSIRO Northern Australia Sustainable Yields Project. CSIRO Water for a Healthy Country Flagship, Canberra.

McBride JL and Nicholls N (1983) Seasonal relationships between Australian rainfall and the Southern Oscillation. Monthly Weather Review 111, 1998-2004.

McVicar TR, Van Niel TG, Li LT, Roderick ML, Rayner DP, Ricciardulli L and Donohue RJ (2008) Wind speed climatology and trends for Australia, 1975-2006: Capturing the stilling phenomenon and comparison with near-surface reanalysis output. Geophysical Research Letters 35, L20403. doi:10.1029/2008GL035627.

Micevski T, Stewart WF and Kuczera G (2006) Multidecadal variability in coastal eastern Australian flood data. Journal of Hydrology 327, 7. DOI: 19.1016/j.jhydrol.2005.11.017.

Mitchell TD (2003) Pattern scaling - An examination of the accuracy of the technique for describing future climates. Climatic Change 60(3), 217-242.

Morton FI (1983) Operational estimates of lake evaporation. Journal of Hydrology 66(1–4), 77–100.

Nicholls N (1988) El Niño-Southern Oscillation and rainfall variability, Journal of Climate. 1: 418-421.

Peel MC, Finlayson BL and McMahon TA (2007) Updated world map of the Koppen-Geiger climate classification. Hydrological and Earth Systems Sciences 11, 1633-1644.

Peel MC, McMahon TA and Finlayson BL (2002) Variability of annual precipitation and its relationship to the El Niño-Southern Oscillation. Journal of Climate 15(5), 545-551.

Peel MC, McMahon TA and Pegram GGS (2005) Global analysis of runs of annual precipitation and runoff equal to or below the median: Run magnitude and severity. International Journal of Climatology 25(5), 549-568. Doi 10.1002/Joc.1147.

Peel MC, McMahon TA, Srikanthan R and Tan KS (2011a) Ensemble Empirical Mode Decomposition: Testing and objective automation. Proceedings of the 33rd Hydrology and Water Resources Symposium, Brisbane, Engineers Australia, pp: 702-709.

Peel MC, Pegram GGS and McMahon TA (2004) Global analysis of runs of annual precipitation and runoff equal to or below the median: Run length. International Journal of Climatology 24(7), 807-822. DOI: Doi 10.1002/Joc.1041.

Peel MC, Srikanthan R, McMahon TA and Karoly DJ (2011b): Ensemble Empirical Mode Decomposition of monthly climatic indices relevant to Australian hydroclimatology. In Chan, F., Marinova, D. and Anderssen, R.S. (eds) MODSIM2011, 19th International Congress on Modelling and Simulation. Modelling and Simulation Society of Australia and New Zealand, December 2011, pp. 3615-3621.

Petheram and Bristow (2008) Towards an understanding of the hydrological constraints and opportunities for irrigation in northern Australia. A review. CSIRO Land and Water Science Report No. 13/08. http://www.clw.csiro.au/publications/science/2008/sr13-08.pdf

Petheram C, McMahon TA and Peel MC (2008) Flow characteristics of rivers in northern Australia: Implications for development. Journal of Hydrology 357(1-2), 93-111.

Petheram C, Rustomji P, McVicar TR, Cai W, Chiew FHS, Vleeshouwer J, Van Niel TG, Li L, Cresswell RG, Donohue RJ, Teng J and Perraud J-M. (2012) Estimating the impact of projected climate change on runoff across the tropical savannas and semiarid rangelands of northern Australia. Journal of Hydrometeorology 13, 21. DOI: 10.1175/JHM-D-11-062.1.

Philander SGH (1990) El Nino – La Nina and the Southern Oscillation. Academic Press 289pp.

Power S, Case T, Folland C, Colman A and Meht V (1999) Inter-decadal modulation of the impact of ENSO on Australia. Clim. Dynam. 15(5), 6.

Prudhomme C and Davies H (2009) Assessing uncertainties in climate change impact analyses on the river flow regimes in the UK. Part 2: future climate. Climatic Change 93(1-2), 197-222. DOI: DOI 10.1007/s10584-008-9461-6.

Rasmusson EM and Arkin PA (1993) A global view of large-scale precipitation variability. Journal of Climate 6: 1495-1522.

Rind D (2008) The consequences of not knowing low-and high-latitude climate sensitivity. Bulletin of the American Meteorological Society 89(6), 855-864. DOI: Doi 10.1175/2007bams2520.1.

Roderick M, Rotstayn L, Farquhar G et al., (2007) On the attribution of changing pan evaporation. Geophysical Research Letters, vol. 34, no. 17, pp. 1-6.

Segui PQ, Ribes A, Martin E, Habets F and Boe J (2010) Comparison of three downscaling methods in simulating the impact of climate change on the hydrology of Mediterranean basins. Journal of Hydrology 383(1-2), 111-124. DOI: DOI 10.1016/j.jhydrol.2009.09.050.

Shuttleworth WJ (1993) Evaporation. In Maidment, D. R. (Ed.) Handbook of Hydrology. New York, McGraw-Hill Inc.

Stephens GL, Le T, Forbes R, Gettlemen A, Golaz J, Bodas-Salcedo A, Suzuki K, Gabriel P and Haynes J. (2010) Dreary state of precipitation in global models. Journal of Geophysical Research 115. DOI: 10.1029/2010JD014532.

Sumner G and Bonell M (1986) Circulation and daily rainfall in the North Queensland wet seasons 1979-1982. Journal of Climatology 6: 531-549.

Teng J, Chiew FHS and Vaze J. (2012) Will CMIP5 GCMs reduce or increase uncertainty in future runoff projections? 34th Hydrology and Water Resources Symposium. Engineers Australia, Sydney.

Todd MC, Taylor RG, Osborn TJ, Kingston DG, Arnell NW and Gosling SN (2011) Uncertainty in climate change impacts on basin-scale freshwater resources - preface to the special issue: the QUEST-GSI methodology and synthesis of results. Hydrology and Earth System Sciences 15(3), 1035-1046. DOI: DOI 10.5194/hess-15-1035-2011.

Warner RF (1986) Hydrology. In 'The Natural Environment' (ed. DN Jeans). Sydney University Press, Sydney, 1986.

Whetton PH, Hennessy KJ, Katzfey JJ, McGregor JL, Jones RN and Nguyen K (2000) Climate averages and variability based on a transient CO_2 simulation, Annual Report 1997–98. Department of Natural Resources and Environment, Victoria.

Whetton PH, McInnes KL, Jones RN, Hennessy KJ, Suppiah R, Page CM, Bathols J and Durack PJ (2005) Australian Climate Change Projections for Impact Assessment and Policy Application: A Review., <http://www.cmar.csiro.au/e-print/open/whettonph_2005a.pdf>Viewed 5 June 2012.

Yevjevich VM (1967) An objective approach to definitions and investigations of continental hydrologic droughts. Colorado State University, Hydrology Paper No. 23.

Appendix A

The figures in this appendix show the distribution of rainfall and maximum temperature data across the Timor Sea, Gulf of Carpentaria and northern North-east Coast drainage divisions.

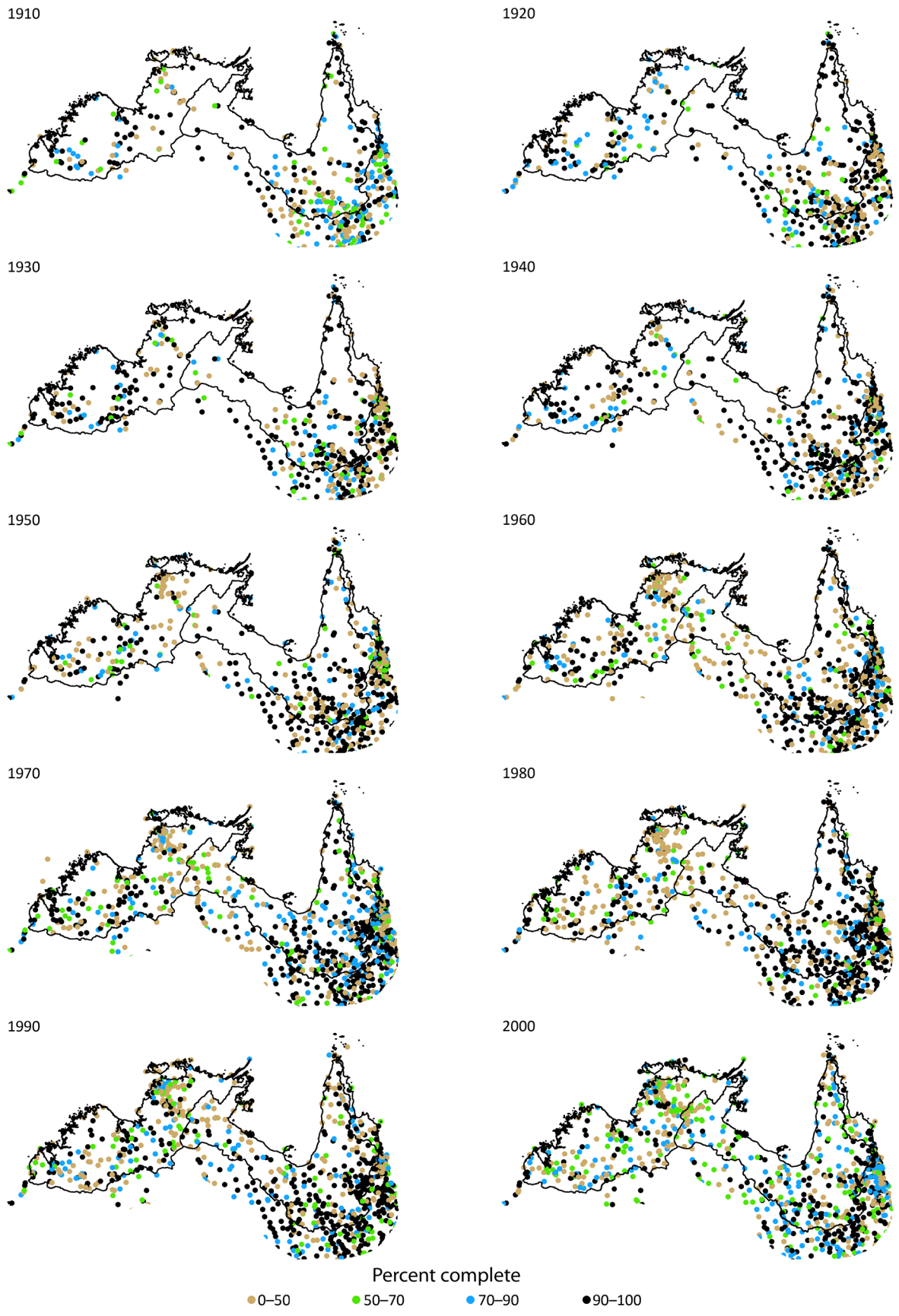

Apx Figure A.1 Decadal analysis of the location and completeness of Bureau of Meteorology stations measuring daily rainfall used in the SILO database. The decade labelled '1910' is defined from 1 January 1910 to 31 December 1919, and so on. At a station, a decade is 100% complete if there are observations for every day in that decade (Li et al., 2009)

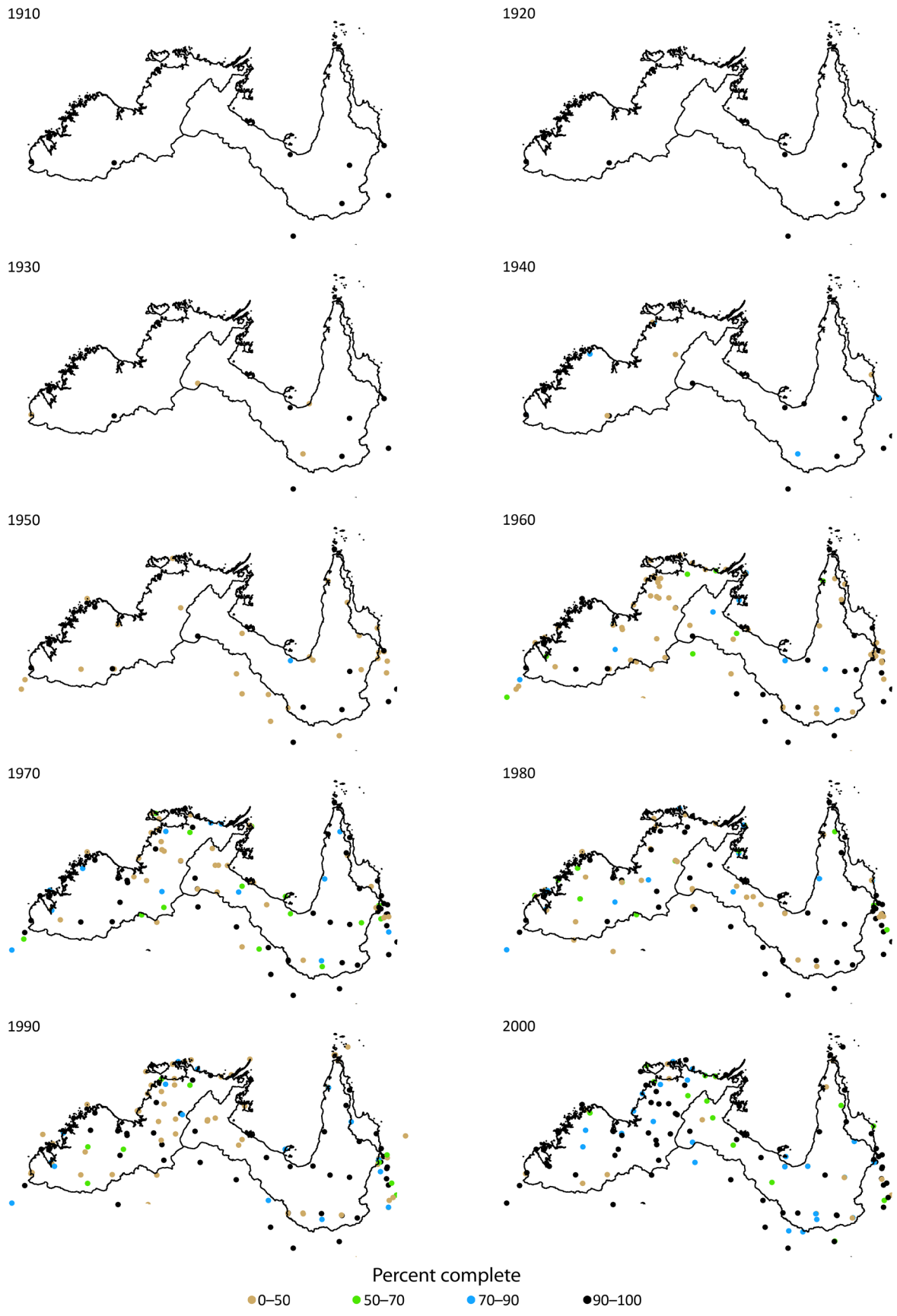

Apx Figure A.2 Decadal analysis of the location and completeness of Bureau of Meteorology stations measuring daily maximum air temperature used in the SILO database. The decade labelled '1910' is defined from 1 January 1910 to 31 December 1919, and so on. At a station, a decade is 100% complete if there are observations for every day in that decade (Li et al., 2009)

Appendix B

The figure in this appendix shows the annual rainfall exceedance for the Flinders and Gilbert catchments.

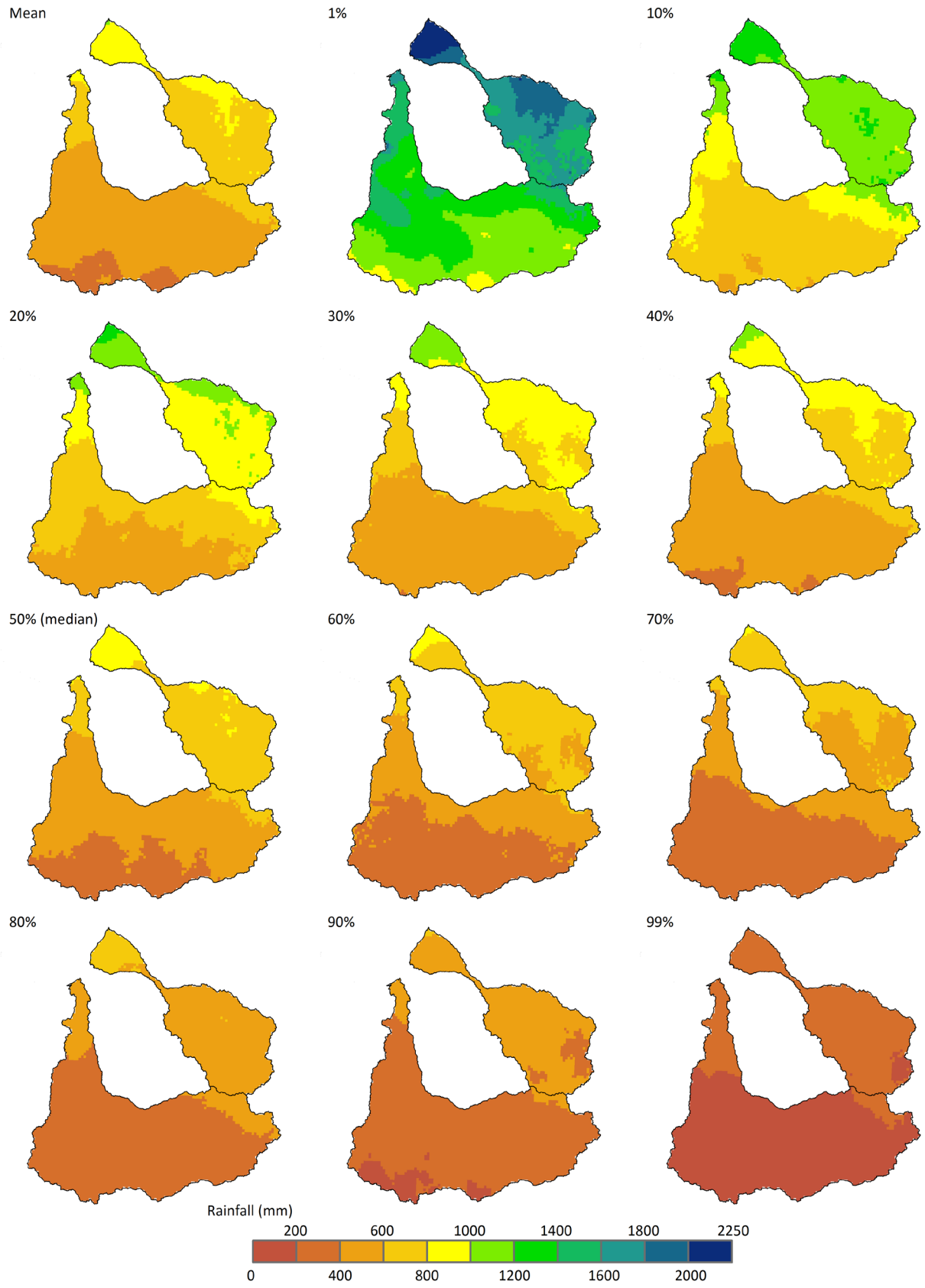

Apx Figure B.1 Annual rainfall exceedance for the Flinders and Gilbert catchments. This diagram illustrates the percentage of years annual rainfall is exceeded

Appendix C

The figures in this appendix show percent exceedance maps for monthly rainfall, potential evaporation, mean daily maximum temperature, mean daily minimum temperature and mean daily relative humidity are provided in Appendix C.

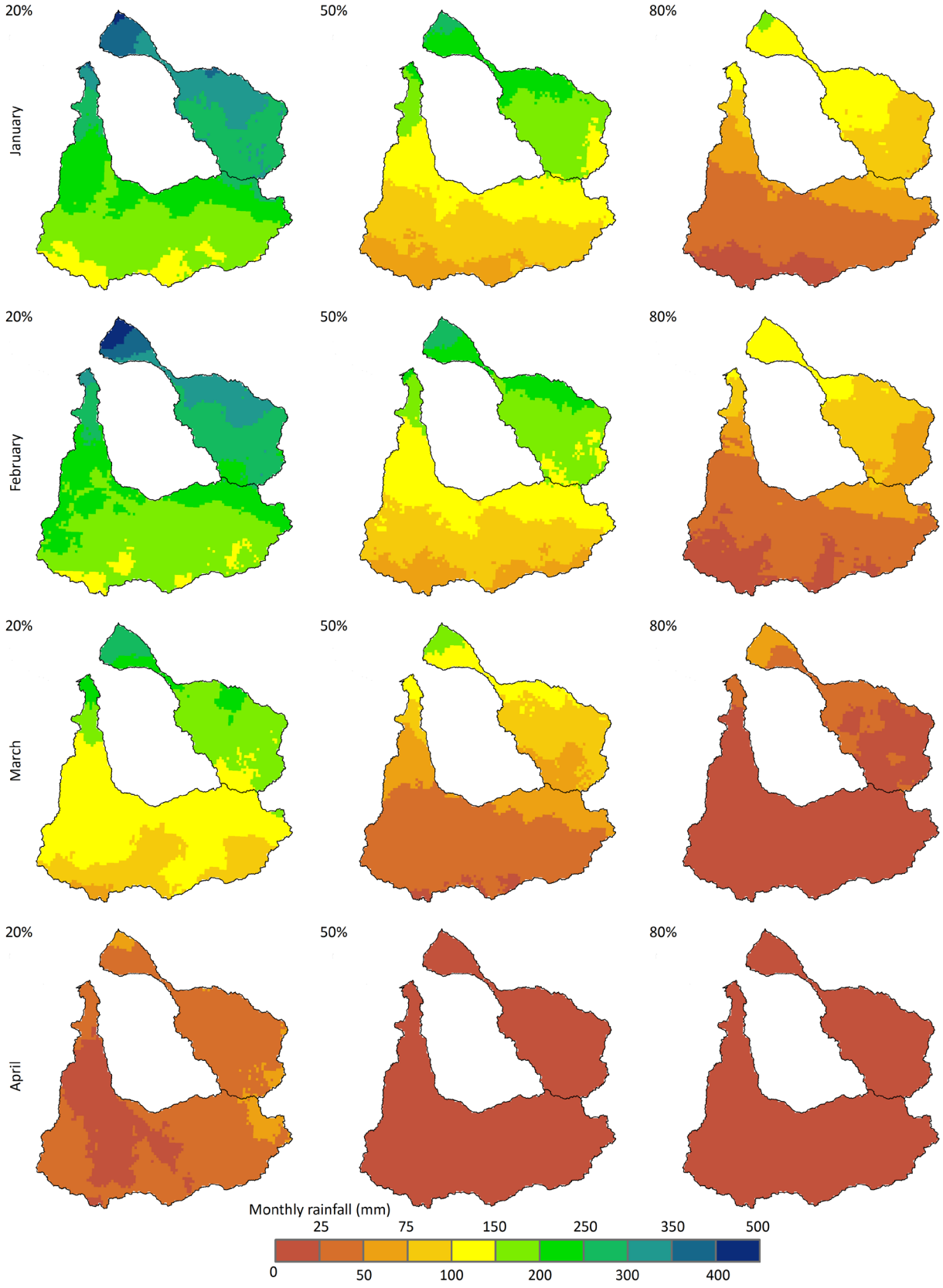

Apx Figure C.1 The rainfall that is exceeded 20%, 50% and 80% of the time for the months of January to April

Apx Figure C.2 The rainfall that is exceeded 20%, 50% and 80% of the time for the months of May to June

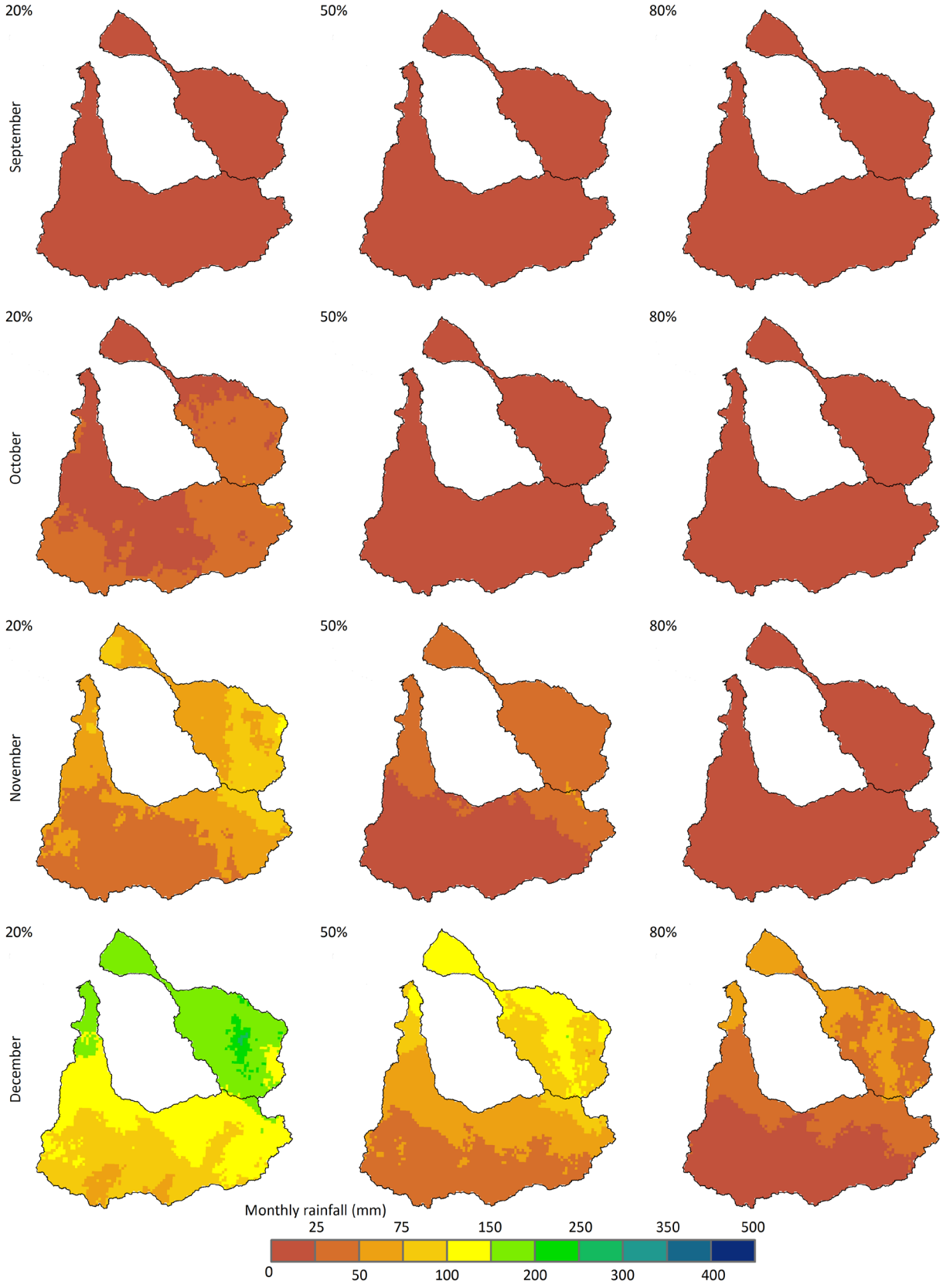

Apx Figure C.3 The rainfall that is exceeded 20%, 50% and 80% of the time for the months of September to December

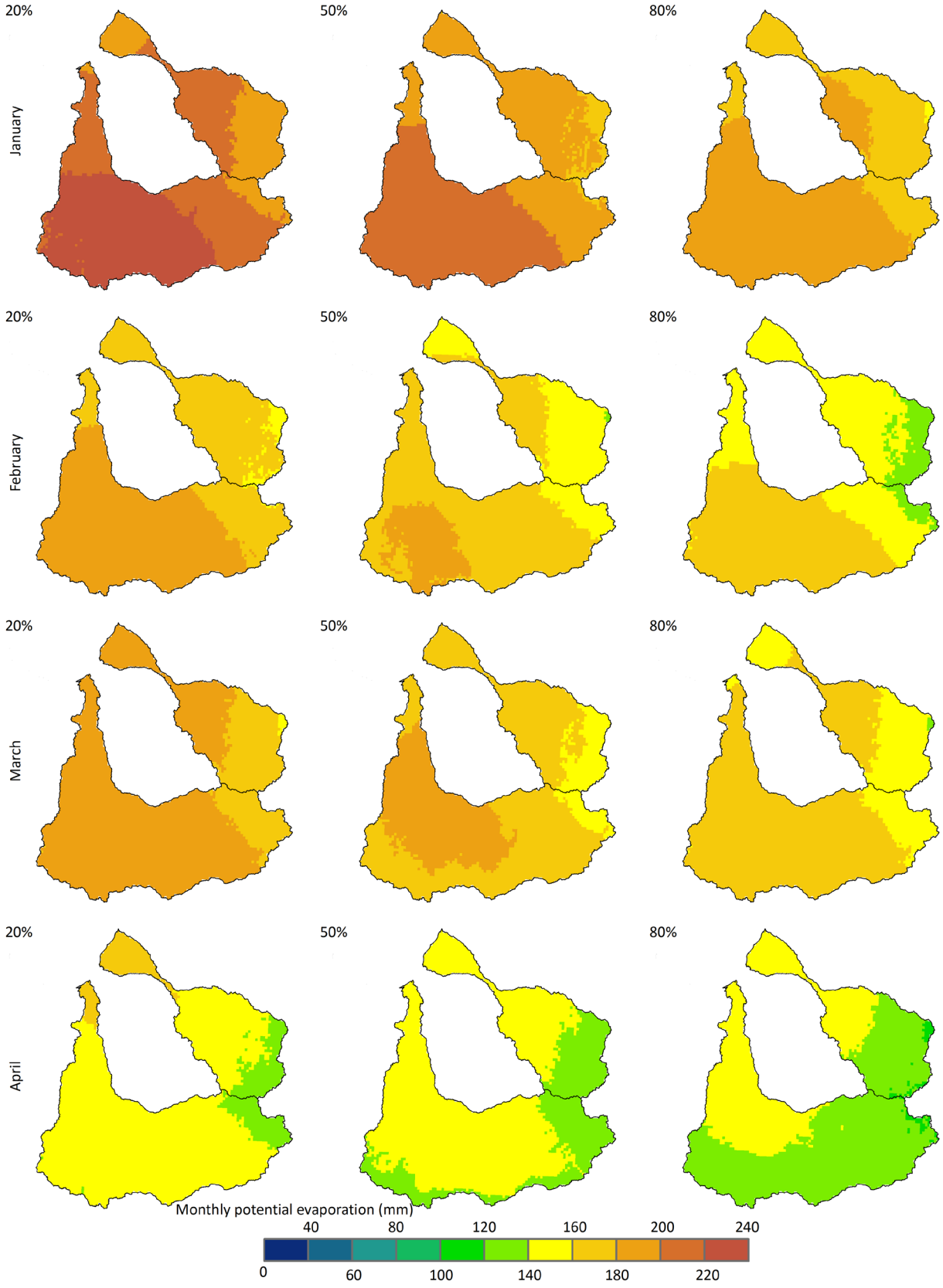

Apx Figure C.4 The areal potential evaporation that is exceeded 20%, 50% and 80% of the time for the months of January to April

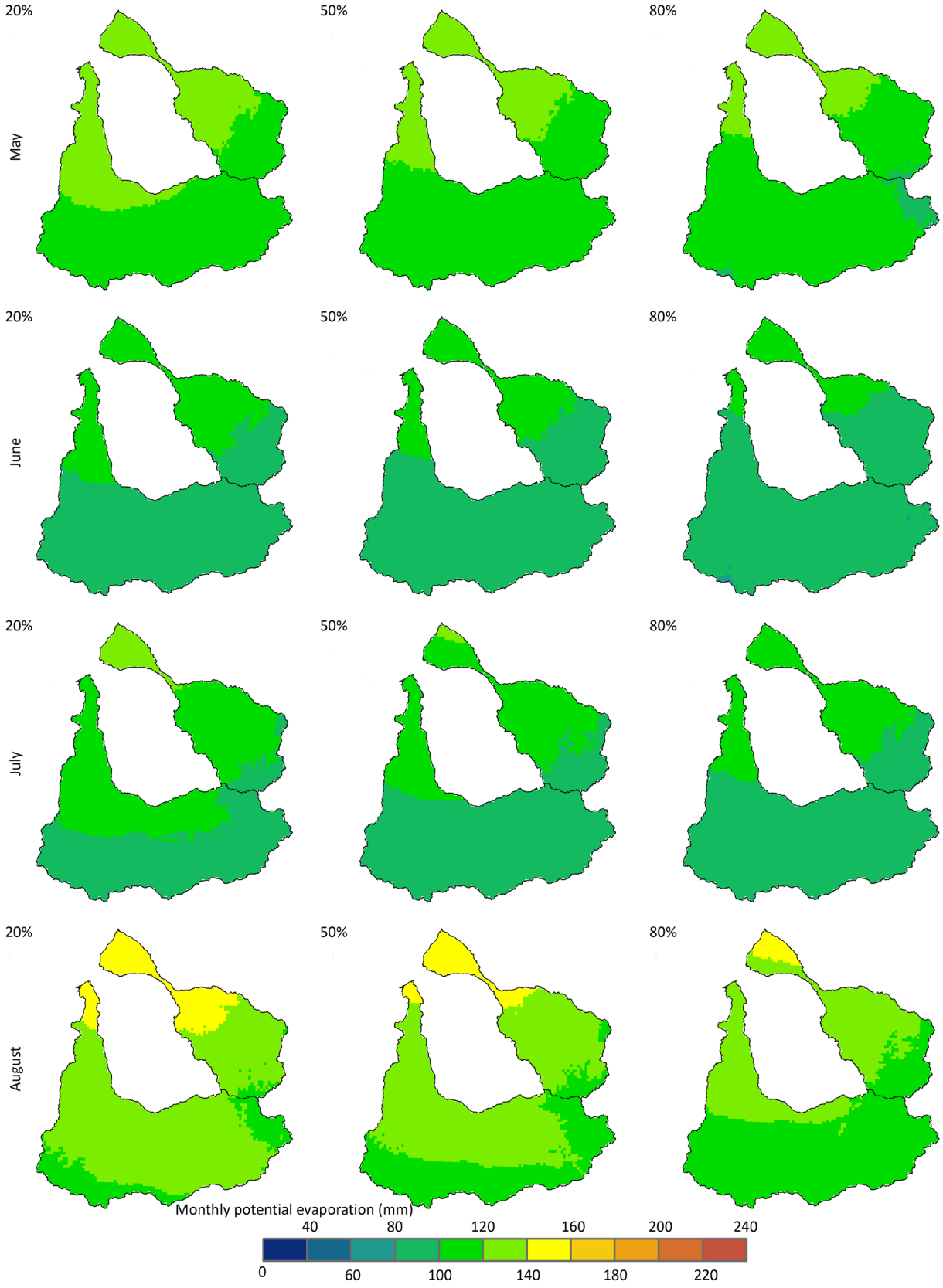

Apx Figure C.5 The areal potential evaporation that is exceeded 20%, 50% and 80% of the time for the months of May to August

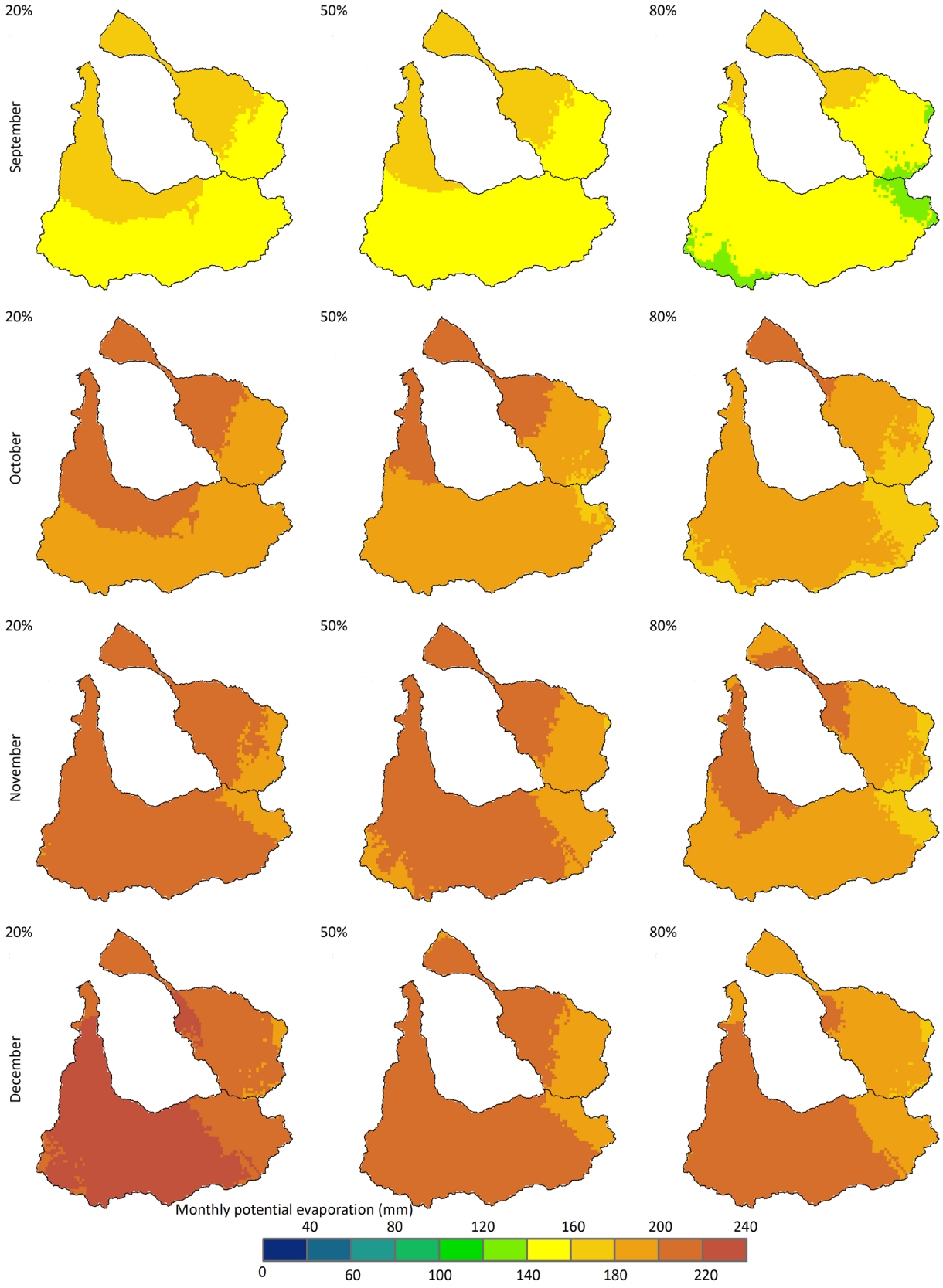

Apx Figure C.6 The areal potential evaporation that is exceeded 20%, 50% and 80% of the time for the months of September to December

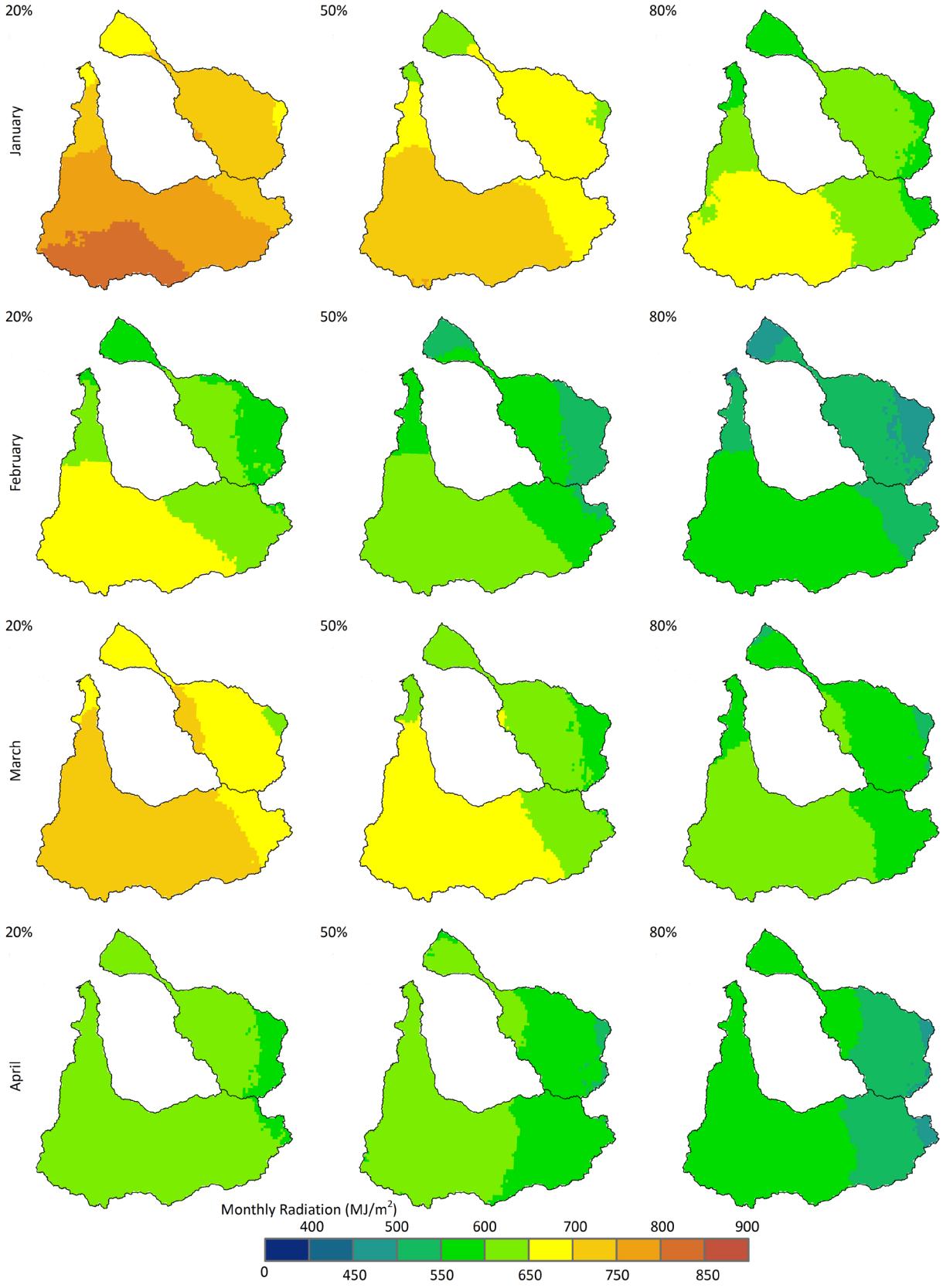

Apx Figure C.7 The short wave radiation that is exceeded 20%, 50% and 80% of the time for the months of January to April

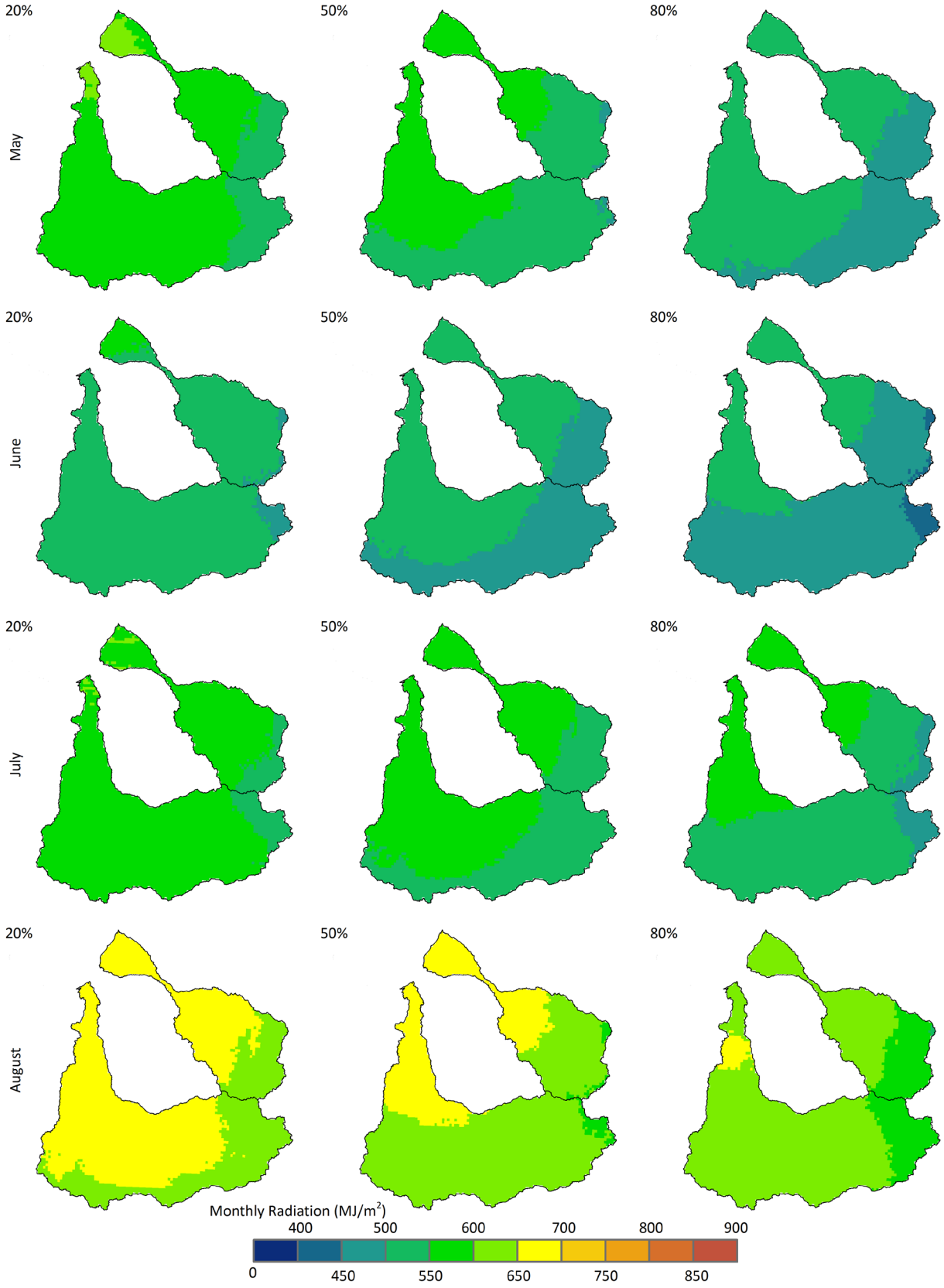

Figure 5.1 The short wave radiation that is exceeded 20%, 50% and 80% of the time for the months of May to August

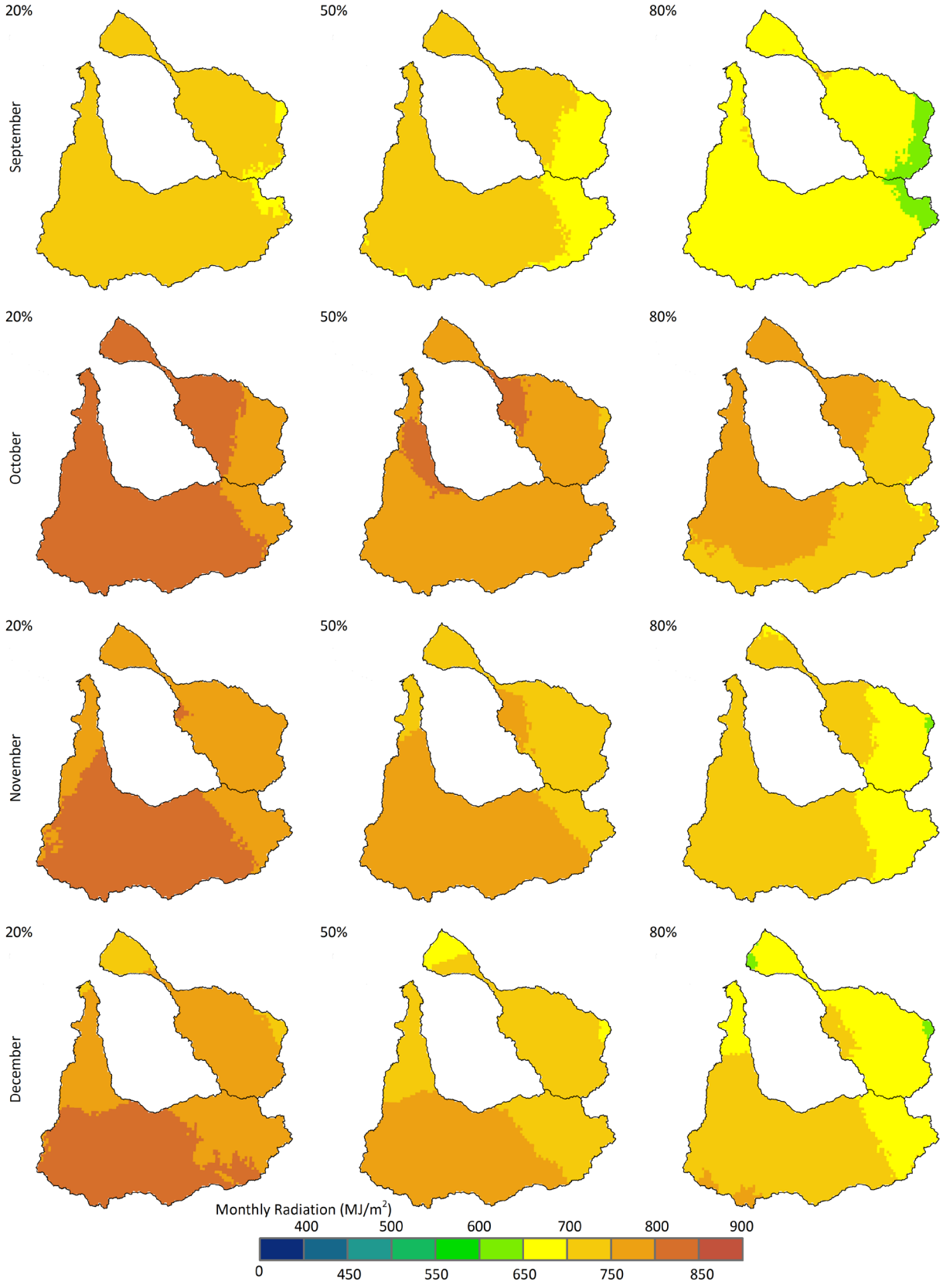

Apx Figure C.8 The short wave radiation that is exceeded 20%, 50% and 80% of the time for the months of September to December

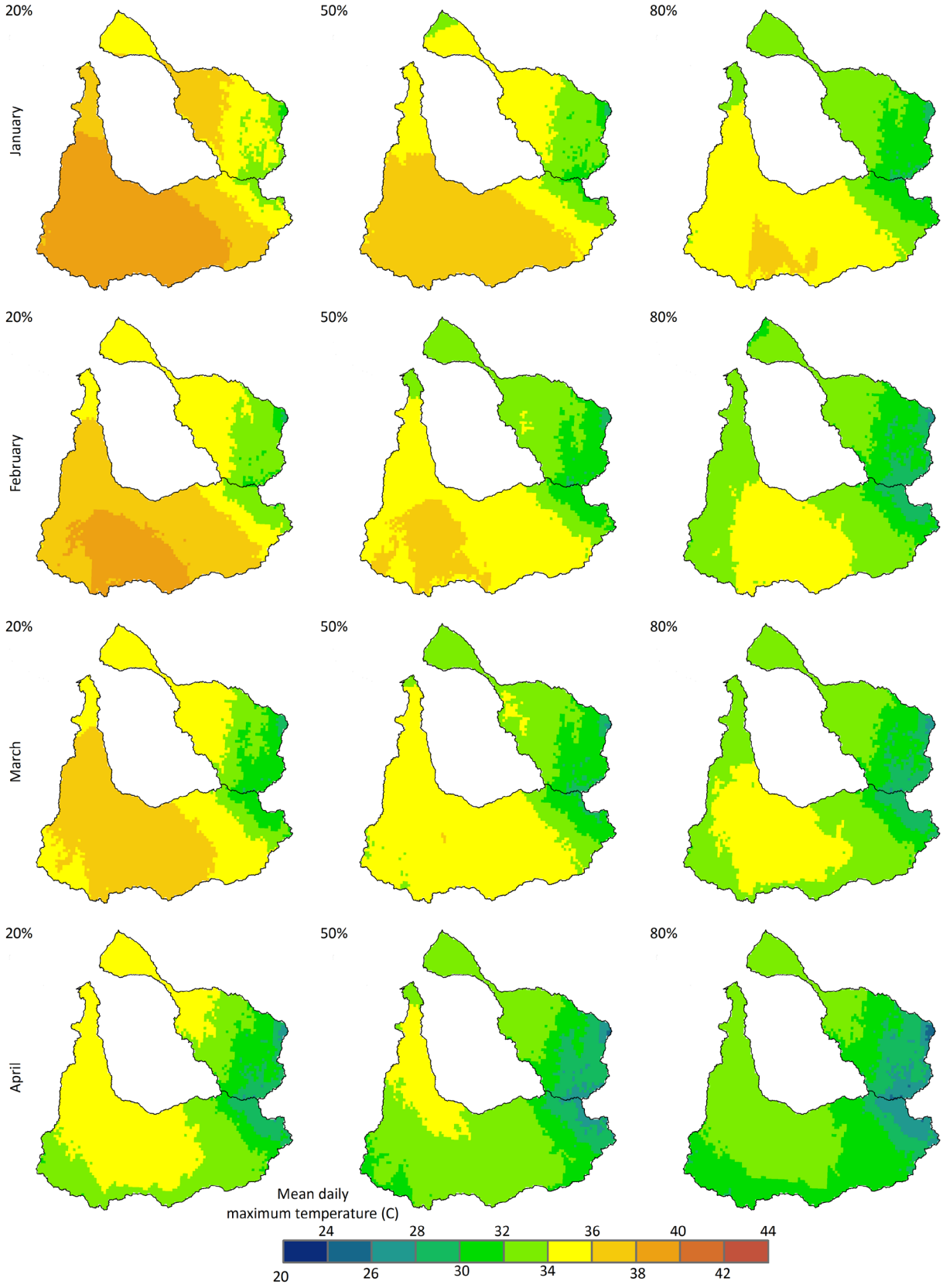

Apx Figure C.9 The mean daily maximum temperature that is exceeded 20%, 50% and 80% of the time for the months of January to April

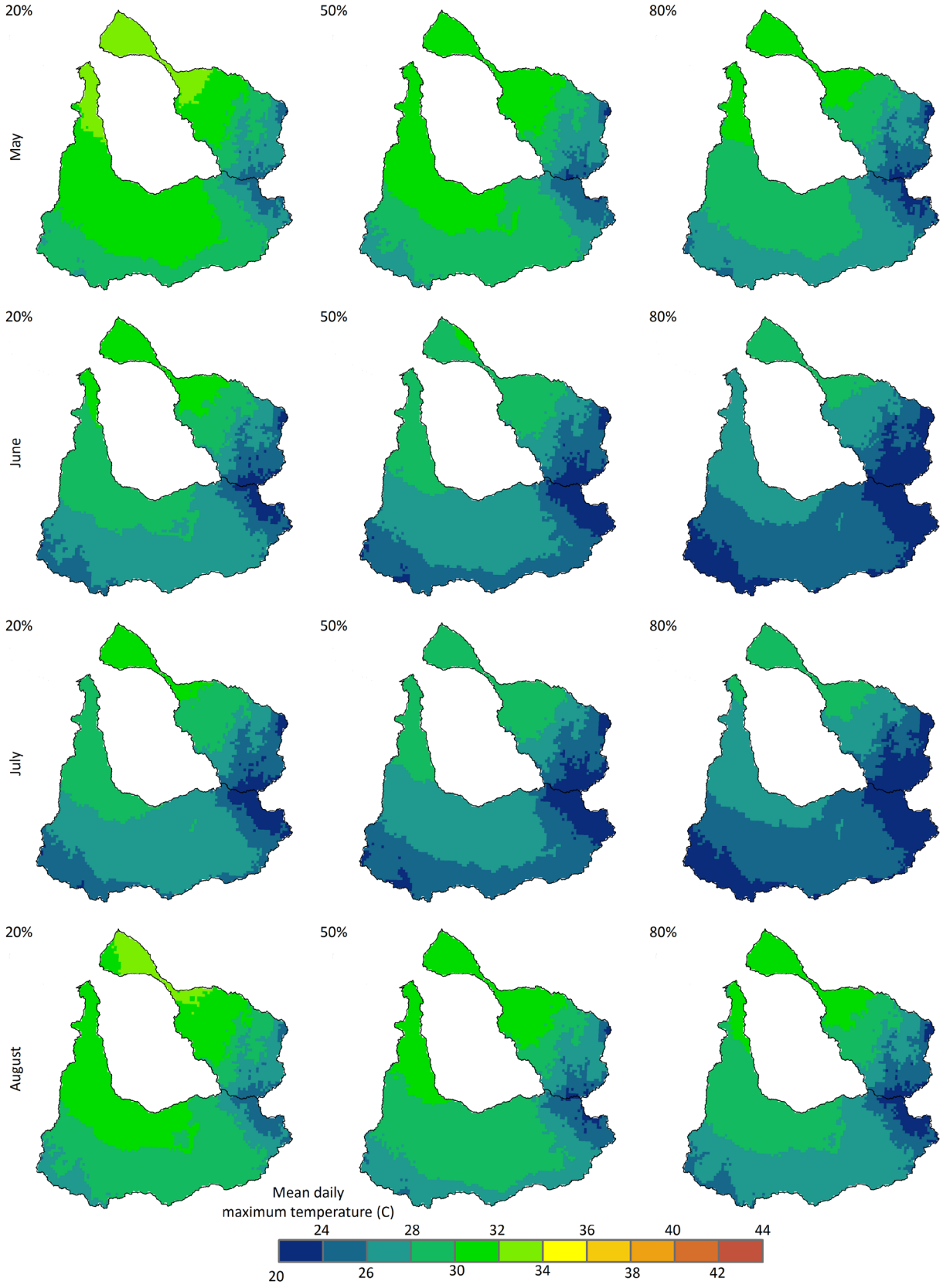

Apx Figure C.10 The mean daily maximum temperature that is exceeded 20%, 50% and 80% of the time for the months of May to August

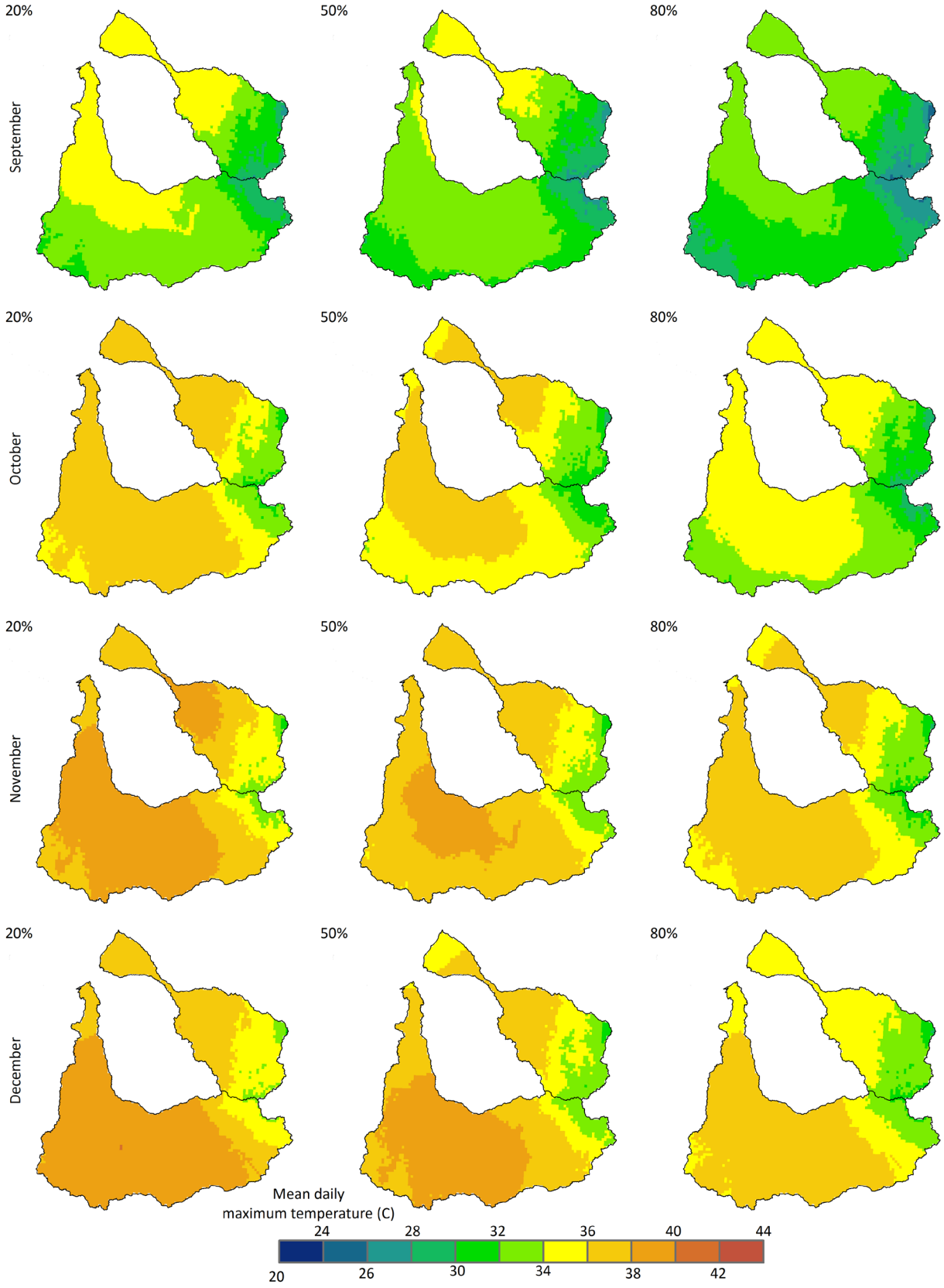

Apx Figure C.11 The mean daily maximum temperature that is exceeded 20%, 50% and 80% of the time for the months of September to December

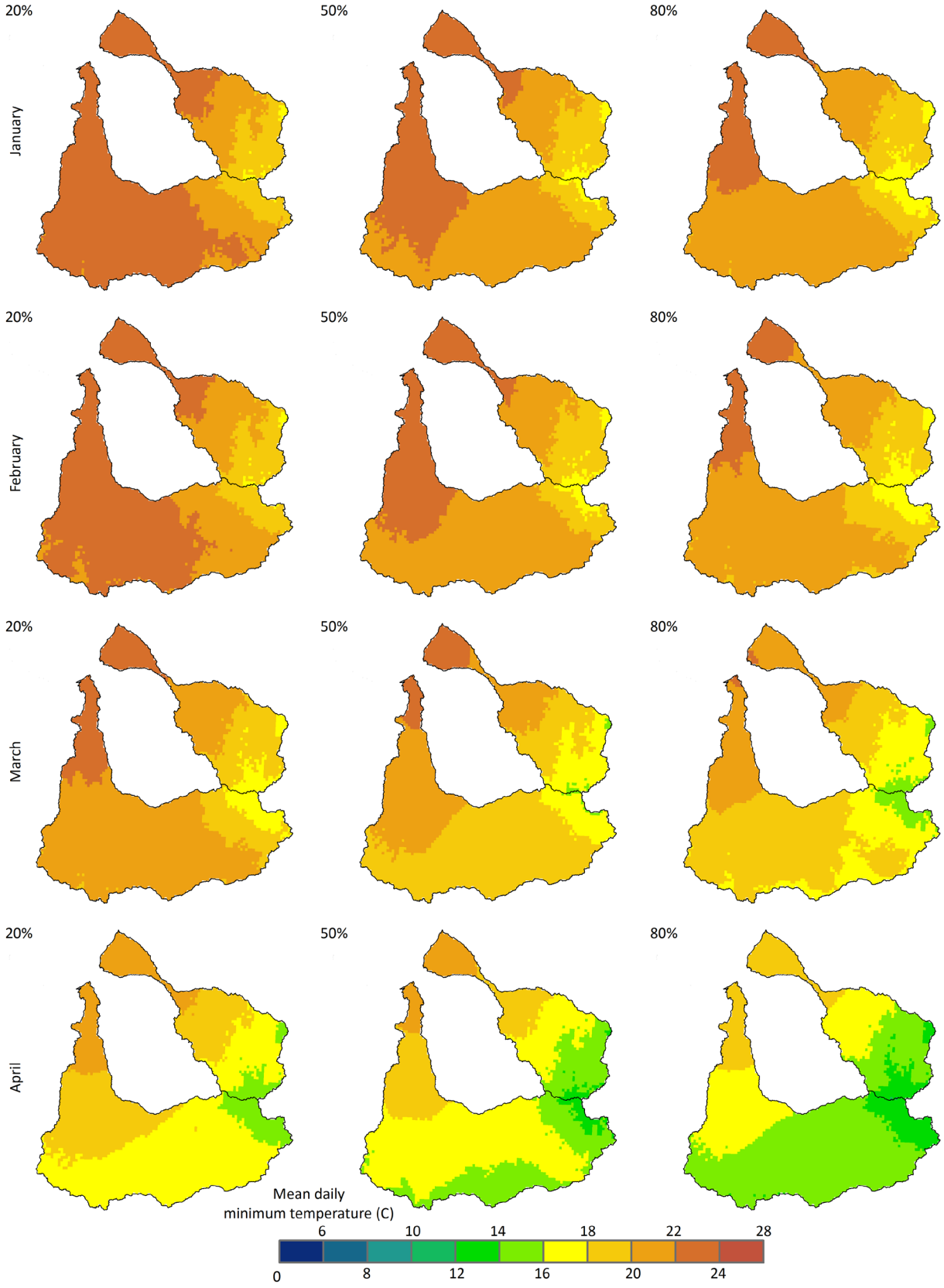

Apx Figure C.12 The mean daily minimum temperature that is exceeded 20%, 50% and 80% of the time for the months of January to April

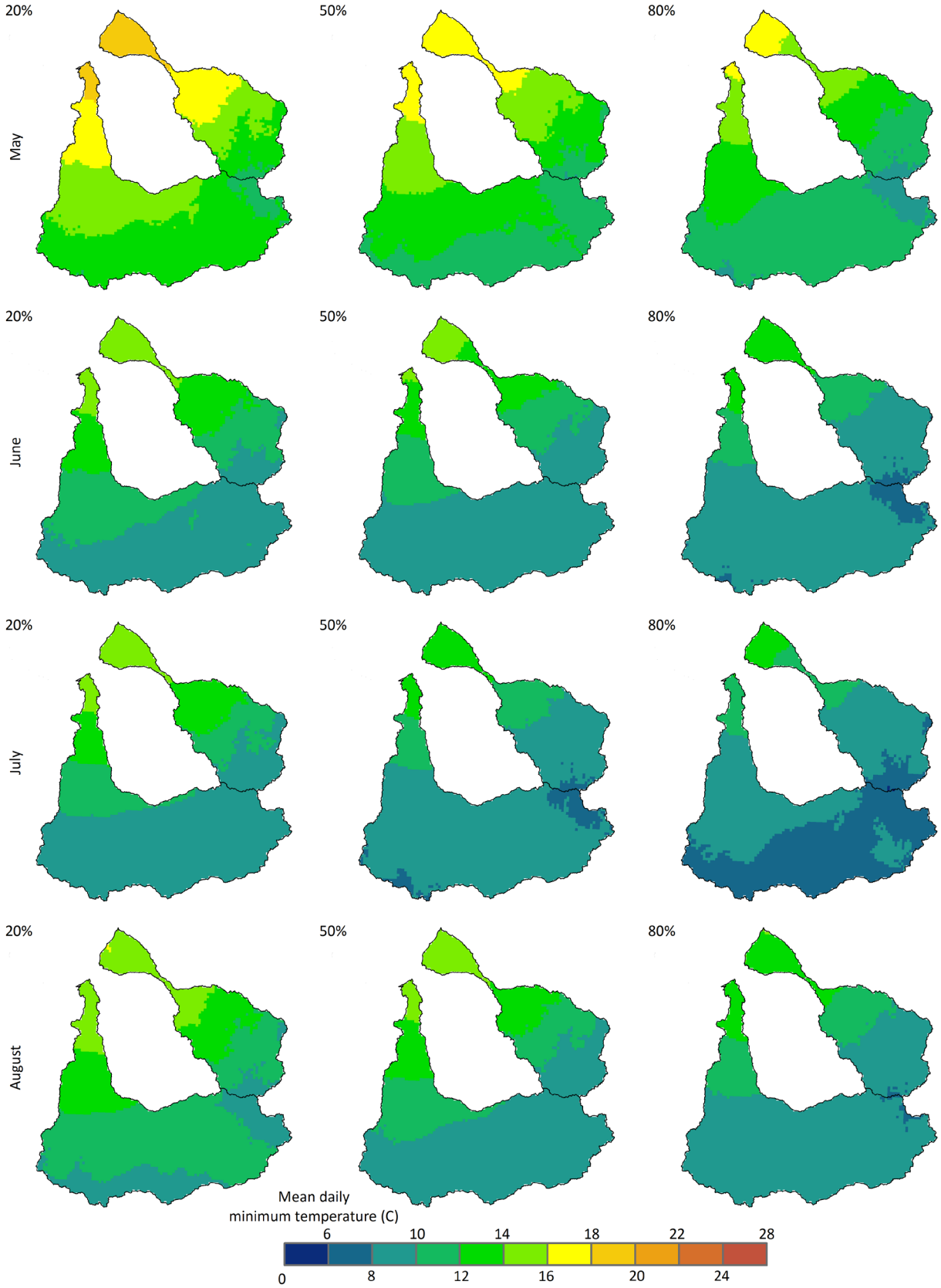

Apx Figure C.13 The mean daily minimum temperature that is exceeded 20%, 50% and 80% of the time for the months of May to August

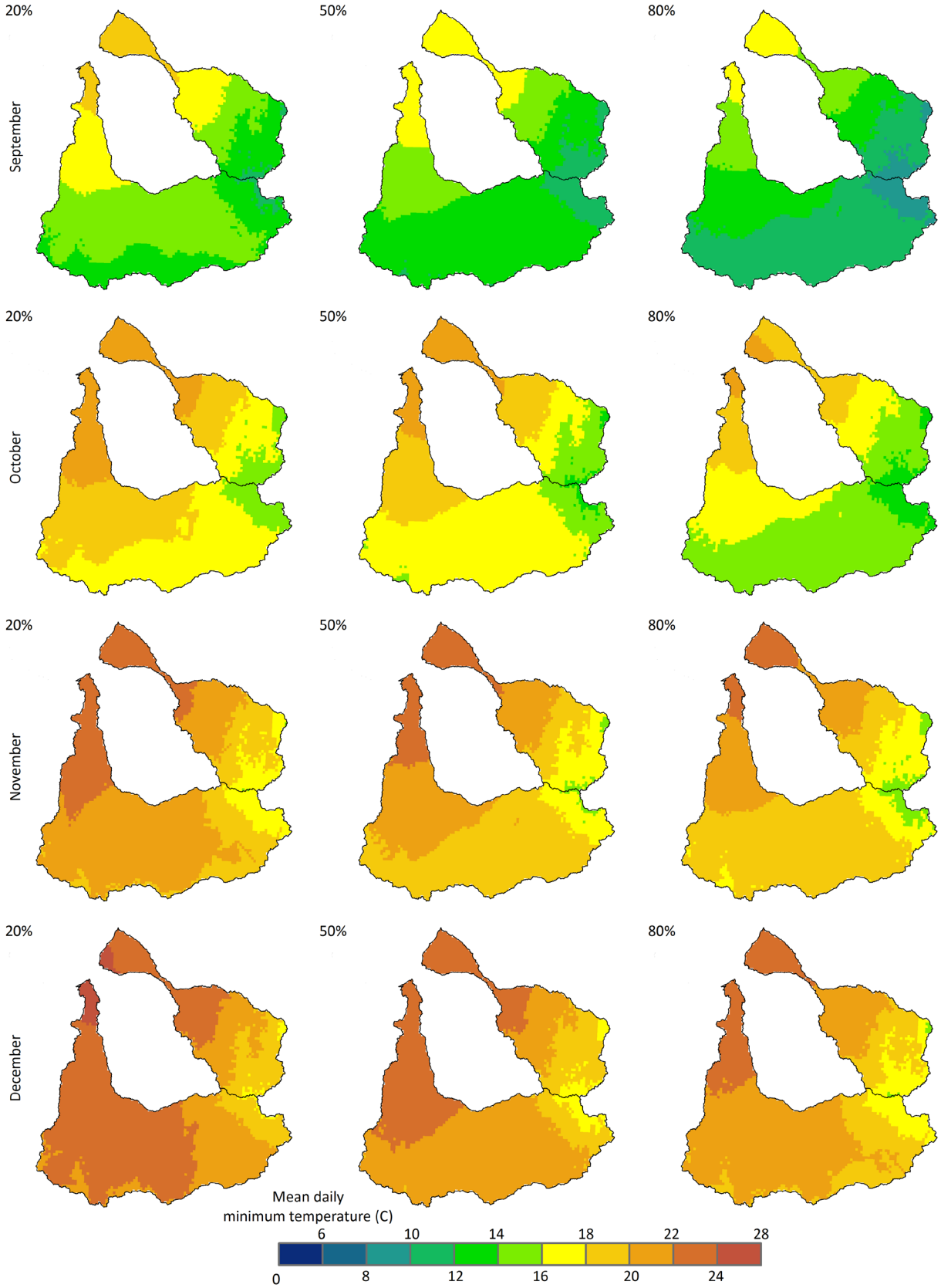

Apx Figure C.14 The mean daily minimum temperature that is exceeded 20%, 50% and 80% of the time for the months of September to December

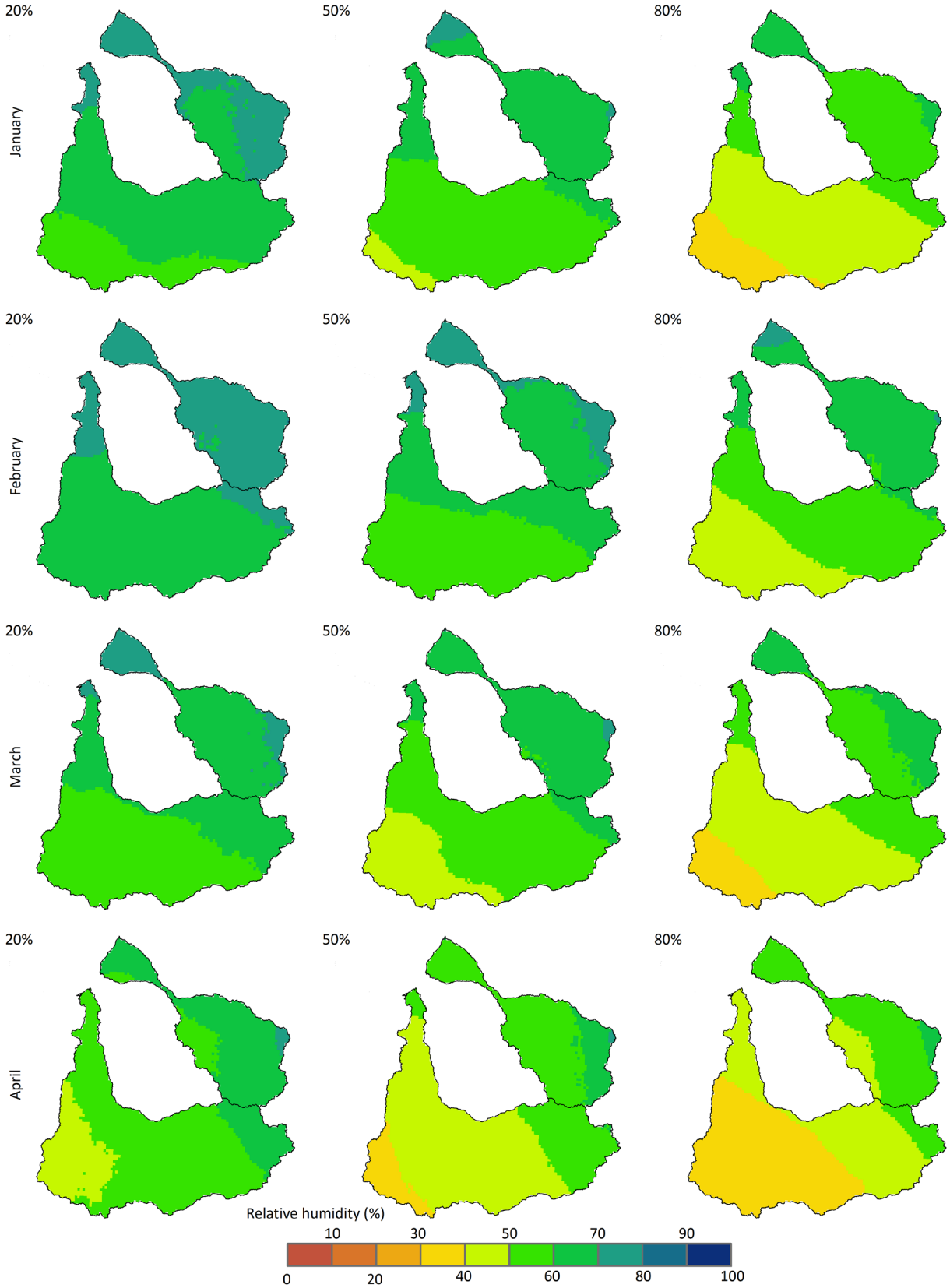

Apx Figure C.15 The mean daily relative humidity that is exceeded 20%, 50% and 80% of the time for the months of January to April

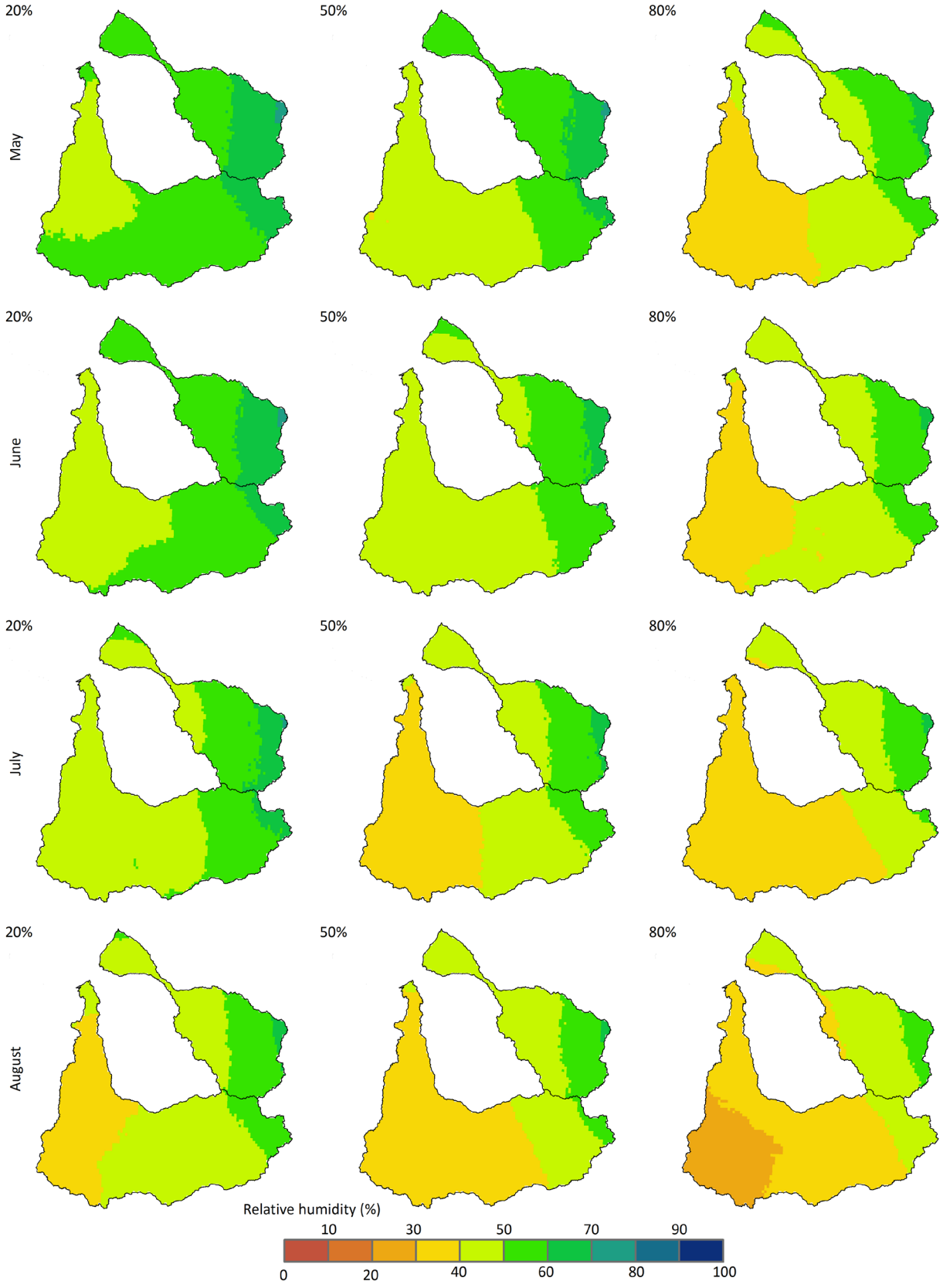

Apx Figure C.16 The mean daily relative humidity that is exceeded 20%, 50% and 80% of the time for the months of May to August

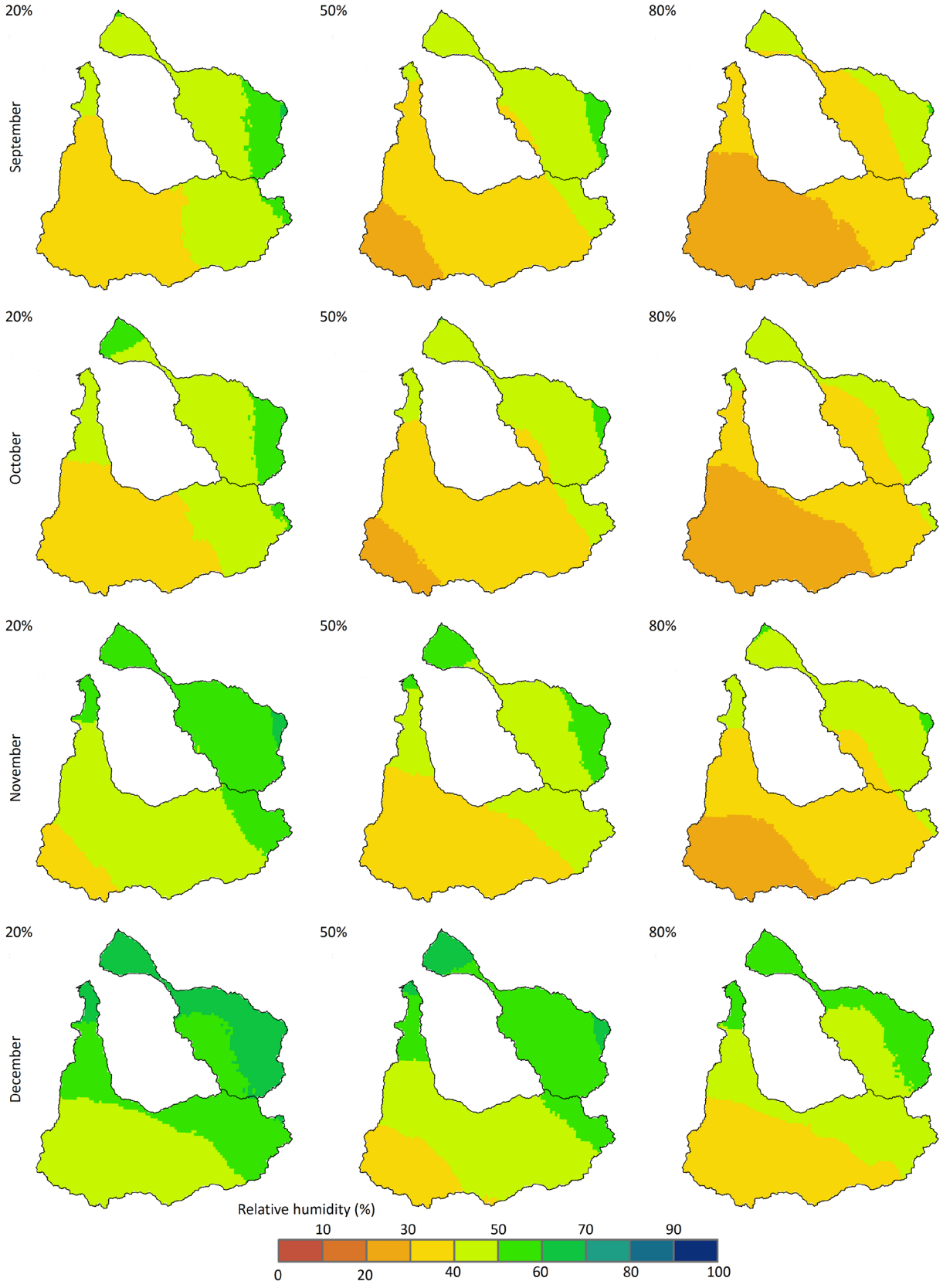

Apx Figure C.17 The mean daily relative humidity that is exceeded 20%, 50% and 80% of the time for the months of September to December

CONTACT US

t 1300 363 400
+61 3 9545 2176
e enquiries@csiro.au
w www.csiro.au

YOUR CSIRO

Australia is founding its future on science and innovation. Its national science agency, CSIRO, is a powerhouse of ideas, technologies and skills for building prosperity, growth, health and sustainability. It serves governments, industries, business and communities across the nation.

FOR FURTHER INFORMATION

Water for a Healthy Country Flagship
Cuan Petheram
t +61 2 6246 5987
e Cuan.Petheram@csiro.au
w www.csiro.au/org/WfHC